The role of ATP-dependent chromatin remodeling enzyme CHD7 in the development and maintenance of murine neural stem cells

by

Joseph Anthony Micucci

A dissertation submitted in partial fulfillment
of the requirements for the degree of
Doctor of Philosophy
(Biological Chemistry)
in the University of Michigan
2013

Dissertation Committee:

Associate Professor Donna M. Martin, Co-Chair
Adjunct Assistant Professor Daniel A. Bochar, Co-Chair
Assistant Professor Shigeki Iwase
Associate Professor Raymond C. Trievel
Professor Michael D. Uhler
Associate Professor Anne B. Vojtek

When I heard the learn’d astronomer;
When the proofs, the figures, were ranged in columns before me;
When I was shown the charts and the diagrams, to add, divide,
and measure them;
When I, sitting, heard the astronomer, where he lectured with much applause in the lecture-room,
How soon, unaccountable, I became tired and sick;
Till rising and gliding out, I wander’d off by myself,
In the mystical moist night-air, and from time to time,
Look’d up in perfect silence at the stars.

Walt Whitman
Leaves of Grass.
1900

Never give up! Trust your instincts!

Peppy Hare
Star Fox 64
1997

2013

Dedication

To Kristen,

Thank you for supporting me and keeping me grounded for the last 10 years, much to your own chagrin.

Acknowledgements

First, I would like to thank my incredible wife, Kristen. I have no idea how we made it through the last five and a half years with our marriage and happiness intact. I think we would both agree that the cats were excellent arbiters. There is absolutely no way that I could have finished graduate school without you. You are the motivating and grounding force in my life for which I am eternally grateful; otherwise, I would never accomplish anything besides being comfortable on the couch watching football. I will do my best to ensure that the next phase in our lives goes much more smoothly and pleasantly than the previous.

There are no words that can adequately express my gratitude to my parents for their unrelenting positivity and unconditional love throughout my life. Despite all of the precocious shenanigans I put you through in the early years of grade school, having you drive me up and down the East Coast to play hockey and paying for my education at Penn State (granted, you two had almost as much fun there as I did), you have never once been anything less than supremely supportive by letting me make my own life decisions and learn from my mistakes. Thank you to my grandparents for always being there for me regardless of their geographical location. I would also like to thank my family for their all of their love and support. I have to specifically thank Aunt Peg and Uncle

Joe for their hospitality whether Kristen and I were with them in South Bend, Ann Arbor or Pittsburgh. We both really appreciated being treated like one of your own children whenever we were at your house for holidays that we couldn't make it back to Jersey or Philly.

Thank you to all of our friends back East (and West now for Robert and Imee) for always meeting us at crazy hours and locations during the holidays and our brief vacations. I look forward to making up for lost time when we return to Philadelphia.

I would also like to thank my friends and lab mates in Ann Arbor. Thanks to Joel and Bruce for their excellent ability to help me forget about things that are troubling me, largely through ridiculous conversations and excessive amounts of playing video games. At times, I'm still completely shocked that we all graduated in reasonable amounts of time. I would like to thank everyone that I have worked with in the Martin Lab, specifically Wanda, Mindy, Mark, Jennifer, Ethan and Sophie. It was a pleasure to come to lab and deal with such fun people. I retroactively apologize for my insane sense of humor and relative lack of filter.

I don't think there is enough space in this dissertation to thank Liz Hurd. Our relationship started out as that of master and apprentice and evolved into some bizarre amalgamation of sister/mother/work-wife. Whatever it was, thank you for it! I don't think I would have adequately made the transition from Dan's lab to Donna's lab without your guidance. Kristen and I greatly appreciate your hospitality and absorbing us into your family. I'm also sorry for putting your cat in a bag and for him giving me necrotizing fasciitis.

I also need to thank Becky Simon for always being up for crying in our beers/Captain and Coke's whenever I needed it. Our friendship may have begun on that fateful van ride to Kalamazoo first year with discussions of diabetes, Wilford Brimley and Crohn's disease, but I think it was solidified when both of us were crying when Penn State locked up the Rose Bowl bid in 2008. Granted, I was crying because my alma mater won the Big Ten championship and you were crying because the Spartans had just been curbstomped by four touchdowns at the feet of the Nittany Lions, but whatever.

I would also like to thank my thesis committee: Ray Trievel, Mike Uhler, Anne Vojtek, Shigeki Iwase and Tom Glaser. Without your patience and guidance throughout the last five years, I would not be prepared to write a dissertation and defend it.

Lastly, I would like to thank my mentors. Dan, thank you for giving me the freedom to be myself, make mistakes and learn from them. It's sad that I didn't get to finish my thesis research in your lab, but I thoroughly enjoyed every second that I got to learn from you. Donna, thank you for giving me boundaries when I needed them and putting me into the right positions to succeed. Also, thank you for taking me in when I needed help the most. I know that we don't often see things the same way, but I'm fairly certain that we've learned a great deal from eachother. I couldn't have asked for better mentors, despite being polar opposite in your outlooks on life and science. You two were exactly what I needed at exactly the right times.

Table of Contents

List of Figures

List of Tables

Abstract

Cell type-specific gene expression is a tightly controlled process which is facilitated by several classes of proteins including transcription factors, histone modifying enzymes and ATP-dependent chromatin remodeling enzymes. The CHD class of chromatin remodelers is important for development and maintenance of mammalian stem cell populations and their progeny. In humans, haploinsufficiency for the CHD family member *CHD7* results in a multiple congenital anomaly disorder called CHARGE syndrome. Defects of the eye, ear, heart, brain, olfactory organs and craniofacial features are commonly observed in CHARGE syndrome. Notably, CHARGE individuals display decreased or absent sense of smell (hyposmia or anosmia) and small or absent olfactory bulbs (OB) and tracts (arrhinencephaly). The OB is populated by neurons born in a neural stem cell niche located along the lateral walls of the lateral ventricles in a region termed the subventricular zone (SVZ). The process of neuronal migration from the SVZ to the OB begins during late embryogenesis and continues into adulthood, implying that *CHD7* deficiency in the SVZ neural stem cell niche may play a role in the olfaction. In order to study the role of CHD7 in SVZ neural stem cell function, I generated conditional *Chd7* knockout mice using a $Chd7^{flox}$ allele and ubiquitous or neural stem cell-specific Cre recombinases. In adult mice,

Chd7 deficiency leads to decreased SVZ proliferation, ventriculomegaly, fewer neuroblasts and mature OB interneurons, and increased glial cells. Conditional adult and perinatal knockout mice display defects in proliferation, self-renewal and neuronal differentiation which can be rescued by modulation of retinoic acid signaling. By chromatin immunoprecipitation, CHD7 binds to the promoters of retinoic acid receptors and pro-neural genes in neural stem cells. Additionally, microarray analysis of SVZ gene expression from control and *Chd7* conditional knockout mice shows that neuronal differentiation, migration and maturation genes are down-regulated upon loss of *Chd7*. Together, these data suggest that CHD7 plays a critical role in the development and maintenance of the SVZ neural stem cell niche. My research has helped to identify molecular mechanisms of CHD7 function in neural stem cells could improve diagnostic and therapeutic approaches for individuals with CHARGE syndrome and related disorders.

Chapter 1

Introduction

The development and maintenance of the mammalian brain requires precise coordination of responses to external signaling events and cell type-specific gene expression. If the delicate balance of transcription factor and epigenetic modifier function and requisite gene expression changes is disturbed, aberrant brain development and maintenance can result in myriad neurological, cognitive and sensory deficits that can severely impact quality of life. The neural stem cell niche in the subventricular zone (SVZ) of the lateral ventricles is of particular importance in brain development due to its role in populating the cerebral cortex and olfactory bulbs (OB) with neurons (Lois et al. 1993; Davis et al. 1994). Interestingly, it is hypothesized that the expansion of the SVZ and its neural stem and progenitor cell pools accounts for the markedly more complex and neuron-rich cerebral cortex observed in humans compared to other animals (Kriegstein et al. 2006). Throughout brain development and maturation, the SVZ plays a number of different neurogenic roles that change in an age-dependent manner and continues to be proliferative into adulthood (Doetsch et al. 1999).

SVZ neural stem cell function during corticogenesis

The mammalian forebrain is created from the closing of the neural tube which traps presumptive cerebrospinal fluid in spaces called the lateral ventricles

(Kriegstein et al. 2006). Neuroepithelial cells, resembling radial glia with a single basal fiber contacting the pia, line the ventricles and begin to express neural stem cell markers such as *Nestin* and *Sox2* (Rakic 1978; Choi 1988; Ferri et al. 2004; Gotz et al. 2005). These neural stem cells form a layer of proliferative cells which will populate the cortex with neurons through a series of symmetric and asymmetric cell divisions termed corticogenesis (Noctor et al. 2001).

In the mouse brain, corticogenesis begins at embryonic day 10 and transitions away from cortical neurogenesis by embryonic day 16 (Wichterle et al. 2001). In the early phases of corticogenesis, neural stem cells in the ventricular zone undergo symmetric cell divisions by vertical cleavage in order to expand the stem cell pool (Fig. 1.1A) (Smart 1973; Chenn et al. 1995). Following this clonal expansion, neural stem cells begin to divide in both symmetric and asymmetric patterns (Noctor et al. 2004; Shitamukai et al. 2011). Symmetric divisions continue to produce two neural stem cells, while asymmetric divisions by horizontal cleavage produce a neural stem cell and a transit amplifying progenitor cell (Noctor et al. 2008). Most neural progenitor cells express *Ascl1*, *Pax6* and *Tbr2* while rapidly dividing to exponentially amplify the pool of progenitor cells, thereby creating a new layer of cells in the presumptive cortex called the subventricular zone (Fig. 1.2) (Parras et al. 2004; Kim et al. 2007; Brill et al. 2009). Progenitor cells in the SVZ also divide asymmetrically to produce a progenitor cell and a *Neurod1*, *Dcx* and *Tbr1*-expressing neuroblast, which migrates radially, matures and integrates to form the layers of the cortex (Brill et al. 2009; Roybon et al. 2009). Interestingly, there are distinct SVZ progenitor

zones surrounding the ventricles that produce a wide variety of neurons depending on spatial location. Progenitor cells produce different types of neurons depending on their expression of various pro-neural and pro-glial genes including: *Ngn2*, *Ascl1*, *Pax6*, *Emx1*, *Gsh2*, *Nkx2.1*, *Dlx1* and *Olig2* (Fig. 1.2) (Anderson et al. 1999; Sussel et al. 1999; Cecchi et al. 2000; Stoykova et al. 2000; Hevner et al. 2001; Stuhmer et al. 2002). For example, neurons created in the lateral ganglionic eminence (LGE) along the lateral wall of the lateral ventricles preferentially express *Gsh2* and *Pax6* and create both dopaminergic tyrosine hydroxylase+ and GABAergic calbindin+ neurons (Marin et al. 2001). In contrast, progenitor cells in the medial ganglionic eminence (MGE), a region ventromedial to the LGE, preferentially expresses *Nkx2.1* and produce only GABAergic calbindin+ and calretinin+ neurons (Marin et al. 2001).

SVZ neural stem cell function during olfactory bulb neurogenesis

As corticogenesis wanes around embryonic day 15 in mice, the SVZ begins to thin and the lateral ventricles reduce in volume, while keeping the neurogenic stem cell niches of the LGE and MGE intact along the dorsoventral axis of the ventricle (Fig. 1.1B) (Wichterle et al. 2001). The SVZ stops producing radially migratory neurons for the cortex and begins to create neurons that move along the rostral migratory stream (RMS), a bundle of neuroblasts and immature neurons ensheathed in blood vessels and supporting glia, that tangentially migrate into the olfactory bulb (Fig. 1.1D) (Lois et al. 1996; Lledo et al. 2008). As the neuroblasts begin to arrive in the OB, they transition into immature olfactory

bulb interneurons, radially migrate to the granule cell and glomerular layers of the OB, and begin to express markers of mature dopaminergic and GABAergic OB interneurons such as tyrosine hydroxylase, calbindin and calretinin (Kosaka et al. 1995; Belluzzi et al. 2003; Carleton et al. 2003). The olfactory bulb is responsible for processing sensory inputs from olfactory sensory neurons in the nasal epithelium (Lledo et al. 2005). Hypoplasia or aplasia of the olfactory bulbs results in a condition called arrhinencephaly, which can impair the sense of smell and lead to hyposmia or anosmia. Additionally, the late embryonic and postnatal SVZ produces GLAST+, O4+ and PDGFR-α+ oligodendrocyte progenitor cells which migrate into the overlying white matter and striatum and differentiate into mature GFAP+ glia (Alvarez-Buylla et al. 2001). This progression of intricate cell divisions and differentiation events from neural stem cell to mature neuron is vital for the proper formation of the mammalian cortex.

The process of OB neurogenesis in the SVZ is not unique to the late embryonic and early postnatal time points; rather, this process continues throughout adulthood (Fig. 1.1C) (Alvarez-Buylla et al. 2004). Adult-born OB interneurons are vital for the creation of olfactory memory and odor discrimination (Wachowiak et al. 2006). Interestingly, the precise molecular programs which govern SVZ neurogenesis, as discussed above, are largely unchanged from corticogenesis to adult olfactory bulb neurogenesis (Alvarez-Buylla et al. 2001; Lledo et al. 2006; Lledo et al. 2008; Hsieh 2012). Consistent with the former identity of the embryonic LGE and MGE, different classes of olfactory bulb interneurons are born from different regions along the dorsoventral axis of the

late embryonic and postnatal SVZ, and migrate tangentially along the RMS into the OB instead of radially into the cortex (Merkle et al. 2007; Young et al. 2007). Two major factors play a role in the precise regulation of SVZ neurogenesis throughout development and maintenance: extracellular morphogens and epigenetic modifiers. These will be discussed separately in the following sections.

Signaling pathways in SVZ neurogenesis

Wnt signaling

The Wnt signaling pathway has been demonstrated to regulate a variety of stem cell populations including those in the skin, blood, muscle and intestinal endothelium, and to promote maintenance of pluripotency in embryonic stem cells (Ciani et al. 2005). In the embryonic forebrain, Wnt serves to promote a cortical identity for the dorsal telencephalon (Wilson et al. 2000; Backman et al. 2005). Beginning at E11 in the SVZ, Wnts are responsible for maintaining an actively proliferating stem cell pool that will populate the cortex with neurons (Chenn et al. 2002; Sato et al. 2004; Hirabayashi et al. 2005). During mid to late corticogenesis, Wnt signaling through β-catenin stimulates the expression of *Neurod1*, *Ngn1* and *Ngn2*, thereby promoting neuronal differentiation (Hirabayashi et al. 2004). Midway through corticogenesis at approximately embryonic day 13, Wnt signaling switches from promoting stem cell self-renewal and proliferation to stimulating neuronal differentiation; this switch is positively influenced by the presence of fibroblast growth factor 2 (FGF2) (Israsena et al.

2004). This interaction between Wnt and growth factor signaling demonstrates the intricacy of the spatiotemporal regulation of the developing and adult brain.

Growth Factor signaling

In the SVZ, several families of growth factors play important roles in the maintenance of neural stem cell identity through activation of receptor tyrosine kinases and downstream MAP kinase activity (Mason 2007). Intraventricular infusion of FGF2 or epidermal growth factor (EGF) has shown that these growth factors are required for maintenance of the stem cell state by promoting neural stem cell self-renewal and proliferation while inhibiting the formation of neural progenitor cells and neuroblasts (Kuhn et al. 1997; Jin et al. 2003; Marshall et al. 2003; Guillemot et al. 2011). Additionally, EGF has been shown to promote neural stem cells to exclusively produce oligodendrocyte precursors at the expense of neural progenitor cells in the SVZ (Burrows et al. 1997; Morrow et al. 2001). Neurosphere assays, a test for the self-renewal, proliferation and differentiation capacity of neural stem cell populations, use a combination of FGF and EGF in the growth medium to maintain neurospheres in a self-renewing state (Reynolds et al. 1992; Pastrana et al. 2011). The growth factor cocktail is removed from the medium to promote differentiation of neurosphere cells into neurons, glia and oligodendrocytes, thus demonstrating the ability of FGF and EGF to maintain the neural stem cell population (Pastrana et al. 2011).

Similar to EGF, platelet derived growth factor (PDGF) and its associated receptor PDGFRα promote the oligodendrocytic fate of SVZ neural stem cells

and neurosphere self-renewal *in vitro* (Williams et al. 1997; Calver et al. 1998). In adult mouse SVZ, reduced PDGF signaling results in decreased stem cell self-renewal, increased apoptosis and hydrocephalus (Carter et al. 2012). Interestingly, vascular endothelial growth factor (VEGF) stimulates the development of and maintains the vasculature that is necessary for the SVZ and RMS to receive signaling molecules and metabolites (Bovetti et al. 2007; Bozoyan et al. 2012). These various growth factor families are required for the proper development and function of the SVZ neural stem cell niche beginning during corticogenesis and continuing throughout life.

Hedgehog signaling

The hedgehog signaling pathway functions through the binding of a soluble hedgehog ligand to a heterodimeric receptor consisting of the inhibitory Patched subunit and the downstream activator subunit Smoothened (Ruiz i Altaba et al. 2002; Fuccillo et al. 2006). Upon hedgehog ligand binding, Patched releases Smoothened and Smoothened activates the Gli affector proteins which promote gene expression (Ruiz i Altaba et al. 2002; Fuccillo et al. 2006). Generally, hedgehog signaling gradients oppose Wnt signaling gradients, thereby creating ventral and dorsal boundaries (Kessaris et al. 2001). Throughout life, hedgehog signaling is necessary for proper maintenance of the SVZ neural stem cell niche and preserves the dorsoventral patterning of the SVZ to produce various types of olfactory bulb interneurons (Lledo et al. 2008; Ihrie et al. 2011). Mice with conditional loss of hedgehog signaling in SVZ neural stem

cells leads to a significant reduction in calbindin+ OB interneurons, demonstrating the requirement for hedgehog signaling in the ventral SVZ (Ihrie et al. 2011).

Retinoic Acid signaling

Retinoic acid signaling is a highly complex process that begins by translocation of retinol into the cytoplasm where it is processed by retinol dehydrogenase to produce retinaldehyde (Fig. 1.3) (Maden 2002; Maden 2007; Niederreither et al. 2008). Retinaldehyde is further processed to the final form of retinoic acid (RA) by retinaldehyde dehydrogenases (Maden 2002; Maden 2007; Niederreither et al. 2008). From this point, RA can function in an autocrine manner, by binding cellular retinoic acid binding proteins (CRABP) and translocating to the nucleus of the cell, or RA can freely diffuse out of the cell and enter an adjacent cell in a paracrine manner before binding CRABP and translocating into the nucleus (Maden 2007). In both cases, RA binds a heterodimer of a single retinoic acid receptor (RAR) and a single retinoid X receptor (RXR) which are bound to consensus retinoic acid response elements (RARE) (Niederreither et al. 2008). Upon activation of the heterodimer by RA binding, target gene expression is activated (Niederreither et al. 2008).

During brain development, RA signaling plays an intermediate role by interacting with both ventral hedgehog signaling and dorsal Wnt signaling (Rhinn et al. 2012). In contrast to growth factor signaling, which generally regulates maintenance of neural stem cells and their differentiation into oligodendrocyte

progenitor cells, RA signaling functions to induce neurogenesis by upregulation of pro-neural genes (Thompson Haskell et al. 2002). RA signaling is particularly important for the differentiation of GABAergic interneurons of the cortex and olfactory bulbs (Anchan et al. 1997). Neurosphere assays have confirmed RA function *in vitro* by demonstrating an increase in proliferation and neuronal differentiation upon treatment with RA, while reduced RA signaling produces the opposite effect (Haskell et al. 2005; Wang et al. 2005). In conjunction with Wnt, growth factor and hedgehog signaling, retinoic acid is necessary for the proper timing of SVZ neural stem cell development and the cell fate and maturation of its pro-neuronal progeny.

Epigenetic regulation of SVZ neurogenesis

Epigenetics is a broad term encompassing any mechanism by which gene expression can be altered without a change in genomic DNA sequence. Epigenetic regulation occurs by a variety of mechanisms including: DNA methylation, regulatory non-coding RNA, covalent histone modifications and ATP-dependent chromatin remodeling. This section will review the roles of histone modifications and ATP-dependent chromatin remodeling in determination of cell fate and differentiation decisions within stem cells and their progeny, focusing on neural stem cells.

Histone modifying enzymes

Promoter and enhancer elements of pro-neural genes can be maintained in one of three states: inactive, poised and active (Fig. 1.4). Inactive genetic elements display histone modifications that are indicative of repressed chromatin including H3K27me3, the defining modification of the Polycomb Repressive Complex, and H3K9me3 (Simon et al. 2009). Active genetic elements favor histone modifications such as mono-, di- and trimethylation H3K4, marks placed by the Trithorax group member MLL1, and a variety of acetylation events including H3K27ac (Azuara et al. 2006). Polycomb group member *Bmi-1* also plays an integral role in SVZ neural stem cell self-renewal and proliferation (Molofsky et al. 2003). When *Bmi-1* is deleted in mice, there is a drastic reduction in neurons due to the reduced size of the neural stem cell pool causing a number of brain abnormalities (Molofsky et al. 2005). Thus, the genome of neural stem cells is tightly regulated by specific histone modifications that can promote or repress gene expression necessary for proper stem cell function.

While it is quite common for genes to be completely active or inactive in fully differentiated cells, the chromatin environment in stem and progenitor cells tends to be more open (euchromatic) and poised for either repression or activation (Azuara et al. 2006; Bernstein et al. 2006). Poised enhancers and promoters typically display both active and repressive marks (Zhou et al. 2011). For example, a poised enhancer element might contain the activating H3K4me1 mark and the repressive H3K9me3 mark, while a poised promoter would contain the activating H3K4me3 modification and the repressive H3K27me3 mark. In the

SVZ, the pro-neural genes *Ascl1* and *Dlx2*, whose expression is indicative of neural differentiation, have high levels of the activating mark H3K4me3 (Lim et al. 2009). In mice, loss of the Trithorax group H3K4 methyltransferase *Mll1* in the SVZ does not affect neural stem cell survival, proliferation or gliogenic differentiation, but severely inhibits neuronal differentiation (Lim et al. 2009). In the wild type mouse SVZ, MLL1 binds to the promoters of *Ascl1* and *Dlx2*, co-localizes with H3K4me3 and stimulates their expression. In *Mll1* null mice, the *Dlx2* promoter switches from an active to a poised status by maintaining the H3K4me3 mark, and gaining the repressive H3K27me3 modification. These epigenetic modifications and reduction in *Dlx2* expression are an example of how chromatin states strongly influence gene expression in developing neural stem cells of the SVZ.

ATP-dependent chromatin remodeling enzymes

Chromatin remodeling enzymes read the histone modifications through specialized protein domains and influence gene expression by disrupting DNA-histone interactions, sliding nucleosomes along the DNA strand to make room for transcription factors, or translocating the nucleosome core particle to another DNA strand (Smith et al. 2005). There are three major superfamilies of ATP-dependent chromatin remodeling enzymes in eukaryotic organisms (SWI/SNF, ISWI and CHD), each of which has a characteristic histone interaction domain (de la Serna et al. 2006). Here, I will discuss the Chromodomain Helicase DNA-

binding (CHD) superfamily of chromatin remodelers focusing on CHD7, the only family member that has a human syndrome associated with its dysfunction.

Structure and function of the CHD superfamily

The CHD family of ATP-dependent chromatin remodeling enzymes consists of nine proteins divided into three subfamilies based on domain homology (Fig. 1.5). All CHD proteins contain two common domains, two tandem chromodomains and a SNF2-like helicase-ATPase (Hall et al. 2007; Layman et al. 2010). Chromodomains were originally characterized in *Drosophila* heterochromatin protein 1 (HP1) which uses its chromodomain to bind nucleosomes and contribute to promotion of closed chromatin states (heterochromatin) at homeotic genes associated with *Drosophila* development (Pearce et al. 1992; Wreggett et al. 1994; Ball et al. 1997). The primary function of chromodomains is to facilitate protein-protein interactions with methylated histone residues as illustrated by the binding affinity of HP1 to the repressive histone modification H3K9me3 leading to formation of heterochromatin (Ball et al. 1997; Brehm et al. 1999; Pray-Grant et al. 2005). Conversely, CHD proteins contain a unique variant of the chromodomain which contains a methyl-binding cage which facilitates interactions with H3K4 (Flanagan et al. 2005; Pray-Grant et al. 2005). While there exists a contrast in chromodomain function dependent on the protein family, these methyl-histone binding protein domains are essential for maintaining the dynamic structure of chromatin necessary for proper gene expression.

The helicase-ATPase domains of CHD proteins are highly similar to those observed in the SWI/SNF superfamily of ATP-dependent chromatin remodeling enzymes (Hirschhorn et al. 1992; Hall et al. 2007). Originally discovered in the SWI2/SNF2 protein, the helicase-ATPase domain functions as a bi-lobed motor by providing the chemical energy to cause mechanical disruption of DNA-histone contacts leading to core histone sliding down a DNA template or core histone evacuation and deposition on another DNA strand (Winston et al. 1992; Peterson et al. 1994; Pazin et al. 1997; Becker et al. 2002).

Additionally, the CHD subfamilies are delineated by the presence of subfamily-specific protein domains. CHD1 and CHD2 contain DNA-binding domains, which have been shown to be similar in function to SANT domains present in CHD6-9 (Ryan et al. 2011). The SANT domain confers non-specific DNA binding, particularly to linker DNA between nucleosomes (Aasland et al. 1996; Schuster et al. 2002; Boyer et al. 2004). In recombinant CHD1 with deletion of the SANT domain, CHD1 loses the ability to bind both DNA and nucleosomes demonstrating that the SANT domain is critical for nucleosomal targeting by the chromatin remodeler (Ryan et al. 2011). CHD3 and CHD4 lack a DNA-binding domain, but contain tandem plant homeo domains (PHD) (Bienz 2006). PHD domains are zinc finger motifs that facilitate interactions with methylated histone residues and protein co-factors including between CHD3/4 and histone deacetylase 1 (HDAC1) which is part of the potent negative transcriptional regulation complex called NuRD (nucleosome-remodeling deactylase complex) (Xue et al. 1998). CHD7-9 also contain tandem BRK

domains that interact with *Drosophila* Brahma and BRG1, but currently have no known function (Daubresse et al. 1999). Regardless of overall protein domain structure, the function of CHD superfamily proteins is intimately tied to regulation of gene expression through modulation of nucleosomes. One of the emerging trends consistent across the entire CHD family is the role of CHD proteins in the maintenance of stem cell populations and directing the cell fate decisions of their progeny.

CHD family members and their functions in stem cells

CHD proteins and embryonic stem cells

Embryonic stem cells are a self-renewing and pluripotent cell population from which the majority of tissues are derived. These cells are viewed as a blank slate with an open chromatin environment, and progressively become more differentiated by activating or repressing various genetic pathways to become neural, hematopoietic and other lineage-specific cells. CHD1 has been shown to regulate the function of embryonic stem cells by maintaining open chromatin (Gaspar-Maia et al. 2009). CHD1 specifically binds to tracts of the active gene marker tri-methylated histone H3 at the residue lysine 4 (H3K4me3) and excludes the repressive marker H3K27me3 (Gaspar-Maia et al. 2009). Furthermore, the Mediator complex, a multi-protein complex responsible for pre-initiation of gene transcription, binds to CHD1 and recruits it to actively expressed genes (Lin et al. 2011). When CHD1 is deleted in embryonic stem cells, chromatin condenses to form heterochromatin and pluripotent differentiation is

impaired, potentially, due to the promotion of ectodermal lineage gene expression at the expense of endodermal lineage gene expression (Gaspar-Maia et al. 2009). Additionally, induction of *CHD1* expression is required for efficient reprograming of mature fibroblasts into induced pluripotent stem cells (iPS) (Gaspar-Maia et al. 2009). These studies show that CHD family proteins are vital for maintaining pluripotency in embryonic stem cells and may play an important role in the development of personalized medicine through iPS cell therapies.

CHD proteins and mesenchymal stem cells

Mesenchymal stem cells are multipotent mesoderm-derived cells that give rise to myoblasts (muscle), adipocytes (fat), osteoblasts (bone) and chondrocytes (cartilage) (Ralston et al. 2006; Chamberlain et al. 2007; Uccelli et al. 2008). The differentiation of mesenchymal stem cells into four distinct lineages has been shown to be regulated by several CHD family proteins. Induction of myogenic cell fates has been shown to require the recruitment of a chromatin destabilizing histone variant histone H3.3 by CHD2 to muscle differentiation genes, which facilitates binding and gene activation by the transcription factor MyoD (Harada et al. 2012). Additionally, CHD9, also known as chromatin-related mesenchymal modulator (CReMM), binds to and promotes the expression of osteocalcin (*Bglap3*), one of the major genes responsible for promoting bone development (Shur et al. 2005; Shur et al. 2006). These findings emphasize the diverse and potentially non-redundant functions of CHD family proteins in mesenchymal cell fate decisions, even within the same stem cell type.

CHD proteins and hematopoietic stem cells

The vast diversity of myeloid and lymphoid cell types present in blood are derived from a common hematopoietic stem cells (Kondo et al. 2003; Ugarte et al. 2013). Hematopoietic stem cells reside largely in the bone marrow and can adopt one of two potential lineages: myeloid and lymphoid (Kondo et al. 2003). Myeloid lineage cells give rise to red blood cells, platelet-producing megakaryocytes and granulocyte immune cells (Bovetti et al. 2007). Lymphoid lineage cells give rise to natural killer, T- and B-cells which play important roles in cellular immunity (Bovetti et al. 2007). CHD4, also known as Mi-2β, is a Nucleosome Remodeling Deacetylase complex (NuRD) component that has been shown to regulate the self-renewal of hematopoietic stem cells (Yoshida et al. 2008). Additionally, loss of *Chd4* in bone marrow leads to an abundance of erythroid progenitors and red blood cells and loss of the lymphoid and remaining myeloid lineage cell types (Yoshida et al. 2008). Further examination of CHD4 activity in the regulation of hematopoietic stem cells may provide novel insights into mechanisms of human diseases such as cancers affecting lymphoid lineage cells including leukemia and lymphoma.

CHD proteins and neural stem cells

Neural stem cells play a vital role in the development and maintenance of the central nervous system and in sensory organs by producing neurons and supporting cells such as glia and oligodendrocytes. CHD4 and CHD5 have been demonstrated to play important roles in the function and differentiation of neural

stem cell niches in the subventricular zone of the forebrain and dentate gyrus of the hippocampus through cooperation with major epigenetic modifiers, transcription factors and signaling pathways. During cortical neurogenesis, CHD4 is expressed in murine SVZ neural progenitor cells and interacts with the Polycomb Repressive Complex 2 (PRC2), specifically with the H3K27 methyltransferase enzyme Ezh2 (Cao et al. 2002; Sparmann et al. 2013). The CHD4/PRC2 complex directly binds to the promoter of the Glial Fibrillar Acidic Protein gene (*Gfap*), represses its expression and prevents glial differentiation (Sparmann et al. 2013). Through inhibition of the *Gfap* locus, CHD4 and PRC2 promote neuronal differentiation during the neurogenic period between E11-E18 in mice (Sparmann et al. 2013).

Similar to CHD4, CHD5 also interacts with the PRC2 complex and specifically associates with the repressive histone modification H3K27me3 in neural stem cells (Egan et al. 2013). CHD5 is highly expressed in neural progenitor and neuroblast cells of the SVZ and subgranular zone (SGZ) of the hippocampus, which produces neurons that are important for learning and memory (Egan et al. 2013). Reduced *Chd5* expression in the developing cortex leads to a significant loss of migratory neuroblasts. Additionally, microarray and gene ontology analysis of *Chd5*-deficient neural stem cells showed downregulation of genes responsible for neuronal migration and maturation (Egan et al. 2013). Taken together, these studies demonstrate that CHD4 and CHD5 play an important role in the inhibition of glial differentiation during key neurogenic phases of mammalian brain development.

CHD7 and stem cells

Chd7 has been implicated in several stem cell populations and appears to be critical for regulating cell fate decisions through modulation of signaling and epigenetic pathways. *Chd7* is highly expressed in embryonic stem cells, where it appears to function similar to CHD1 by associating with signals of active gene expression and open chromatin at enhancer elements of critical stem cell pluripotency genes including *Sox2*, *Oct4* and *Nanog* (Zentner et al. 2011). CHD7 preferentially binds active (H3K4me1+, H3K27ac+) and poised (H3K4me1+, H3K27me3+) enhancer elements at ectodermal lineage genes in embryonic stem cells (Zentner et al. 2011). This finding is particularly intriguing due to the contribution of ectodermal lineages to tissues affected in CHARGE syndrome including the brain, retina and neural crest-derived structures in the heart and craniofacial structures. Similar to MLL1, co-localization of CHD7 with poised genetic elements presents a paradigm where CHD7 may play a role in recruitment of transcription factor, histone modifier and/or chromatin remodeling complexes in a cell type-specific manner to promote the activation or repression of certain classes of genes by resolution of the poised status.

Studies in mesenchymal stem cells have shown that CHD7 is critical for Wnt-mediated repression of PPAR-γ through recruitment of a complex containing CHD7, NLK and SETDB1 (an H3K9 methyltransferase), thus leading to an osteoblast fate (Takada et al. 2007). Notably, upon reduction of CHD7, PPAR-γ is free to perform its function as a potent activator of adipocyte lineage genes, demonstrating a clear role for CHD7 in cell fate decisions (Takada et al. 2007).

In neural stem cells, co-immunoprecipitation and chromatin immunoprecipitation studies have shown that CHD7 physically interacts with SOX2 at genes that are associated with human diseases including Alagille syndrome (*JAG1*, a Notch signaling ligand), Feingold syndrome (*MYCN*, a bHLH transcription factor) and Pallister-Hall syndrome (*GLI3*, a mediator of Sonic hedgehog signaling) (Engelen et al. 2011). Many phenotypes that are present in these syndromes are also seen in CHARGE including genital abnormalities (Pallister-Hall and *SOX2* deficiency), tracheoesophageal defects (Alagille, Feingold and *SOX2* deficiency), pituitary defects (Pallister-Hall and *SOX2* deficiency) and semicircular canal hypoplasia (Alagille) (Fig. 1.6). These observations demonstrate that CHD7 activity is important for a variety of stem cell differentiation and cell fate decisions.

Recently, CHD7 was shown to be expressed in the subgranular zone (SGZ) of the hippocampus and the SVZ of adult mice where it co-localizes with markers of neural stem cells (GFAP), neural progenitor cells (Ascl1) and neuroblasts (DCX) (Feng et al. 2013). Longitudinal studies in temporally induced conditional knockout of *Chd7* in adult SVZ neural stem cells show that *Chd7*-deficiency leads to a reduction in mature dopaminergic and GABAergic olfactory bulb interneurons and reduced expression of pro-neural genes *Sox4* and *Sox11* (Feng et al. 2013). In the SGZ of the hippocampus, conditional knockout of *Chd7* also leads to a reduction in neurogenesis, which can be rescued through exercise (Feng et al. 2013). These data provide additional evidence that CHD7 is critical for stem cell function in a variety of tissues.

CHD7 and CHARGE syndrome

CHARGE syndrome, a multiple congenital anomaly disorder that occurs in approximately 1 in 10,000 births, is characterized by Coloboma of the eye, Heart defects, Atresia of the choanae, Retardation of growth and development, Genital and Ear abnormalities (Pagon et al. 1981; Issekutz et al. 2005). Heterozygous mutations in *CHD7* are present in over 90% of individuals with CHARGE syndrome (Vissers et al. 2004; Bergman et al. 2011; Janssen et al. 2012). Despite identification of *CHD7* mutations as the etiology of most CHARGE cases, there are no definitive genotype/phenotype correlations, likely due to the tremendous diversity of *CHD7* nonsense, missense, deletion and truncation mutations and the variable expressivity of CHARGE features (Janssen et al. 2012). Biochemical assays with recombinant CHD7 protein have determined that CHD7 is an ATP-dependent chromatin remodeling enzyme capable of modulating DNA-histone interactions (Bouazoune et al. 2012). Interestingly, when point mutations observed in CHARGE individuals are introduced into recombinant CHD7, its enzymatic activity is reduced in a mutation-specific manner (Bouazoune et al. 2012).

CHD7 haploinsufficiency causes dysfunction in sensory processes leading to impaired hearing, vision, balance, and olfaction in CHARGE individuals. In order to more fully understand the role of *CHD7* in development and its impact on sensory processes, mouse models have been created. A *Chd7* gene trap null allele was generated in our lab through insertion of the *lacZ* reporter into the *Chd7* allele, creating a functionally null allele with β-galactosidase reporter

activity (Hurd et al. 2007). Interestingly, *Chd7* null embryos do not survive past embryonic day 10.5, presumably from cardiovascular defects, while *Chd7* heterozygous mice display many of the same defects observed in CHARGE (Hurd et al. 2007).

Chd7 is widely expressed in the embryonic mouse, most notably in tissues affected in CHARGE syndrome including the heart, inner ear, eye, olfactory epithelium and brain (Hurd et al. 2007; Layman et al. 2010). In each organ thus far analyzed, *Chd7* expression has been predictive of tissue or cellular defects in mutant mice. In the inner ear, *Chd7* heterozygous mice display hypoplasia or aplasia of the lateral and posterior semicircular canals and innervation defects of the vestibular sensory epithelium (Adams et al. 2007; Hurd et al. 2010). Conditional knockout of *Chd7* using a floxed *Chd7* allele causes complete aplasia of vestibular and cochlear structures, reductions in FGF signaling leading to decreased proliferation and reduced expression of pro-neural genes such as *Ngn1* and *Neurod1* (Hurd et al. 2010). These data imply that CHD7 may function in brain neural stem cells as it does sensory tissues, through regulation of similar signaling pathways and activation of pro-neural gene expression.

Hyposmia and anosmia, reduction or loss of the sense of smell, are two of the most highly penetrant phenotypes observed in CHARGE individuals. Olfactory deficits are commonly accompanied by hypoplasia or aplasia of the olfactory bulbs in the brain (Pinto et al. 2005; Layman et al. 2009; Bergman et al. 2011; Legendre et al. 2012). *Chd7* heterozygous mice display complete

anosmia, lack of odor discrimination, and olfactory bulb hypoplasia (Layman et al. 2009). *Chd7* is expressed in olfactory epithelium neural stem and progenitor cells as demonstrated by co-localization with Sox2, Ascl1 and Neurod1 (Layman et al. 2009). Loss of *Chd7* correlates with a marked decrease in olfactory epithelium proliferation, a subsequent loss of innervation, and an inability to recover from damage (Layman et al. 2009). Interestingly, *Chd7* heterozygous mice show decreased dopaminergic tyrosine hydroxylase+ interneurons in the olfactory bulb, which could be due to lack of efferent signals from the olfactory epithelium or a defect in neurogenesis from the SVZ neural stem cell niche (Layman et al. 2009).

Novel insights into CHD7 regulation of SVZ neural stem cells

Neural stem cells play a vital role in the development and maintenance of the central nervous system and in sensory organs by producing neurons and supporting cells such as glia and oligodendrocytes. Dysregulation of the transcriptional programs of neural stem cells and their progeny (neurons, glia and oligodendrocytes) can cause neurological disease and, in the case of *CHD7* haploinsufficiency, lead to the severe defects in multiple neural-derived tissues observed in CHARGE syndrome. Thus, understanding the molecular and regulatory mechanisms of CHD7 function in neural stem cells is of vital importance to developing diagnostic and therapeutic techniques, and may improve the quality of life for CHARGE individuals. In this dissertation, I have focused my analysis on the function of *Chd7* in the olfactory bulb and SVZ neural

stem cell population in the embryonic, early postnatal and adult mouse in order to identify mechanisms that may help explain some of the neurological defects that are hallmarks of CHARGE syndrome.

In Chapter 2, I thoroughly analyzed the function of CHD7 in the adult and perinatal SVZ. In adult mice, I found that loss of *Chd7* led to fewer olfactory bulb interneurons, impaired neural stem cell function and a potential switch from a neuronal fate to a glial fate of migrating neuroblasts. *Chd7*-deficiency in perinatal mice caused defects neural stem cell self-renewal, proliferation and neuronal differentiation which could be rescued with modulation of retinoic acid signaling. These studies suggest that *Chd7* plays an important role in SVZ neural stem cell function throughout life and loss of *Chd7* in the SVZ partially contributes to olfactory bulb and olfaction deficits.

In Chapter 3, I performed genome-wide analysis of the SVZ in *Chd7*-deficient mice and further investigated the link between CHD7 and retinoic acid signaling. Upon loss of *Chd7*, microarray analysis of SVZ gene expression showed reduction in genes important for learning, memory, cognition, neuronal differentiation, migration and maturation. Interestingly, expression of genes encoding the retinoic acid receptors *Rarb* and *Rxrg* was down-regulated in the *Chd7*-deficient SVZ, consistent with data shown in Chapter 2. Using P19 embryonal carcinoma cells, I have shown that CHD7 directly binds retinoic acid receptors and knockdown of *Chd7* led to impaired P19 cell growth and pro-neural gene expression.

In Chapter 4, I investigated the role of CHD7 in the development of the mouse cerebral cortex. CHD7 co-localized with neural stem and progenitor cell markers in the SVZ during corticogenesis. Conditional knockout of *Chd7* in neural stem cells showed no impairment of proliferation, self-renewal or differentiation. These data imply that CHD7 is not required for proper neural stem cell function during corticogenesis, but leave the possibility for a role for CHD7 in neuroblasts migration and maturation. Taken together, I have demonstrated an important role for CHD7 function in the developing and adult mouse SVZ neural stem cell niche, which may provide insights into sensory phenotypes associated with CHARGE syndrome.

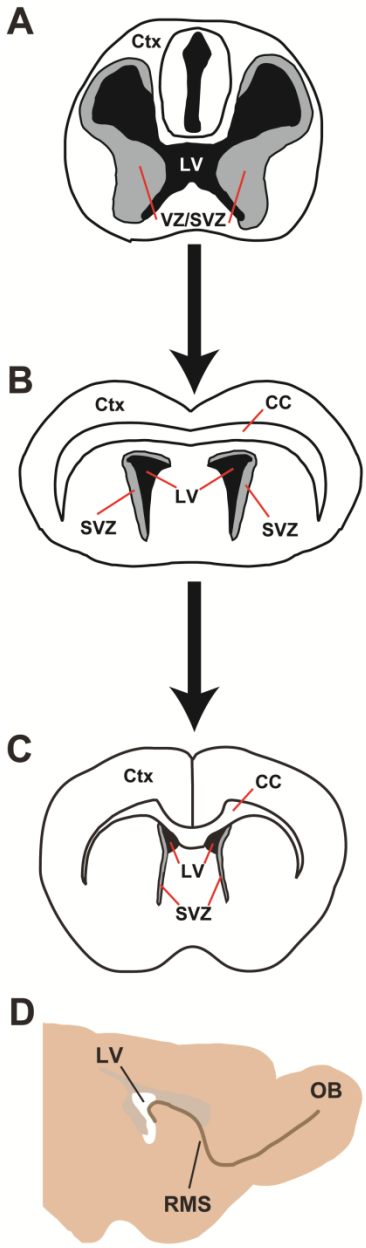

Figure 1.1: Morphogenesis of the mouse forebrain throughout development. (**A**) Schematic showing a coronal section of the forebrain at embryonic day 13.5 (E13.5) with neural stem and progenitor cells in the ventricular and subventricular zones (gray, VZ/SVZ) surrounding the lateral ventricles (black, LV), which produce neurons bound for the cortex (Ctx). (**B**) Schematic showing a coronal section of the forebrain at postnatal day 1 (P1) with a constricted SVZ that produces neurons bound for the olfactory bulb (OB). (**C**) Schematic showing a coronal section of the adult forebrain with an SVZ that is restricted to the lateral wall of the LV. (**D**) Schematic showing a sagittal section of the forebrain where neurons are born along the LV, migrate through the rostral migratory stream (RMS) and integrate into the OB. Other abbreviations: CC: corpus callosum.

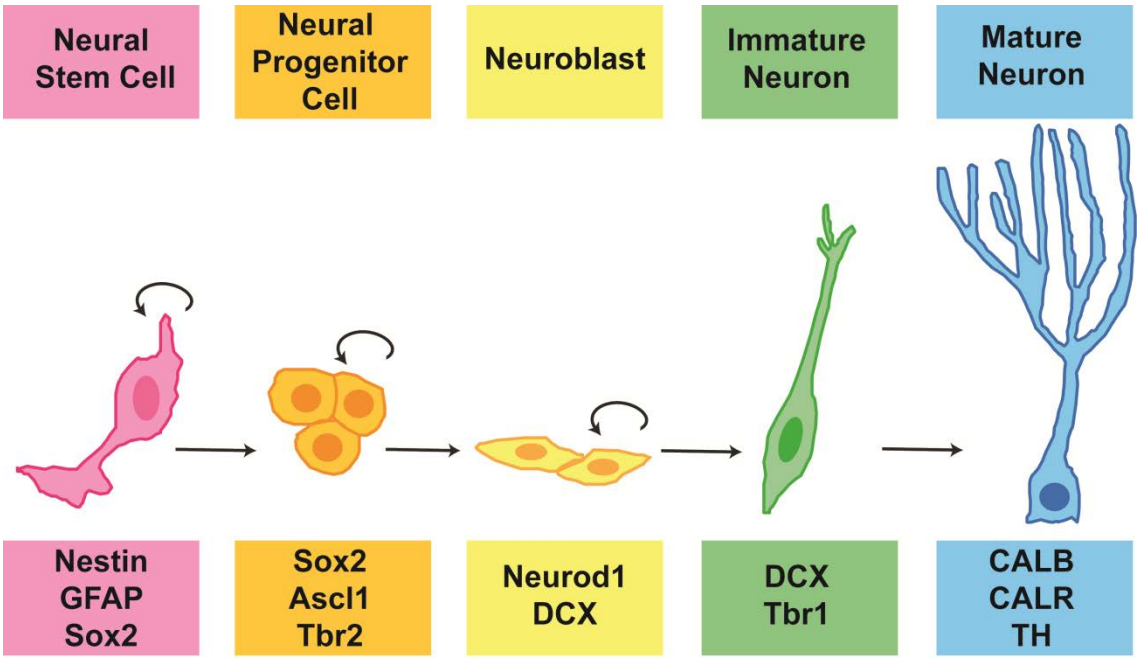

Figure 1.2: Lineage-specific markers of SVZ-derived cells.
Nestin, GFAP and Sox2 are present in SVZ neural stem cells, which can self-renew to make another stem cell or produce a neural progenitor cell. Neural progenitor cells continue to express Sox2, begin expression of pro-neural markers Ascl1 and Tbr2 and produce Neurod1- and DCX-expressing neuroblasts. As neuroblasts migrate through the RMS and into the OB, they begin to express Tbr1 in addition to DCX. Upon reaching the proper OB layer, neurons express GABAergic (CALB and CALR) or dopaminergic (TH) markers, then mature and integrate into the OB circuitry. Re-created from Hsieh et al. 2012. Genes Dev.

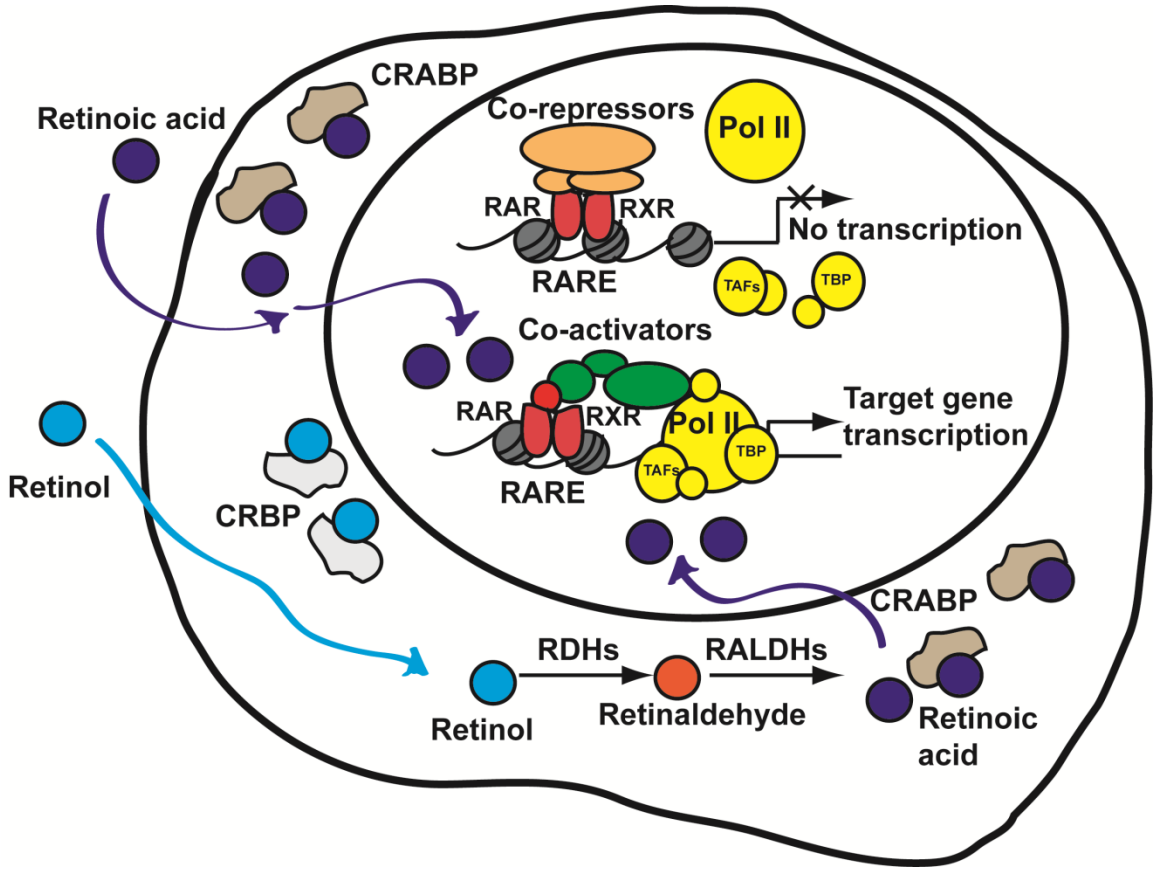

Figure 1.3: Transcriptional regulation by retinoic acid signaling.
Retinol traverses the cell membrane and is bound by cellular retinol binding protein (CRBP). Retinol dehydrogenases (RDH) metabolize retinol into retinaldehyde which is subsequently converted to retinoic acid (RA) by retinaldehyde dehydrogenases (RALDH). Cellular retinoic acid binding protein (CRABP) binds RA that has either freely diffused into the cell or produced intracellularly by RDH and RALDH from retinol and translocates RA into the nucleus. RA binds retinoic acid receptor and retinoid X receptor heterodimers (RAR/RXR) that are associated with retinoic acid response elements (RARE) at RA target genes. Upon RA binding, co-activators or co-repressors are recruited to the activated RAR/RXR complex which can recruit or block RNA polymerase II (Pol II), TATA binding protein (TBP) and TBP-associated factors (TAF). Re-created from Rhinn and Dollé. 2012. Development.

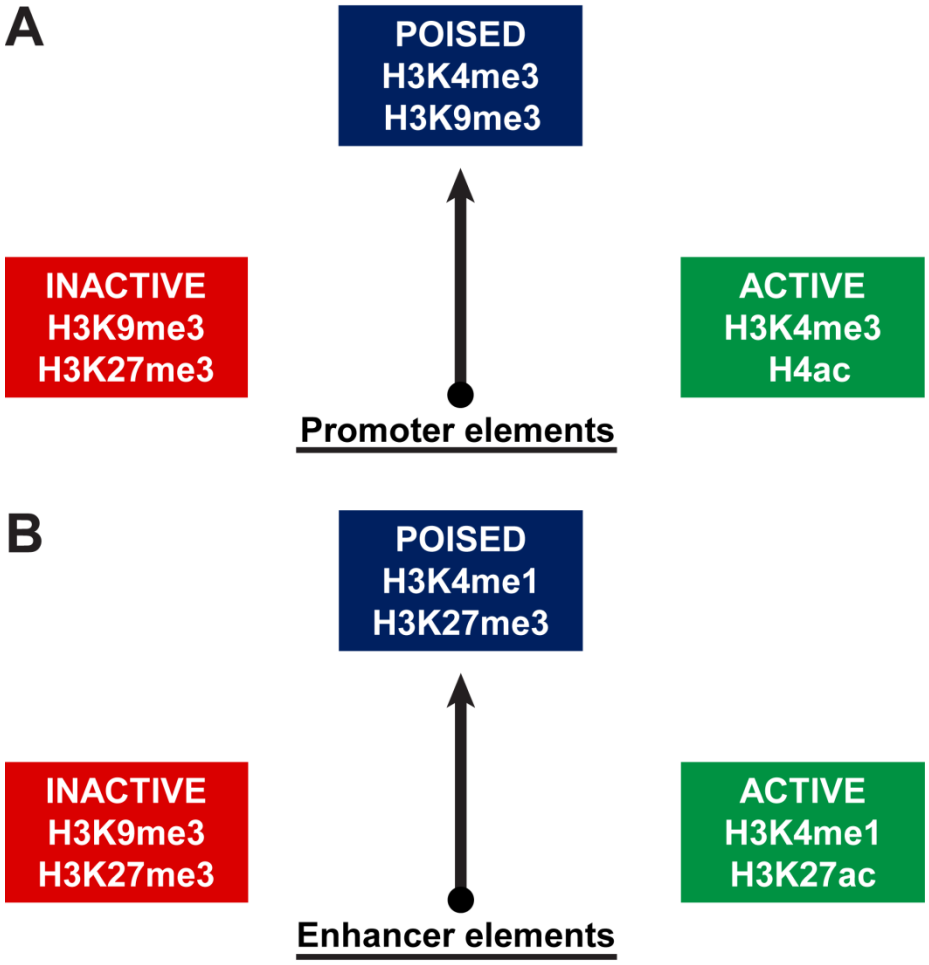

Figure 1.4: Distinct histone modifications mark the status of promoter and enhancer elements. (**A**) Promoter elements can possess three sets of chromatin modifications that denote active (H3K4me3 and acetylation of histone H4), poised (H3K4me3 and H3K9me3) or inactive genes (H3K9me3 and H3K27me3). (**B**) Similar to promoters, enhancer elements can also contain histone modification indicative of active (H3K4me1 and K3K27ac), poised (H3K4me1 and H3K27me3) or inactive genes (H3K9me3 and H3K27me3).

Figure 1.5: Domain schematic of CHD superfamily members.
The CHD superfamily is comprised of three subfamilies. CHD1 and CHD2 comprise subfamily I and contain tandem chromodomains (purple), an ATPase-helicase domain (blue) and a loosely-specific DNA-binding domain (orange). Subfamily II is composed of CHD3 and CHD4 which lack the DNA-binding domain of subfamily I, but contain tandem PHD zinc finger domains (yellow). While CHD5 is considered a member of subfamily II, it only contains tandem chromodomains and an ATPase-helicase domain with no known additional structural motifs. CHD6 through CHD9 comprise subfamily III and have characteristic SANT (red) and tandem BRK domains (green) in addition to tandem chromodomains and an ATPase-helicase domain.

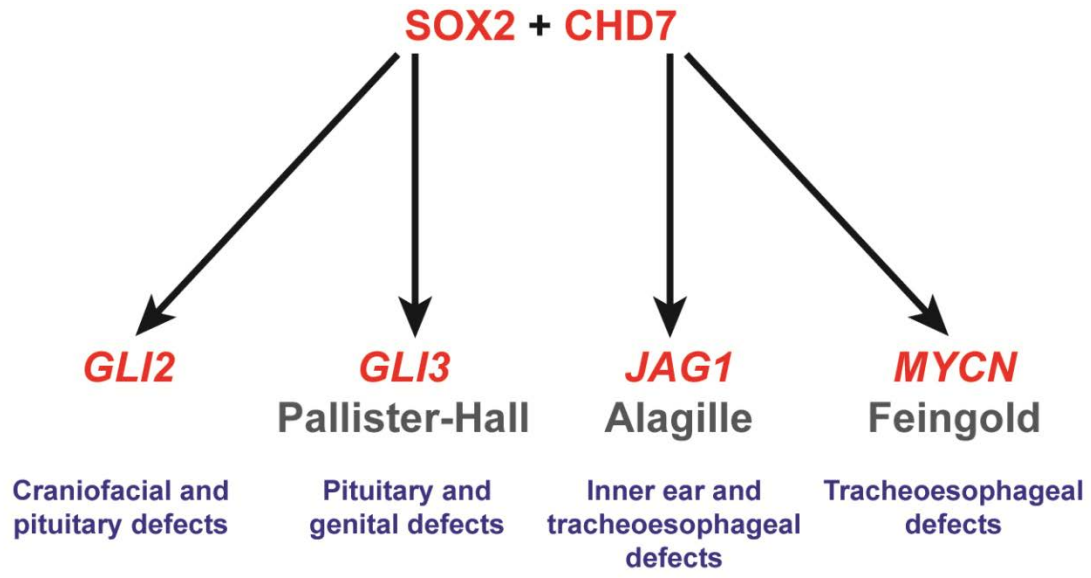

Figure 1.6: The SOX2/CHD7 complex regulates genes involved in human syndromes. SOX2 and CHD7 form a complex in neural stem cells and bind pro-neural genes including: sonic hedgehog signaling genes (*GLI2* and *GLI3*), a notch signaling gene (*JAG1*) and a basic helix-loop-helix transcription factor gene (*MYCN*). Genetic deficiency of *CHD7* results in CHARGE syndrome which shares phenotypes with human syndromes associated with *GLI2*-deficiency, Pallister-Hall syndrome (*GLI3*-deficiency), Alagille syndrome (*JAG1*-deficiency) and Feingold syndrome (*MYCN*-deficiency).

References

Aasland, R., A. F. Stewart and T. Gibson (1996). "The SANT domain: a putative DNA-binding domain in the SWI-SNF and ADA complexes, the transcriptional co-repressor N-CoR and TFIIIB." Trends Biochem Sci **21**(3): 87-88.

Adams, M. E., E. A. Hurd, L. A. Beyer, D. L. Swiderski, Y. Raphael and D. M. Martin (2007). "Defects in vestibular sensory epithelia and innervation in mice with loss of Chd7 function: implications for human CHARGE syndrome." J Comp Neurol **504**(5): 519-532.

Alvarez-Buylla, A., J. M. Garcia-Verdugo and A. D. Tramontin (2001). "A unified hypothesis on the lineage of neural stem cells." Nat Rev Neurosci **2**(4): 287-293.

Alvarez-Buylla, A. and D. A. Lim (2004). "For the long run: maintaining germinal niches in the adult brain." Neuron **41**(5): 683-686.

Anchan, R. M., D. P. Drake, C. F. Haines, E. A. Gerwe and A. S. LaMantia (1997). "Disruption of local retinoid-mediated gene expression accompanies abnormal development in the mammalian olfactory pathway." J Comp Neurol **379**(2): 171-184.

Anderson, S., M. Mione, K. Yun and J. L. Rubenstein (1999). "Differential origins of neocortical projection and local circuit neurons: role of Dlx genes in neocortical interneuronogenesis." Cereb Cortex **9**(6): 646-654.

Azuara, V., P. Perry, S. Sauer, M. Spivakov, H. F. Jorgensen, R. M. John, M. Gouti, M. Casanova, G. Warnes, M. Merkenschlager and A. G. Fisher (2006). "Chromatin signatures of pluripotent cell lines." Nat Cell Biol **8**(5): 532-538.

Backman, M., O. Machon, L. Mygland, C. J. van den Bout, W. Zhong, M. M. Taketo and S. Krauss (2005). "Effects of canonical Wnt signaling on dorso-ventral specification of the mouse telencephalon." Dev Biol **279**(1): 155-168.

Ball, L. J., N. V. Murzina, R. W. Broadhurst, A. R. Raine, S. J. Archer, F. J. Stott, A. G. Murzin, P. B. Singh, P. J. Domaille and E. D. Laue (1997). "Structure of the chromatin binding (chromo) domain from mouse modifier protein 1." EMBO J **16**(9): 2473-2481.

Belluzzi, O., M. Benedusi, J. Ackman and J. J. LoTurco (2003). "Electrophysiological differentiation of new neurons in the olfactory bulb." J Neurosci **23**(32): 10411-10418.

Bergman, J. E., N. Janssen, L. H. Hoefsloot, M. C. Jongmans, R. M. Hofstra and C. M. van Ravenswaaij-Arts (2011). "CHD7 mutations and CHARGE syndrome: the clinical implications of an expanding phenotype." J Med Genet **48**(5): 334-342.

Bernstein, B. E., T. S. Mikkelsen, X. Xie, M. Kamal, D. J. Huebert, J. Cuff, B. Fry, A. Meissner, M. Wernig, K. Plath, R. Jaenisch, A. Wagschal, R. Feil, S. L. Schreiber and E. S. Lander (2006). "A bivalent chromatin structure marks key developmental genes in embryonic stem cells." Cell **125**(2): 315-326.

Bienz, M. (2006). "The PHD finger, a nuclear protein-interaction domain." Trends in biochemical sciences **31**(1): 35-40.
Bouazoune, K. and R. E. Kingston (2012). "Chromatin remodeling by the CHD7 protein is impaired by mutations that cause human developmental disorders." Proc Natl Acad Sci U S A **109**(47): 19238-19243.
Bovetti, S., Y. C. Hsieh, P. Bovolin, I. Perroteau, T. Kazunori and A. C. Puche (2007). "Blood vessels form a scaffold for neuroblast migration in the adult olfactory bulb." J Neurosci **27**(22): 5976-5980.
Boyer, L. A., R. R. Latek and C. L. Peterson (2004). "The SANT domain: a unique histone-tail-binding module?" Nat Rev Mol Cell Biol **5**(2): 158-163.
Bozoyan, L., J. Khlghatyan and A. Saghatelyan (2012). "Astrocytes control the development of the migration-promoting vasculature scaffold in the postnatal brain via VEGF signaling." J Neurosci **32**(5): 1687-1704.
Brehm, A., S. J. Nielsen, E. A. Miska, D. J. McCance, J. L. Reid, A. J. Bannister and T. Kouzarides (1999). "The E7 oncoprotein associates with Mi2 and histone deacetylase activity to promote cell growth." EMBO J **18**(9): 2449-2458.
Brill, M. S., J. Ninkovic, E. Winpenny, R. D. Hodge, I. Ozen, R. Yang, A. Lepier, S. Gascon, F. Erdelyi, G. Szabo, C. Parras, F. Guillemot, M. Frotscher, B. Berninger, R. F. Hevner, O. Raineteau and M. Gotz (2009). "Adult generation of glutamatergic olfactory bulb interneurons." Nat Neurosci **12**(12): 1524-1533.
Burrows, R. C., D. Wancio, P. Levitt and L. Lillien (1997). "Response diversity and the timing of progenitor cell maturation are regulated by developmental changes in EGFR expression in the cortex." Neuron **19**(2): 251-267.
Calver, A. R., A. C. Hall, W. P. Yu, F. S. Walsh, J. K. Heath, C. Betsholtz and W. D. Richardson (1998). "Oligodendrocyte population dynamics and the role of PDGF in vivo." Neuron **20**(5): 869-882.
Cao, R., L. Wang, H. Wang, L. Xia, H. Erdjument-Bromage, P. Tempst, R. S. Jones and Y. Zhang (2002). "Role of histone H3 lysine 27 methylation in Polycomb-group silencing." Science **298**(5595): 1039-1043.
Carleton, A., L. T. Petreanu, R. Lansford, A. Alvarez-Buylla and P. M. Lledo (2003). "Becoming a new neuron in the adult olfactory bulb." Nat Neurosci **6**(5): 507-518.
Carter, C. S., T. W. Vogel, Q. Zhang, S. Seo, R. E. Swiderski, T. O. Moninger, M. D. Cassell, D. R. Thedens, K. M. Keppler-Noreuil, P. Nopoulos, D. Y. Nishimura, C. C. Searby, K. Bugge and V. C. Sheffield (2012). "Abnormal development of NG2+PDGFR-alpha+ neural progenitor cells leads to neonatal hydrocephalus in a ciliopathy mouse model." Nat Med **18**(12): 1797-1804.
Cecchi, C. and E. Boncinelli (2000). "Emx homeogenes and mouse brain development." Trends Neurosci **23**(8): 347-352.
Chamberlain, G., J. Fox, B. Ashton and J. Middleton (2007). "Concise review: mesenchymal stem cells: their phenotype, differentiation capacity,

immunological features, and potential for homing." Stem cells **25**(11): 2739-2749.
Chenn, A. and S. K. McConnell (1995). "Cleavage orientation and the asymmetric inheritance of Notch1 immunoreactivity in mammalian neurogenesis." Cell **82**(4): 631-641.
Chenn, A. and C. A. Walsh (2002). "Regulation of cerebral cortical size by control of cell cycle exit in neural precursors." Science **297**(5580): 365-369.
Choi, B. H. (1988). "Prenatal gliogenesis in the developing cerebrum of the mouse." Glia **1**(5): 308-316.
Ciani, L. and P. C. Salinas (2005). "WNTs in the vertebrate nervous system: from patterning to neuronal connectivity." Nat Rev Neurosci **6**(5): 351-362.
Daubresse, G., R. Deuring, L. Moore, O. Papoulas, I. Zakrajsek, W. R. Waldrip, M. P. Scott, J. A. Kennison and J. W. Tamkun (1999). "The Drosophila kismet gene is related to chromatin-remodeling factors and is required for both segmentation and segment identity." Development **126**(6): 1175-1187.
Davis, A. A. and S. Temple (1994). "A self-renewing multipotential stem cell in embryonic rat cerebral cortex." Nature **372**(6503): 263-266.
de la Serna, I. L., Y. Ohkawa and A. N. Imbalzano (2006). "Chromatin remodelling in mammalian differentiation: lessons from ATP-dependent remodellers." Nat Rev Genet **7**(6): 461-473.
Doetsch, F., I. Caille, D. A. Lim, J. M. Garcia-Verdugo and A. Alvarez-Buylla (1999). "Subventricular zone astrocytes are neural stem cells in the adult mammalian brain." Cell **97**(6): 703-716.
Egan, C. M., U. Nyman, J. Skotte, G. Streubel, S. Turner, D. J. O'Connell, V. Rraklli, M. J. Dolan, N. Chadderton, K. Hansen, G. J. Farrar, K. Helin, J. Holmberg and A. P. Bracken (2013). "CHD5 is required for neurogenesis and has a dual role in facilitating gene expression and polycomb gene repression." Developmental cell **26**(3): 223-236.
Engelen, E., U. Akinci, J. C. Bryne, J. Hou, C. Gontan, M. Moen, D. Szumska, C. Kockx, W. van Ijcken, D. H. Dekkers, J. Demmers, E. J. Rijkers, S. Bhattacharya, S. Philipsen, L. H. Pevny, F. G. Grosveld, R. J. Rottier, B. Lenhard and R. A. Poot (2011). "Sox2 cooperates with Chd7 to regulate genes that are mutated in human syndromes." Nat Genet **43**(6): 607-611.
Feng, W., M. A. Khan, P. Bellvis, Z. Zhu, O. Bernhardt, C. Herold-Mende and H. K. Liu (2013). "The Chromatin Remodeler CHD7 Regulates Adult Neurogenesis via Activation of SoxC Transcription Factors." Cell Stem Cell **13**(1): 62-72.
Ferri, A. L., M. Cavallaro, D. Braida, A. Di Cristofano, A. Canta, A. Vezzani, S. Ottolenghi, P. P. Pandolfi, M. Sala, S. DeBiasi and S. K. Nicolis (2004). "Sox2 deficiency causes neurodegeneration and impaired neurogenesis in the adult mouse brain." Development **131**(15): 3805-3819.
Flanagan, J. F., L. Z. Mi, M. Chruszcz, M. Cymborowski, K. L. Clines, Y. Kim, W. Minor, F. Rastinejad and S. Khorasanizadeh (2005). "Double chromodomains cooperate to recognize the methylated histone H3 tail." Nature **438**(7071): 1181-1185.

Fuccillo, M., A. L. Joyner and G. Fishell (2006). "Morphogen to mitogen: the multiple roles of hedgehog signalling in vertebrate neural development." Nat Rev Neurosci **7**(10): 772-783.

Gaspar-Maia, A., A. Alajem, F. Polesso, R. Sridharan, M. J. Mason, A. Heidersbach, J. Ramalho-Santos, M. T. McManus, K. Plath, E. Meshorer and M. Ramalho-Santos (2009). "Chd1 regulates open chromatin and pluripotency of embryonic stem cells." Nature **460**(7257): 863-868.

Gotz, M. and W. B. Huttner (2005). "The cell biology of neurogenesis." Nat Rev Mol Cell Biol **6**(10): 777-788.

Guillemot, F. and C. Zimmer (2011). "From cradle to grave: the multiple roles of fibroblast growth factors in neural development." Neuron **71**(4): 574-588.

Hall, J. A. and P. T. Georgel (2007). "CHD proteins: a diverse family with strong ties." Biochem Cell Biol **85**(4): 463-476.

Harada, A., S. Okada, D. Konno, J. Odawara, T. Yoshimi, S. Yoshimura, H. Kumamaru, H. Saiwai, T. Tsubota, H. Kurumizaka, K. Akashi, T. Tachibana, A. N. Imbalzano and Y. Ohkawa (2012). "Chd2 interacts with H3.3 to determine myogenic cell fate." The EMBO journal **31**(13): 2994-3007.

Haskell, G. T. and A. S. LaMantia (2005). "Retinoic acid signaling identifies a distinct precursor population in the developing and adult forebrain." J Neurosci **25**(33): 7636-7647.

Hevner, R. F., L. Shi, N. Justice, Y. Hsueh, M. Sheng, S. Smiga, A. Bulfone, A. M. Goffinet, A. T. Campagnoni and J. L. Rubenstein (2001). "Tbr1 regulates differentiation of the preplate and layer 6." Neuron **29**(2): 353-366.

Hirabayashi, Y. and Y. Gotoh (2005). "Stage-dependent fate determination of neural precursor cells in mouse forebrain." Neurosci Res **51**(4): 331-336.

Hirabayashi, Y., Y. Itoh, H. Tabata, K. Nakajima, T. Akiyama, N. Masuyama and Y. Gotoh (2004). "The Wnt/beta-catenin pathway directs neuronal differentiation of cortical neural precursor cells." Development **131**(12): 2791-2801.

Hsieh, J. (2012). "Orchestrating transcriptional control of adult neurogenesis." Genes Dev **26**(10): 1010-1021.

Hurd, E. A., P. L. Capers, M. N. Blauwkamp, M. E. Adams, Y. Raphael, H. K. Poucher and D. M. Martin (2007). "Loss of Chd7 function in gene-trapped reporter mice is embryonic lethal and associated with severe defects in multiple developing tissues." Mamm Genome **18**(2): 94-104.

Hurd, E. A., H. K. Poucher, K. Cheng, Y. Raphael and D. M. Martin (2010). "The ATP-dependent chromatin remodeling enzyme CHD7 regulates pro-neural gene expression and neurogenesis in the inner ear." Development **137**(18): 3139-3150.

Ihrie, R. A., J. K. Shah, C. C. Harwell, J. H. Levine, C. D. Guinto, M. Lezameta, A. R. Kriegstein and A. Alvarez-Buylla (2011). "Persistent sonic hedgehog signaling in adult brain determines neural stem cell positional identity." Neuron **71**(2): 250-262.

Israsena, N., M. Hu, W. Fu, L. Kan and J. A. Kessler (2004). "The presence of FGF2 signaling determines whether beta-catenin exerts effects on proliferation or neuronal differentiation of neural stem cells." Dev Biol **268**(1): 220-231.

Issekutz, K. A., J. M. Graham, Jr., C. Prasad, I. M. Smith and K. D. Blake (2005). "An epidemiological analysis of CHARGE syndrome: preliminary results from a Canadian study." Am J Med Genet A **133A**(3): 309-317.

Janssen, N., J. E. Bergman, M. A. Swertz, L. Tranebjaerg, M. Lodahl, J. Schoots, R. M. Hofstra, C. M. van Ravenswaaij-Arts and L. H. Hoefsloot (2012). "Mutation update on the CHD7 gene involved in CHARGE syndrome." Hum Mutat **33**(8): 1149-1160.

Jin, K., Y. Sun, L. Xie, S. Batteur, X. O. Mao, C. Smelick, A. Logvinova and D. A. Greenberg (2003). "Neurogenesis and aging: FGF-2 and HB-EGF restore neurogenesis in hippocampus and subventricular zone of aged mice." Aging Cell **2**(3): 175-183.

Kessaris, N., N. Pringle and W. D. Richardson (2001). "Ventral neurogenesis and the neuron-glial switch." Neuron **31**(5): 677-680.

Kim, E. J., C. T. Leung, R. R. Reed and J. E. Johnson (2007). "In vivo analysis of Ascl1 defined progenitors reveals distinct developmental dynamics during adult neurogenesis and gliogenesis." J Neurosci **27**(47): 12764-12774.

Kondo, M., A. J. Wagers, M. G. Manz, S. S. Prohaska, D. C. Scherer, G. F. Beilhack, J. A. Shizuru and I. L. Weissman (2003). "Biology of hematopoietic stem cells and progenitors: implications for clinical application." Annual review of immunology **21**: 759-806.

Kosaka, K., Y. Aika, K. Toida, C. W. Heizmann, W. Hunziker, D. M. Jacobowitz, I. Nagatsu, P. Streit, T. J. Visser and T. Kosaka (1995). "Chemically defined neuron groups and their subpopulations in the glomerular layer of the rat main olfactory bulb." Neurosci Res **23**(1): 73-88.

Kriegstein, A., S. Noctor and V. Martinez-Cerdeno (2006). "Patterns of neural stem and progenitor cell division may underlie evolutionary cortical expansion." Nat Rev Neurosci **7**(11): 883-890.

Kuhn, H. G., J. Winkler, G. Kempermann, L. J. Thal and F. H. Gage (1997). "Epidermal growth factor and fibroblast growth factor-2 have different effects on neural progenitors in the adult rat brain." J Neurosci **17**(15): 5820-5829.

Layman, W. S., E. A. Hurd and D. M. Martin (2010). "Chromodomain proteins in development: lessons from CHARGE syndrome." Clin Genet **78**(1): 11-20.

Layman, W. S., D. P. McEwen, L. A. Beyer, S. R. Lalani, S. D. Fernbach, E. Oh, A. Swaroop, C. C. Hegg, Y. Raphael, J. R. Martens and D. M. Martin (2009). "Defects in neural stem cell proliferation and olfaction in Chd7 deficient mice indicate a mechanism for hyposmia in human CHARGE syndrome." Hum Mol Genet **18**(11): 1909-1923.

Legendre, M., M. Gonzales, G. Goudefroye, F. Bilan, P. Parisot, M. J. Perez, M. Bonniere, B. Bessieres, J. Martinovic, A. L. Delezoide, F. Jossic, C. Fallet-Bianco, M. Bucourt, J. Tantau, P. Loget, L. Loeuillet, N. Laurent, B. Leroy, H. Salhi, N. Bigi, C. Rouleau, F. Guimiot, C. Quelin, A. Bazin, C. Alby, A.

Ichkou, R. Gesny, A. Kitzis, Y. Ville, S. Lyonnet, F. Razavi, B. Gilbert-Dussardier, M. Vekemans and T. Attie-Bitach (2012). "Antenatal spectrum of CHARGE syndrome in 40 fetuses with CHD7 mutations." J Med Genet **49**(11): 698-707.

Lim, D. A., Y. C. Huang, T. Swigut, A. L. Mirick, J. M. Garcia-Verdugo, J. Wysocka, P. Ernst and A. Alvarez-Buylla (2009). "Chromatin remodelling factor Mll1 is essential for neurogenesis from postnatal neural stem cells." Nature **458**(7237): 529-533.

Lin, J. J., L. W. Lehmann, G. Bonora, R. Sridharan, A. A. Vashisht, N. Tran, K. Plath, J. A. Wohlschlegel and M. Carey (2011). "Mediator coordinates PIC assembly with recruitment of CHD1." Genes & development **25**(20): 2198-2209.

Lledo, P. M., M. Alonso and M. S. Grubb (2006). "Adult neurogenesis and functional plasticity in neuronal circuits." Nat Rev Neurosci **7**(3): 179-193.

Lledo, P. M., G. Gheusi and J. D. Vincent (2005). "Information processing in the mammalian olfactory system." Physiol Rev **85**(1): 281-317.

Lledo, P. M., F. T. Merkle and A. Alvarez-Buylla (2008). "Origin and function of olfactory bulb interneuron diversity." Trends Neurosci **31**(8): 392-400.

Lois, C. and A. Alvarez-Buylla (1993). "Proliferating subventricular zone cells in the adult mammalian forebrain can differentiate into neurons and glia." Proc Natl Acad Sci U S A **90**(5): 2074-2077.

Lois, C., J. M. Garcia-Verdugo and A. Alvarez-Buylla (1996). "Chain migration of neuronal precursors." Science **271**(5251): 978-981.

Maden, M. (2002). "Retinoid signalling in the development of the central nervous system." Nat Rev Neurosci **3**(11): 843-853.

Maden, M. (2007). "Retinoic acid in the development, regeneration and maintenance of the nervous system." Nat Rev Neurosci **8**(10): 755-765.

Marin, O. and J. L. Rubenstein (2001). "A long, remarkable journey: tangential migration in the telencephalon." Nat Rev Neurosci **2**(11): 780-790.

Marshall, C. A., S. O. Suzuki and J. E. Goldman (2003). "Gliogenic and neurogenic progenitors of the subventricular zone: who are they, where did they come from, and where are they going?" Glia **43**(1): 52-61.

Mason, I. (2007). "Initiation to end point: the multiple roles of fibroblast growth factors in neural development." Nat Rev Neurosci **8**(8): 583-596.

Merkle, F. T., Z. Mirzadeh and A. Alvarez-Buylla (2007). "Mosaic organization of neural stem cells in the adult brain." Science **317**(5836): 381-384.

Molofsky, A. V., S. He, M. Bydon, S. J. Morrison and R. Pardal (2005). "Bmi-1 promotes neural stem cell self-renewal and neural development but not mouse growth and survival by repressing the p16Ink4a and p19Arf senescence pathways." Genes Dev **19**(12): 1432-1437.

Molofsky, A. V., R. Pardal, T. Iwashita, I. K. Park, M. F. Clarke and S. J. Morrison (2003). "Bmi-1 dependence distinguishes neural stem cell self-renewal from progenitor proliferation." Nature **425**(6961): 962-967.

Morrow, T., M. R. Song and A. Ghosh (2001). "Sequential specification of neurons and glia by developmentally regulated extracellular factors." Development **128**(18): 3585-3594.

Niederreither, K. and P. Dolle (2008). "Retinoic acid in development: towards an integrated view." Nat Rev Genet **9**(7): 541-553.
Noctor, S. C., A. C. Flint, T. A. Weissman, R. S. Dammerman and A. R. Kriegstein (2001). "Neurons derived from radial glial cells establish radial units in neocortex." Nature **409**(6821): 714-720.
Noctor, S. C., V. Martinez-Cerdeno, L. Ivic and A. R. Kriegstein (2004). "Cortical neurons arise in symmetric and asymmetric division zones and migrate through specific phases." Nat Neurosci **7**(2): 136-144.
Noctor, S. C., V. Martinez-Cerdeno and A. R. Kriegstein (2008). "Distinct behaviors of neural stem and progenitor cells underlie cortical neurogenesis." J Comp Neurol **508**(1): 28-44.
Pagon, R. A., J. M. Graham, Jr., J. Zonana and S. L. Yong (1981). "Coloboma, congenital heart disease, and choanal atresia with multiple anomalies: CHARGE association." J Pediatr **99**(2): 223-227.
Parras, C. M., R. Galli, O. Britz, S. Soares, C. Galichet, J. Battiste, J. E. Johnson, M. Nakafuku, A. Vescovi and F. Guillemot (2004). "Mash1 specifies neurons and oligodendrocytes in the postnatal brain." EMBO J **23**(22): 4495-4505.
Pastrana, E., V. Silva-Vargas and F. Doetsch (2011). "Eyes wide open: a critical review of sphere-formation as an assay for stem cells." Cell Stem Cell **8**(5): 486-498.
Pearce, J. J., P. B. Singh and S. J. Gaunt (1992). "The mouse has a Polycomb-like chromobox gene." Development **114**(4): 921-929.
Pinto, G., V. Abadie, R. Mesnage, J. Blustajn, S. Cabrol, J. Amiel, L. Hertz-Pannier, A. M. Bertrand, S. Lyonnet, R. Rappaport and I. Netchine (2005). "CHARGE syndrome includes hypogonadotropic hypogonadism and abnormal olfactory bulb development." J Clin Endocrinol Metab **90**(10): 5621-5626.
Pray-Grant, M. G., J. A. Daniel, D. Schieltz, J. R. Yates, 3rd and P. A. Grant (2005). "Chd1 chromodomain links histone H3 methylation with SAGA- and SLIK-dependent acetylation." Nature **433**(7024): 434-438.
Rakic, P. (1978). "Neuronal migration and contact guidance in the primate telencephalon." Postgrad Med J **54 Suppl 1**: 25-40.
Ralston, S. H. and B. de Crombrugghe (2006). "Genetic regulation of bone mass and susceptibility to osteoporosis." Genes & development **20**(18): 2492-2506.
Reynolds, B. A. and S. Weiss (1992). "Generation of neurons and astrocytes from isolated cells of the adult mammalian central nervous system." Science **255**(5052): 1707-1710.
Rhinn, M. and P. Dolle (2012). "Retinoic acid signalling during development." Development **139**(5): 843-858.
Roybon, L., T. Deierborg, P. Brundin and J. Y. Li (2009). "Involvement of Ngn2, Tbr and NeuroD proteins during postnatal olfactory bulb neurogenesis." Eur J Neurosci **29**(2): 232-243.
Ruiz i Altaba, A., V. Palma and N. Dahmane (2002). "Hedgehog-Gli signalling and the growth of the brain." Nat Rev Neurosci **3**(1): 24-33.

Ryan, D. P., R. Sundaramoorthy, D. Martin, V. Singh and T. Owen-Hughes (2011). "The DNA-binding domain of the Chd1 chromatin-remodelling enzyme contains SANT and SLIDE domains." The EMBO journal **30**(13): 2596-2609.

Sato, N., L. Meijer, L. Skaltsounis, P. Greengard and A. H. Brivanlou (2004). "Maintenance of pluripotency in human and mouse embryonic stem cells through activation of Wnt signaling by a pharmacological GSK-3-specific inhibitor." Nat Med **10**(1): 55-63.

Schuster, E. F. and R. Stoger (2002). "CHD5 defines a new subfamily of chromodomain-SWI2/SNF2-like helicases." Mamm Genome **13**(2): 117-119.

Shitamukai, A., D. Konno and F. Matsuzaki (2011). "Oblique radial glial divisions in the developing mouse neocortex induce self-renewing progenitors outside the germinal zone that resemble primate outer subventricular zone progenitors." J Neurosci **31**(10): 3683-3695.

Shur, I. and D. Benayahu (2005). "Characterization and functional analysis of CReMM, a novel chromodomain helicase DNA-binding protein." Journal of molecular biology **352**(3): 646-655.

Shur, I., R. Socher and D. Benayahu (2006). "In vivo association of CReMM/CHD9 with promoters in osteogenic cells." Journal of cellular physiology **207**(2): 374-378.

Simon, J. A. and R. E. Kingston (2009). "Mechanisms of polycomb gene silencing: knowns and unknowns." Nat Rev Mol Cell Biol **10**(10): 697-708.

Smart, I. H. (1973). "Proliferative characteristics of the ependymal layer during the early development of the mouse neocortex: a pilot study based on recording the number, location and plane of cleavage of mitotic figures." J Anat **116**(Pt 1): 67-91.

Smith, C. L. and C. L. Peterson (2005). "ATP-dependent chromatin remodeling." Curr Top Dev Biol **65**: 115-148.

Sparmann, A., Y. Xie, E. Verhoeven, M. Vermeulen, C. Lancini, G. Gargiulo, D. Hulsman, M. Mann, J. A. Knoblich and M. van Lohuizen (2013). "The chromodomain helicase Chd4 is required for Polycomb-mediated inhibition of astroglial differentiation." The EMBO journal **32**(11): 1598-1612.

Stoykova, A., D. Treichel, M. Hallonet and P. Gruss (2000). "Pax6 modulates the dorsoventral patterning of the mammalian telencephalon." J Neurosci **20**(21): 8042-8050.

Stuhmer, T., L. Puelles, M. Ekker and J. L. Rubenstein (2002). "Expression from a Dlx gene enhancer marks adult mouse cortical GABAergic neurons." Cereb Cortex **12**(1): 75-85.

Sussel, L., O. Marin, S. Kimura and J. L. Rubenstein (1999). "Loss of Nkx2.1 homeobox gene function results in a ventral to dorsal molecular respecification within the basal telencephalon: evidence for a transformation of the pallidum into the striatum." Development **126**(15): 3359-3370.

Takada, I., M. Mihara, M. Suzawa, F. Ohtake, S. Kobayashi, M. Igarashi, M. Y. Youn, K. Takeyama, T. Nakamura, Y. Mezaki, S. Takezawa, Y. Yogiashi,

H. Kitagawa, G. Yamada, S. Takada, Y. Minami, H. Shibuya, K. Matsumoto and S. Kato (2007). "A histone lysine methyltransferase activated by non-canonical Wnt signalling suppresses PPAR-gamma transactivation." Nat Cell Biol **9**(11): 1273-1285.

Thompson Haskell, G., T. M. Maynard, R. A. Shatzmiller and A. S. Lamantia (2002). "Retinoic acid signaling at sites of plasticity in the mature central nervous system." J Comp Neurol **452**(3): 228-241.

Uccelli, A., L. Moretta and V. Pistoia (2008). "Mesenchymal stem cells in health and disease." Nature reviews. Immunology **8**(9): 726-736.

Ugarte, F. and E. C. Forsberg (2013). "Haematopoietic stem cell niches: new insights inspire new questions." The EMBO journal **32**(19): 2535-2547.

Vissers, L. E., C. M. van Ravenswaaij, R. Admiraal, J. A. Hurst, B. B. de Vries, I. M. Janssen, W. A. van der Vliet, E. H. Huys, P. J. de Jong, B. C. Hamel, E. F. Schoenmakers, H. G. Brunner, J. A. Veltman and A. G. van Kessel (2004). "Mutations in a new member of the chromodomain gene family cause CHARGE syndrome." Nat Genet **36**(9): 955-957.

Wachowiak, M. and M. T. Shipley (2006). "Coding and synaptic processing of sensory information in the glomerular layer of the olfactory bulb." Semin Cell Dev Biol **17**(4): 411-423.

Wang, T. W., H. Zhang and J. M. Parent (2005). "Retinoic acid regulates postnatal neurogenesis in the murine subventricular zone-olfactory bulb pathway." Development **132**(12): 2721-2732.

Wichterle, H., D. H. Turnbull, S. Nery, G. Fishell and A. Alvarez-Buylla (2001). "In utero fate mapping reveals distinct migratory pathways and fates of neurons born in the mammalian basal forebrain." Development **128**(19): 3759-3771.

Williams, B. P., J. K. Park, J. A. Alberta, S. G. Muhlebach, G. Y. Hwang, T. M. Roberts and C. D. Stiles (1997). "A PDGF-regulated immediate early gene response initiates neuronal differentiation in ventricular zone progenitor cells." Neuron **18**(4): 553-562.

Wilson, S. W. and J. L. Rubenstein (2000). "Induction and dorsoventral patterning of the telencephalon." Neuron **28**(3): 641-651.

Wreggett, K. A., F. Hill, P. S. James, A. Hutchings, G. W. Butcher and P. B. Singh (1994). "A mammalian homologue of Drosophila heterochromatin protein 1 (HP1) is a component of constitutive heterochromatin." Cytogenetics and cell genetics **66**(2): 99-103.

Xue, Y., J. Wong, G. T. Moreno, M. K. Young, J. Cote and W. Wang (1998). "NURD, a novel complex with both ATP-dependent chromatin-remodeling and histone deacetylase activities." Molecular cell **2**(6): 851-861.

Yoshida, T., I. Hazan, J. Zhang, S. Y. Ng, T. Naito, H. J. Snippert, E. J. Heller, X. Qi, L. N. Lawton, C. J. Williams and K. Georgopoulos (2008). "The role of the chromatin remodeler Mi-2beta in hematopoietic stem cell self-renewal and multilineage differentiation." Genes & development **22**(9): 1174-1189.

Young, K. M., M. Fogarty, N. Kessaris and W. D. Richardson (2007). "Subventricular zone stem cells are heterogeneous with respect to their

embryonic origins and neurogenic fates in the adult olfactory bulb." J Neurosci **27**(31): 8286-8296.
Zentner, G. E., P. J. Tesar and P. C. Scacheri (2011). "Epigenetic signatures distinguish multiple classes of enhancers with distinct cellular functions." Genome Res **21**(8): 1273-1283.
Zhou, V. W., A. Goren and B. E. Bernstein (2011). "Charting histone modifications and the functional organization of mammalian genomes." Nat Rev Genet **12**(1): 7-18.

Chapter 2

CHD7 and retinoic acid signaling cooperate to regulate neural stem cell and inner ear development in mouse models of CHARGE syndrome

Abstract

CHARGE syndrome is a multiple congenital anomaly disorder that leads to life-threatening birth defects such as choanal atresia and cardiac malformations as well as multiple sensory impairments that affect hearing, vision, olfaction, and balance. CHARGE is caused by heterozygous mutations in *CHD7*, which encodes an ATP-dependent chromatin remodeling enzyme. Identification of the mechanisms underlying neurological and sensory defects in CHARGE is a first step toward developing treatments for CHARGE individuals. Here I used mouse models of *Chd7*-deficiency to explore the function of CHD7 in the development of the subventricular zone (SVZ) neural stem cell niche and inner ear, structures that are important for olfactory bulb neurogenesis and hearing and balance, respectively. I found that loss of *Chd7* results in cell-autonomous proliferative, neurogenic, and self-renewal defects in the perinatal and mature mouse SVZ stem cell niche. Modulation of retinoic acid (RA) signaling prevented *in vivo* inner ear and *in vitro* neural stem cell defects caused by *Chd7*-deficiency. My findings demonstrate critical, cooperative roles for RA and CHD7 in SVZ neural stem cell function and inner ear development, suggesting that altered RA signaling may be an effective method for treating *Chd7*-deficiency.

Introduction

CHARGE syndrome is a multiple anomaly disorder occurring in 1:10,000 live births and characterized by ear and heart defects, choanal atresia, retardation of growth and/or development, and delayed puberty (Pagon et al. 1981; Issekutz et al. 2005). In addition, olfactory bulb (OB) hypoplasia and hyposmia/anosmia are highly penetrant in CHARGE individuals; strikingly, arrhinencephaly and ventriculomegaly have been reported in CHARGE fetuses (Pinto et al. 2005; Layman et al. 2009; Bergman et al. 2011; Legendre et al. 2012). Heterozygous mutations in *CHD7*, which encodes an ATP-dependent chromatin remodeling enzyme, account for over 90% of CHARGE syndrome cases, yet no clear genotype-phenotype correlations have emerged (Vissers et al. 2004; Bergman et al. 2011; Janssen et al. 2012). Beyond supportive treatments and surgical intervention, there are no curative therapies for CHARGE-related defects.

Mouse models of CHARGE syndrome recapitulate most phenotypes observed in humans, including inner ear defects (semicircular canal and cochlear hypoplasia/dysplasia), OB hypoplasia, and hyposmia/anosmia (Bosman et al. 2005; Hurd et al. 2007; Layman et al. 2009; Bergman et al. 2010; Hurd et al. 2010; Hurd et al. 2011; Hurd et al. 2012). The underlying causes of inner ear defects and OB hypoplasia in *Chd7*-deficiency states are unknown, but there is evidence for disrupted neural stem cell proliferation in the otocyst and olfactory epithelium (Layman et al. 2009; Hurd et al. 2010). In the olfactory system, OB interneurons (granule and periglomerular cells) arise from neural stem cells in the

subventricular zone (SVZ) of the lateral ventricles (LV), which give rise to neuroblasts that migrate through the rostral migratory stream (RMS) over a 2-3 week period (Lledo et al. 2008). SVZ-derived neuroblasts then terminally differentiate and integrate into the granule cell (GCL) and glomerular (GL) layers of the OB, where they mature into inhibitory interneurons that modulate mitral and tufted cells, which relay olfactory sensory signals to the olfactory cortex (Lledo et al. 2008). In rodents, OB neurogenesis begins around embryonic day 15 (E15) and continues throughout life (Luskin 1993; Wichterle et al. 2001). Thus, OB neurogenesis is an excellent system for studying CHD7 function in neural development and maintenance.

Development and maintenance of the inner ear, SVZ, RMS, and OB are regulated in part by retinoic acid (RA) signaling (Anchan et al. 1997; Thompson Haskell et al. 2002; Romand et al. 2013). Notably, treatment of SVZ neural stem cell cultures with RA promotes neurogenesis (Wang et al. 2005), whereas reduction or absence of RA signaling results in proliferative and neurogenic defects in both the adult and developing SVZ (Haskell et al. 2005). Interestingly, deficiency in RA receptors or synthetic enzymes leads to phenotypes similar to those observed in CHARGE syndrome including eye, heart and brain abnormalities (Mark et al. 2009; Janssen et al. 2012). Despite having highly similar developmental effects in mammalian tissues, potential interactions between CHD7 and RA signaling pathways have not been explored.

The highly penetrant OB hypoplasia/aplasia and olfaction deficits in CHARGE individuals and *Chd7*-deficient mice suggest that *Chd7* may have a

role in the maintenance and differentiation of neural stem cells in the SVZ. Recently, CHD7 was shown to be expressed in the adult SVZ and in the subgranular zone (SGZ) of the dentate gyrus in the hippocampus (Feng et al. 2013). Additionally, OB and hippocampal neurogenesis was impaired in adult *Tlx-CreERT2 Chd7* conditional knockout mice (Feng et al. 2013). These findings demonstrate that CHD7 activity is required for ongoing neurogenesis in the mature SVZ; however, it is not known whether similar defects are present earlier in development or with heterozygous *Chd7* deletion. To investigate these questions, I generated conditional *Chd7*-deficient adult and neonatal mice and monitored changes in SVZ proliferation, self-renewal and neuronal differentiation. I also examined potential links between CHD7 and RA signaling by modulating RA levels in neurosphere assays and during inner ear development. My findings demonstrate that proper *Chd7* dosage is required for optimal function of SVZ neural stem cells during development and throughout adulthood, while modulation of retinoic acid signaling can attenuate inner ear and neural stem cell defects that arise from *Chd7*-deficiency.

Materials and Methods

Mouse strains, breeding and genotyping.

Chd7$^{Gt/+}$ and *Chd7*$^{flox/flox}$ mice were maintained as previously described (Hurd et al. 2007; Hurd et al. 2010). *Ubc-CreERT2*, *Nestin-Cre* and *Nestin-CreERT2* mice were maintained on a C57BL/6 background and mated with *Chd7*$^{flox/flox}$ mice to generate *Cre*;*Chd7*$^{flox/+}$ mice. *Cre;Chd7*$^{flox/+}$ mice were

crossed to *Chd7*$^{flox/flox}$ to produce control (*Chd7*$^{flox/+}$ and *Chd7*$^{flox/flox}$), *Chd7* conditional heterozygous (*Cre;Chd7*$^{flox/+}$), and conditional knockout (*Cre;Chd7*$^{flox/flox}$) mice. Genomic DNA was isolated from tail and brain tissue and PCR genotyped as previously described (Hurd et al. 2010). All procedures were approved by The University of Michigan University Committee on the Use and Care of Animals (UCUCA).

Tamoxifen administration.

Tamoxifen (Sigma-Aldritch, St. Louis, MO) was dissolved in sterile corn oil at a concentration of 10 mg/ml. For adult studies, Tamoxifen (0.2 mg/gbw) was administered by intraperitoneal injection to 5 week-old littermate mice once daily for five days. Mice were allowed to recover for 14 days, then euthanized and processed for further analysis. For perinatal studies, a single dose of Tamoxifen (0.2 mg/gbw) was administered by intraperitoneal injection to pregnant females at embryonic day 15.5.

Histology and embedding.

P1 mice were decapitated, skin was dissected away and heads were placed in 4% paraformaldehyde for 4 hrs, then cryoprotected in 30% sucrose, embedded in OCT (Tissue Tek, Torrance, CA), frozen and sectioned at 14 µm. Adult 7 week-old mice underwent terminal cardiac perfusion with 4% paraformaldehyde, then heads were removed, post-fixed with 4% paraformaldehyde, cryoprotected in 30% sucrose and embedded in OCT (Tissue Tek), then frozen and sectioned at 14 µm. For histological analyses, sections

were stained with hematoxylin and eosin (Sigma) and imaged with bright field microscopy on a Leica upright DMRB microscope (Leica Camera AG, Solms, Germany) and processed in Photoshop CS5.1 (Adobe, San Jose, CA).

Immunofluorescence.

Cryosections from 7 week-old and P1 mice (*n* = 3 per genotype) were processed for immunofluorescence with antibodies against CHD7 (1:7500; Cell Signaling Technology, Beverly, MA), Ki67 (1:200; Vector Laboratories, Burlingame, CA), tyrosine hydroxylase (1:150; Pel-Freeze, Rogers, AR), cleaved caspase 3 (1:800, Cell Signaling Technology), calbindin (1:5000; Sigma), GFAP (1:500; Sigma), O4 (1:800; Developmental Studies Hybridoma Bank, University of Iowa, Iowa City, IA), Tuj1 (1:400; Covance, Princeton, NJ), DCX (1:4000; a gift from Jack M. Parent) and SOX2 (1:250; EMD Millipore). All secondary antibodies were used at 1:200 with Alexa Fluor 488, Alexa Fluor 555 or biotinylated secondary antibodies (Vector Laboratories) conjugated with streptavidin-Horseradish Peroxidase and Alexa Fluor 488 Tyramide Signal Amplification or Alexa Fluor 555 Tyramide Signal Amplification (Life Technologies, Carlsbad, CA). Nuclear staining was performed with 4',6-diamidino-2-phenylindole (DAPI, 1:100; Life Technologies). Images were produced by single channel fluorescence microscopy on a Leica upright DMRB microscope and processed in Photoshop CS5.1.

Olfactory bulb interneuron quantification.

7 week-old *Chd7*$^{+/+}$ and *Chd7*$^{Gt/+}$ littermate mice (*n* = 3 per genotype) were processed for immunofluorescence with antibodies against tyrosine hydroxylase, calretinin, and calbindin. Images were captured by single channel fluorescence microscopy on a Leica upright DMRB microscope and processed in Adobe Photoshop CS5.1. For quantification of OB interneurons, 25 images using the 10X objective lens were taken of nine olfactory bulb sections per genotype and analyzed using the cell counter function of Image J (National Institutes of Health, Bethesda, MD) by sampling ten squares (40 µm x 40 µm) in the granule cell and glomerular cell layers.

Fluorescence intensity measurements.

Tamoxifen-treated 7 week-old mice (*n* = 3 per genotype) were processed for immunofluorescence with antibodies against GFAP and DCX. Images were captured at the same exposure for each antibody by single channel fluorescence microscopy on a Leica upright DMRB microscope. Fluorescence intensity was measured on 25-45 images using the 20X objective lens from nine OB, RMS and SVZ sections per genotype, then processed in ImageJ by using the freehand selection and measurement tool. Experimental fluorescence intensities and were reported as fluorescence intensity units (FIU) per µm^2.

SVZ proliferation and apoptosis studies.

7 week-old and P1 mice (*n* = 3 per genotype) were processed for immunofluorescence with antibody against Ki67 and cleaved caspase 3. Nuclei were stained with DAPI. Images were captured by single channel fluorescence microscopy on a Leica upright DMRB microscope and processed in Adobe Photoshop CS5.1. For quantification of Ki67+ cells, 36 images using the 20X objective lens were taken of nine SVZ sections per genotype and the number of Ki67+ cells and total number of cells present in the SVZ was counted using the cell counter function of Image J. For quantification of cleaved caspase 3+ cells, 27 SVZ sections per genotype were scored for the total number of cleaved caspase 3+ cells per section.

Cortex and corpus callosum measurements.

7 week-old control, *Nestin* Cond Het, and *Nestin* Cond KO mice (*n* = 3 per genotype) were perfusion fixed and brains were sectioned and processed for hematoxylin and eosin staining as above. Cortical thickness measurements were made on 27 SVZ sections per genotype by drawing a line perpendicular to, and extending from, the lateral ventricle to the outer edge of the cortex. For corpus callosum thickness, measurements were made on 27 SVZ sections per genotype by drawing a line at the midline transversely through the corpus callosum. Both measurements were performed using the Leica Applications Suite – Advanced Fluorescence software (Leica Camera AG) on 10X images.

Neurosphere cultures.

7 week-old adult and P1 mice (*n* = 3 per genotype) were euthanized, whole brain was dissected and coronal sections were cut between the pre-optic area and caudal OB. The lateral wall of the lateral ventricle was microdissected, dissociated in trypsin/EDTA (Life Technologies) and DNase1, filtered through a 0.45 µm mesh (BD Biosciences, East Rutherford, NJ) and counted on a hemacytometer. For primary neurosphere formation assays, 1000 cells were plated on ultra-low binding 6 well plates (Corning, Corning, NY) under self-renewal conditions (media with EGF and FGF), incubated at 37°C with 6.5% CO_2 for 8 days then measured and imaged using an Olympus IX81 motorized inverted microscope (Olympus, Tokyo, Japan). For primary neurosphere differentiation, single neurospheres were plated under adherent conditions with FGF and without EGF (24 well tissue culture-treated plates (Corning) with poly-D-lysine and human fibronectin (Biomedical Technologies, Stoughton, MA)) then incubated at 37°C with 6.5% CO_2 for 12 days. Secondary neurospheres were generated by dissociating single primary neurospheres and re-plating them under self-renewing conditions. Measurement, counting, imaging and differentiation of secondary neurospheres were performed as described for primary neurospheres. Neurosphere diameter (*n*=150 per genotype) was measured using the arbitrary line tool in the Olympus cellSens Dimension software package. Neurosphere frequency was determined by counting the total number of neurospheres greater than 50 µm in diameter in each well of a 6 well plate and dividing by the total

number of cells plated per well. Statistical significance was determined by unpaired Student's t-test.

Neurosphere differentiation, staining and scoring.

Primary and secondary neurospheres were differentiated as described above then treated with 1:800 anti-O4 antibody for 1 h and fixed with ice cold 95% ethanol/ 5% glacial acetic acid at -20ºC for 20 min. Fixed neurospheres were blocked for 1 h at room temperature with light rocking with blocking buffer (0.05% octylphenoxypolyethoxyethanol (NP-40, Sigma), 2 mg/ml bovine serum albumin (Sigma) in phosphate buffered saline). Alexa Fluor 647 conjugated goat anti-mouse IgM (1:500, Life Technologies) diluted in blocking buffer was added to each well and incubated at room temperature for 1 h with light rocking. Each well was washed three times with blocking buffer then a cocktail of 1:500 anti-Tuj1 and 1:200 anti-GFAP primary antibodies was added to each well and incubated at room temperature for 1 h with light rocking. Each well was washed three times with blocking buffer then incubated in a cocktail of 1:500 Alexa Fluor 555 goat anti-mouse IgG_{2a} and 1:500 Alexa Fluor 488 goat anti-mouse IgG_1 at room temperature for 1 h with light rocking. Each well was washed three times and nuclei were stained with 1:1000 DAPI for 15 min. Stained colonies were imaged with an Olympus IX81 motorized inverted microscope and scored for the presence or absence of cell type-specific immunofluorescence (n = 36 neurospheres per genotype). Statistical significance was determined by unpaired Student's t-test.

Retinoic acid and citral treatment of neurosphere cultures.

Neurosphere assays were performed as above on control, *Nestin-ERT2* Cond Het, and *Nestin-ERT2* Cond KO P1 mice. Secondary neurospheres (*n* = 3 per genotype) were plated in ultra-low binding 6 well plates in self-renewal medium or medium supplemented with 0.1μM retinoic acid (Sigma), 1 μM retinoic acid, 1 μM citral (Sigma) or 10 μM citral (*n* = 18 wells per genotype). For differentiation, untreated secondary neurospheres from each genotype were plated in 24 well plates in differentiation medium or medium supplemented with 1 μM retinoic acid, 1 μM citral, or 10 μM citral (*n* = 18 neurospheres per condition), and scored for differentiation as above.

Embryonic retinoic acid and citral treatment and inner ear paint fills.

Timed pregnancies were established between *Chd7*$^{Gt/+}$ males and females with the morning of the plug scored as embryonic day 0.5 (E0.5). At E7.5, pregnant females were treated with either retinoic acid (Sigma; in corn oil at 5 mg/kg by oral gavage), or citral (Sigma; in corn oil at 3μM/g body weight by intraperitoneal injection). At E14.5, *Chd7*$^{+/+}$ (n = 12 embryos; 24 ears) and *Chd7*$^{Gt/+}$ (n = 18 embryos; 36 ears) embryos were dissected and processed for inner ear paint filling. Briefly, embryos were washed in PBS, fixed in Bodian's fixative, cleared in methyl salicylate, heads were bisected and ears were injected with a solution with 3% Wite-Out (BIC, Shelton, CT) diluted in methyl salicylate (Hurd et al. 2007).

Gene expression analysis.

Subventricular zones from littermate control and *Ubc* Cond KO P1 mice (*n* = 4 per genotype) were microdissected and RNA was isolated using the RNAqueous-Micro RNA Isolation Kit (Ambion, Austin, TX, USA). cDNA was generated using the Superscript First-Strand cDNA Synthesis system with random hexamers (Life Technologies). Relative gene expression levels were assayed using TaqMan Gene Expression Master Mix and TaqMan probes (Applied Biosystems, Foster City, CA, USA) for *Gapdh*, *Ccnd1*, *Ccnd2*, *Cdk4*, *Cdkn1a*, *Cdkn1b*, *Rarb*, *Rxrg*, *Neurod1,* and *Sox2* or SYBR Green Master Mix (Applied Biosystems) for 45S pre-rRNA (Zentner et al. 2010). Each sample was run in triplicate using an Applied Biosystems StepOne-Plus Real-Time qPCR System. The gene expression level of *Gapdh* was used as an internal positive control. The difference in threshold cycle (C_T) between the assayed gene and *Gapdh* for any given sample was defined as the change in threshold cycle (ΔC_T). The difference in ΔC_T between two samples was defined as $\Delta\Delta C_T$ which represents a relative difference in expression of the assayed gene. The fold change of the assayed gene relative to *Gapdh* was defined as $2^{-\Delta\Delta CT}$. Unpaired Student's t-test was performed on *Gapdh* normalized ΔC_T values for each sample to determine statistical significance.

P19 neurosphere cultures.

P19 embryonal carcinoma cells were passaged in MEMα (Life Technologies) + 10% FBS (Life Technologies) + 1X penicillin/streptomycin (Life

Technologies) and gently treated with 0.25% trypsin. Cells were plated on 0.7% agarose in bacterial culture plates in MEMα + 7.5% calf serum + 2.5% FBS + 1 μM retinoic acid + 1X penicillin/streptomycin. Neurospheres were confirmed to form two days after plating by bright field microscopy and medium was changed two and four days after initial plating. Six days after plating, neurospheres were collected by gentle centrifugation then fixed for 20 min with formaldehyde and processed for chromatin immunoprecipitation.

Chromatin immunoprecipitation and quantitative real-time PCR.

Chromatin immunoprecipitation with anti-CHD7 antibody (Cell Signaling) and normal rabbit IgG (EMD Millipore) was performed using the EZ ChIP Chromatin Immunoprecipitation Kit (EMD Millipore) following the manufacturer's instructions on crosslinked P19 neurospheres. Conserved and non-conserved regions within 10 kb of the transcription start site for each of *Rarb*, *Rxrg*, and *Neurod1* were identified using the 60 vertebrate PhastCons track in the UCSC Genome Browser (build GRCm38/mm10) (Siepel et al. 2005). A conserved region was defined by a series of adjacent LOD score hits conserved in ≥ 80% of the vertebrates. Primers were designed against nine conserved regions and one non-conserved region for each gene and assayed for a single melting point by quantitative real-time PCR (qRT-PCR) melt curve analysis using SYBR-Green reagents (Applied Biosystems). Primer pairs which demonstrated non-specific amplification were removed prior to further analysis. Nine replicates of qRT-PCR were performed on the input, IgG, and anti-CHD7 samples for each primer pair.

Percent input was calculated for both the IgG and anti-Chd7 samples across each primer pair.

Results

Chd7-deficient mice display neuronal defects in the adult olfactory bulb and rostral migratory stream.

I sought to determine the cell type specificity of *Chd7* in the mature mouse OB and to clarify whether *Chd7* is required for proper formation and maintenance of OB interneurons. In the adult OB, CHD7 co-localized with markers of immature (Doublecortin, DCX) and mature interneurons (Calbindin, CALB, Calretinin, CALR and Tyrosine Hydroxylase, TH) (Fig. 2.1) consistent with recently published observations (Feng et al. 2013). In the OB glomerular layer of $Chd7^{Gt/+}$ mice, there were 35% fewer CALB+ cells, 48% fewer TH+ cells, and no change in the number of CALR+ cells compared to wild type (Fig. 2.2C-E, F-H, I-K). In the OB granule cell layer of $Chd7^{Gt/+}$ mice, there were 15% fewer CALR+ cells compared to wild type (Fig. 2.2F-H). My data are consistent with a recent report showing reduced numbers of olfactory interneurons in adult *Tlx-CreERT2 Chd7* conditional knockout mice (Feng et al. 2013), and suggest that haploinsufficiency of *Chd7* also disrupts mature OB interneurons.

There are no reported cases of humans with homozygous *CHD7* mutations, and mice with complete loss of *Chd7* die by embryonic day 11 (E11), presumably from cardiovascular defects (Bosman et al. 2005; Hurd et al. 2007). To study the postnatal effects of complete *Chd7* deficiency, I used $Chd7^{flox/flox}$

and *Ubc-CreERT2* mice which ubiquitously express a Tamoxifen-inducible Cre (Ruzankina et al. 2007). Five week-old control (*Chd7*$^{flox/+}$ or *Chd7*$^{flox/flox}$), *Ubc* conditional heterozygous (*Ubc-CreERT2; Chd7*$^{flox/+}$, *Ubc* Cond Het), and *Ubc* conditional knockout (*Ubc-CreERT2; Chd7*$^{flox/flox}$, *Ubc* Cond KO) mice were treated with Tamoxifen by daily intraperitoneal injection for five days, then allowed to recover for 14 days (Fig. 2.3A). Immunofluorescence and fluorescence intensity (FI) quantification on coronal cryosections of the OB from control, *Ubc* Cond Het, and *Ubc* Cond KO adult mice was performed to characterize DCX+ migrating neurons and Glial Fibrillary Acidic Protein+ (GFAP) glia in the RMS and OB. In the RMS, there was a reduction in DCX-FI and a corresponding increase in GFAP-FI in *Ubc* Cond Het and *Ubc* Cond KO mice compared to controls (Fig. 2.3C-E, I, J). Interestingly, GFAP-FI was also increased in the glomerular layer (GL) of the OB in *Ubc* Cond KO mice compared to controls (Fig. 2.3F,H,K), while *Ubc* Cond Het mice were unaffected (Fig. 2.3F,G,K). Thus, adult-onset reduction of *Chd7* dosage leads to fewer immature and mature OB neurons and a visible expansion of glia, consistent with ongoing postnatal requirements for *Chd7*.

Reduced *Chd7* dosage leads to neurogenic and proliferative defects in the adult mouse SVZ.

Reduction of neurons in the olfactory bulb could be due to abnormalities in SVZ-derived neuronal production, migration, differentiation or survival. In the SVZ, CHD7 was present in a subset of neural stem and progenitor cells marked

by GFAP and SOX2 (Fig. 2.4C,D). In the RMS, CHD7 co-localized with DCX+ neuroblasts (progeny of SOX2+ SVZ cells), and was absent in GFAP+ glia (Fig. 2.4E,F). Therefore, *Chd7* is expressed in SVZ neural stem and progenitor cells and continues to be expressed in DCX+ neuroblasts as they migrate through the RMS into the olfactory bulb where they differentiate into mature interneurons. These data are in agreement with co-localization studies by Feng et al., which showed CHD7 present in a subset of GFAP+ neural stem cells as well as the majority of Mash1+ neural progenitors and DCX+ neuroblasts (Feng et al. 2013).

Next, I examined whether loss of *Chd7* leads to abnormalities in SVZ and RMS of adult mice. Hematoxylin and eosin (H&E) staining of SVZ tissue from *Ubc* Cond KO adult mice revealed ventriculomegaly, consistent with hydrocephalus (Fig. 2.5A,C), while *Ubc* Cond Het mice were unaffected (Fig. 2.5B). Immunofluorescence with anti-CHD7 confirmed deletion of CHD7+ cells in the SVZ of *Ubc* Cond Het and *Ubc* Cond KO mice compared to controls (Fig. 2.5D-F). As observed in the OB (Fig. 2.3J), there was decreased DCX-FI, disorganization of the RMS, and increased GFAP-FI in the RMS of adult *Ubc* Cond Het and *Ubc* Cond KO adult mice as compared to controls (Fig. 2.5G-I). The trend of decreased DCX-FI and increased GFAP-FI was also observed in adult *Ubc* Cond KO SVZ as compared to controls (Fig. 2.6). These observations suggest that *Chd7* is required for proper maintenance of the SVZ stem cell niche and the rostral migratory stream. The number of proliferating Ki67+ cells was reduced by 11% in the SVZ of *Ubc* Cond KO compared to controls and was unchanged in *Ubc* Cond Het mice (Fig. 2.5J-M), consistent with a minor role for

Chd7 in positive regulation of mature SVZ neural stem and progenitor cell proliferation. My results differ slightly from Feng et al., who showed no abnormalities in proliferating cells in the SVZ of adult *Tlx-CreERT2 Chd7* conditional knockout mice (Feng et al. 2013). This difference may reflect the timing of tamoxifen-induced deletion, assay sensitivity, or the specificity/efficiency of the Cre line.

Considering that *Ubc-CreERT2* deletes *Chd7* in all cells, ventriculomegaly and SVZ deficits may be influenced by secondary, non-cell autonomous deletion of *Chd7* in tissues or cells that interact with the SVZ. To test this, I used *Nestin-Cre* mice which express a neural stem cell-specific *Cre* that is active by embryonic day 11 (E11) in the central nervous system (Tronche et al. 1999; Sclafani et al. 2006). Ki67+ cells in the SVZ of adult *Nestin* Cond KO were reduced by 15% compared to controls and were unchanged in *Nestin* Cond Het (Fig. 2.5N-Q), consistent with mild lineage specific proliferative defects.

Since E11-E15 is a period of active cortical neurogenesis (Marin et al. 2001), *Nestin* Cond KO mice were tested for defects in forebrain structures including the cortex, corpus callosum, and lateral ventricles. H&E staining of forebrains revealed no differences in thickness of the cortex or corpus callosum between adult control and *Nestin* Cond KO mice (Fig. 2.7). Similar to adult *Ubc* Cond KO mice, *Nestin* Cond KO also displayed ventriculomegaly. Thus, *Nestin-Cre* mediated loss of *Chd7* in the brain results in ventriculomegaly without major abnormalities in cortex or corpus callosum.

SVZ neural stem and progenitor cells exhibit impaired proliferation, self-renewal and neurogenesis in *Chd7*-deficient adult mice.

To test whether *Chd7* is necessary for maintenance of proliferation, self-renewal, and multipotency of SVZ neural stem and progenitor cells, I generated and analyzed neurospheres from the SVZ of adult mice (Reynolds et al. 1992; Pastrana et al. 2011). The neurosphere assay can be used to determine the *in vitro* potential of a stem cell population, and to explore the regulatory mechanisms underlying self-renewal and differentiation (Fig. 2.8A-C). *Ubc* Cond Het and *Ubc* Cond KO primary neurospheres were smaller than controls, but there were no differences in primary neurosphere frequency (Fig. 2.8D,E). To test the self-renewal potential of neural stem and progenitor cells over time, I generated secondary neurospheres by dissociating and re-plating primary neurospheres under non-adherent conditions (Fig. 2.9). *Ubc* Cond KO secondary neurospheres were smaller than controls, while *Ubc* Cond Het secondary neurosphere size was unchanged (Fig. 2.8G). There were fewer *Ubc* Cond Het and *Ubc* Cond KO secondary neurospheres compared to controls (Fig. 2.8H). Both primary and secondary neurospheres from *Nestin* Cond Het and *Nestin* Cond KO mice were reduced in size and frequency in a *Chd7* dosage-dependent and cell-autonomous manner (Fig. 2.8J-K, M-N).

A hallmark of stem cells derived from neural tissue is their ability to differentiate *in vitro* into the three major cell types present in the central nervous system: glia (GFAP+), oligodendrocytes (O4+), and neurons (TUJ1+) (Alvarez-Buylla et al. 2001). TUJ1+ colonies derived from *Ubc* Cond Het, *Ubc* Cond KO,

and *Nestin* Cond KO adult secondary neurospheres, and *Nestin* Cond KO primary neurospheres, were significantly reduced compared to controls (Fig. 2.8I,L,O). Alternatively, neuronal potentials of *Ubc* Cond Het, *Ubc* Cond KO, and *Nestin* Cond Het primary neurospheres were unaffected compared to controls (Fig. 2.8F,L). Oligodendrocyte and glial potentials were normal for all *Ubc* and *Nestin* Cond Het and Cond KO neurospheres (data not shown). Due to the plating of whole, undissociated neurospheres for differentiation, I was unable to quantify specific lineages beyond presence or absence in the culture dish; thus, experimentally induced increases in glial cells would not be detected in this assay. I conclude that *Chd7*-deficient neurospheres exhibit cell-autonomous reductions in neuronal potential, with preserved or potentially enhanced differentiation into both oligodendrocytes and astrocytes.

Perinatal mice with reduced *Chd7* dosage have impaired proliferation, self-renewal and neurogenesis of SVZ neural stem and progenitor cells.

In the rodent SVZ, OB neurogenesis is a lifelong process that begins during late embryogenesis and continually populates the olfactory bulb with new interneurons (Luskin 1993; Wichterle et al. 2001). Considering that *Nestin-Cre* is active *in utero* before E11, defects in SVZ neural stem cell proliferation in *Nestin-Cre Chd7* CKO mice could be secondary to early *Chd7* deletion. In order to determine whether late embryonic *Chd7* deletion impacts perinatal SVZ function, I induced deletion of *Chd7* with *Ubc-CreERT2* and *Nestin-CreERT2* (Ables et al. 2010) at E15.5 (Fig. 2.10A), when mouse SVZ neural stem cells begin to

transition from cortical neurogenesis to olfactory bulb neurogenesis (Anderson et al. 1997). In the SVZ of postnatal day 1 (P1) *Ubc* Cond KO and *NestinERT2* Cond KO mice, there were 38% and 37% fewer Ki67+ cells than controls, whereas Ki67+ cells in *Ubc* Cond Het and *NestinERT2* Cond Het mice were unchanged (Fig. 2.10B-I), consistent with impaired proliferation. Additionally, there was no change in apoptosis frequency in the SVZ of *NestinERT2* Cond Het and *NestinERT2* Cond KO perinatal mice compared to controls (Fig. 2.10K-N).

To explore potential mechanisms for the moderate decrease in SVZ proliferation with loss of *Chd7*, I performed quantitative RT-PCR for genes involved in proliferation and cell cycle regulation on RNA derived from SVZ of control and *Ubc* Cond KO perinatal mice (Fig. 2.11). There were no significant changes in expression of the positive cell cycle regulators *Ccnd1* (cyclinD1), *Ccnd2* (cyclinD2), and *Cdk4,* or the negative regulators *Cdkn1a* ($p21^{Cip1}$) and *Cdkn1b* ($p27^{Kip1}$) (Beukelaers et al. 2012). Previous studies in mouse embryonic stem cells have demonstrated that CHD7 directly binds to precursor ribosomal RNA genes (rRNA) and regulates their transcription, resulting in global reductions in cell proliferation and protein levels upon loss of *Chd7* (Zentner et al. 2010). I observed a 26% reduction in 45S pre-rRNA transcripts in RNA isolated from *Ubc* Cond KO SVZ compared to controls (Fig. 2.10J). This is consistent with the 20-40% decrease in rRNA in *Chd7*-deficient mouse embryonic stem cells, inner ears, and eyes reported by Zentner et al. (Zentner et al. 2010). These data suggest that CHD7 effects on SVZ cell proliferation may be caused by global reductions in protein translation and ribosomal RNA. Importantly, my

studies do not rule out the possibility of smaller effects of CHD7 on other downstream genes that, in combination, may exert robust effects on the cell cycle.

I then tested the *in vitro* proliferation, self-renewal, and differentiation capacity of neonatal *Chd7*-deficient SVZ neural stem and progenitor cells by generating primary neurospheres from control, *Ubc* Cond Het, *Ubc* Cond KO, *Nestin-ERT2* Cond Het, and *Nestin-ERT2* Cond KO P1 mice (Figs. 2.12 and 2.13). As in adult mice, primary and secondary neurospheres from *Ubc* Cond KO and *Nestin-ERT2* Cond KO mice were reduced in size, frequency, self-renewal, and neuronal potential compared to controls. Neurospheres from *Ubc* Cond Het and *Nestin-ERT2* Cond Het mice exhibited intermediate phenotypes, with milder reductions compared to Cond KO mice. Together, the *in vivo* proliferation and *in vitro* neurosphere data from neonatal mice indicate that *Chd7* deficiency contributes to altered SVZ neural stem and progenitor cell function as early as P1.

Modulation of retinoic acid signaling attenuates defects in *Chd7*-deficient neurospheres and semicircular canals.

Retinoic acid (RA) signaling is necessary for proper development and maintenance of the forebrain and olfactory bulbs (LaMantia et al. 1993). RA treatment of neurospheres promotes self-renewal and neuronal differentiation (Wang et al. 2005), while inhibition of retinoic acid signaling leads to fewer, but larger neurospheres (Haskell et al. 2005). I hypothesized that alteration of RA

signaling by addition of RA or citral (inhibitor of RA synthesis) (Kikonyogo et al. 1999) in SVZ neurosphere cultures may influence the size, self-renewal and/or neuronal differentiation of *Chd7*-deficient neurospheres. Treatment of secondary neurospheres with RA produced smaller and more abundant neurospheres from control, *Nestin-ERT2* Cond Het, and *Nestin-ERT2* Cond KO mice (Fig. 2.14A,B). Interestingly, RA increased neuronal potential by 46% in *Nestin-ERT2* Cond KO secondary neurospheres, suggesting partial rescue of the observed neuronal differentiation defect (Fig. 2.14E).

Nestin-ERT2 Cond Het and *Nestin-ERT2* Cond KO secondary neurospheres increased in size by 19% and 39%, respectively, with 10 µM citral treatment, whereas the control was unchanged (Fig. 2.14C). Self-renewal of *Nestin-ERT2* Cond Het and *Nestin-ERT2* Cond KO secondary neurospheres was reduced by 15% and 27%, respectively, with 10 µM citral exposure, while self-renewal of control neurospheres was decreased by 58% (Fig. 2.14D). These data indicate that reduced *Chd7* dosage may confer protection against the reduction in self-renewal that occurs with citral treatment. Citral treatment did not alter the neuronal potential of control, *Nestin-ERT2* Cond Het, and *Nestin-ERT2* Cond KO secondary neurospheres (Fig. 2.14F). I conclude that decreased RA signaling does not further inhibit neuronal differentiation in *Chd7*-deficient neurospheres. Interestingly, glial and oligodendrocyte potential was unaffected for all genotypes regardless of RA or citral exposure (data not shown). My results provide evidence that increased RA signaling partially attenuates neuronal differentiation defects in *Chd7*-deficient neurospheres, without affecting

size or self-renewal. Conversely, inhibition of RA signaling with citral (1) moderately corrects size deficits in *Chd7* Cond Het and Cond KO neurospheres, (2) partially protects against further reduction of self-renewal capacity, and (3) has no effect on neuronal differentiation.

To test the *in vivo* effects of RA modulation in *Chd7*-deficient mice, I chose to investigate the inner ear, a tissue that displays highly penetrant defects and is easily accessible to pharmacological manipulation (Hurd et al. 2010; Hurd et al. 2011). Inner ears from *Chd7*$^{Gt/+}$ mice displayed truncation or agenesis of the E14.5 lateral semicircular canal (LC) (Fig. 2.14G,J) that was more severe after *in utero* exposure to RA (Fig. 2.14H,K). Interestingly, intrauterine citral treatment had no effect on wild-type ears (18/18) and on most *Chd7*$^{Gt/+}$ inner ears (20/28), whereas in roughly one-third of *Chd7*$^{Gt/+}$ inner ears (8/28), citral fully prevented the semicircular canal defects (Fig. 2.14L, Fig. 2.15). This rescue or prevention of inner ear defects in *Chd7*-deficient ears with modulation of RA levels suggests a mechanistic interaction between CHD7 function and RA signaling.

Chd7 directly regulates RA receptor and neuronal differentiation genes in neural stem and progenitor cells.

Given that CHD7 regulates transcription through chromatin remodeling (Hurd et al. 2010; Layman et al. 2011; Bouazoune et al. 2012), I predicted that loss of *Chd7* may disrupt expression of genes coding for transcription factors and retinoic acid signaling mediators involved in neuronal differentiation. To test this, I selected three genes (*Rarb*, *Rxrg*, and *Neurod1*) known to be involved in either

SVZ neurogenesis or neuronal differentiation by qRT-PCR. *Rarb* and *Rxrg* encode receptors that facilitate RA signaling (Rochette-Egly et al. 2009) and *Neurod1* encodes a basic helix-loop-helix transcription factor that promotes neuronal differentiation (Roybon et al. 2009). In *Ubc* Cond KO P1 SVZ, expression of *Rarb, Rxrg,* and *Neurod1* was reduced by 58%, 57%, and 55%, respectively, relative to controls (Fig. 2.16A). Consistent with prior studies showing that CHD7 and SOX2 interact in neural stem cells (Engelen et al. 2011), *Sox2* expression was unchanged in the SVZ of P1 *Ubc* Cond KO mice relative to control. Therefore, loss of *Chd7* results in down-regulation of key retinoic acid and neuronal differentiation genes but does not affect global expression of neural stem cell specific genes.

To determine whether CHD7 participates in a complex that binds directly to *Rarb*, *Rxrg,* and *Neurod1* promoter regions, I performed chromatin immunoprecipitation (ChIP) on chromatin isolated from P19 mouse embryonal carcinoma cells followed by qRT-PCR at evolutionarily conserved promoter regions. P19 cells are known to form neural stem cell-like neurospheres and differentiate in response to RA (McBurney et al. 1988; MacPherson et al. 1997). I observed enrichment for CHD7 at a subset of conserved promoter regions for *Rarb*, *Rxrg*, and *Neurod1* (Fig. 2.16B-D). Additionally, CHD7 was not bound to non-conserved regions in these genes. Together, my findings data provide new insights into interactions between RA signaling pathways and CHD7 in neural stem cells and the inner ear.

Discussion

Here I show that *Chd7* is expressed throughout the SVZ, RMS, and OB in adult mice. In both the adult and neonatal mouse, conditional loss of *Chd7* leads to proliferative, self-renewal, and neurogenic deficits both *in vivo* and *in vitro* with preserved or enhanced glial potential. Modulation of retinoic acid signaling by treatment with retinoic acid increases neuronal potential of *Chd7*-deficient neurospheres, while inhibition of retinoic acid signaling attenuates size and self-renewal deficits. Additionally, inhibition of retinoic acid signaling *in vivo* leads to correction of semicircular canal defects in the inner ears of *Chd7*-deficient mouse embryos. Expression of key retinoic acid receptor genes (*Rarb, Rxrg*) and at least one neurogenic transcription factor gene (*Neurod1*) is significantly reduced in the *Chd7* knockout SVZ; moreover, these genes are directly bound by CHD7-containing complexes in P19 neurospheres. Together, these findings indicate that *Chd7* and RA signaling promote proliferation, self-renewal, and neurogenesis during late embryogenesis and into adulthood, thereby suggesting a therapeutic avenue for intervention during pregnancy.

I propose a model whereby CHD7 regulates retinoic acid signaling and pro-neuronal genes to facilitate the transition from neural progenitor cell to neuroblast (Fig. 2.16E). *Chd7*-deficiency also leads to decreased progenitor cell differentiation into neuroblasts and a shift in cell fate towards the glial lineage. Interestingly, *in vitro* modification of retinoic acid signaling partially compensates for loss of *Chd7*, but does not fully correct the observed deficits in size, self-renewal, and neuronal differentiation. Like retinoic acid, CHD7 has been shown

to participate in several signaling pathways including Wnt (Takada et al. 2007), BMP (Hurd et al. 2012), FGF (Hurd et al. 2010; Layman et al. 2011; Hurd et al. 2012), and Notch (Hurd et al. 2012). Loss of *Chd7* in the SVZ and inner ear may cause deficits in these pathways, potentially explaining the partial rescue of neurosphere and inner ear defects by RA modulators.

Disrupted retinoic acid signaling leads to a variety of organ defects, many of which occur with *Chd7*-deficiency including abnormalities of the eye, heart, urogenital system, brain, and skeleton (Mark et al. 2009; Janssen et al. 2012). Treatment of *Nestin*-lineage *Chd7*-deficient neurospheres with retinoic acid increased neuronal potential, whereas citral treatment restored neurosphere size to control levels. Two retinoic acid receptor genes, *Rarb* and *Rxrg*, were also down-regulated in *Ubc* Cond KO SVZ. Interestingly, CHD7 was present in a complex that was directly bound to the highly conserved promoter regions of *Rarb* and *Rxrg* in P19 neurospheres. In the SVZ, reduced or absent retinoic acid signaling results in proliferative and neurogenic defects both *in vivo* and *in vitro* during development and in the adult, while increased retinoic acid leads to increased neurogenesis (Haskell et al. 2005; Wang et al. 2005). Consistent with these studies, my data imply a direct relationship between CHD7 and retinoic acid signaling that may contribute to the defects associated with CHARGE syndrome.

My findings also imply that decreased numbers of OB interneurons derived from the SVZ may contribute to OB hypoplasia in *Chd7*-deficient mice, in addition to the influence of reduced olfactory sensory neurons, as previously

reported (Layman et al. 2009). This result is in agreement with recently published data showing reduced olfactory bulb interneurons in adult mice with *Tlx-CreERT2* mediated conditional deletion of *Chd7* (Feng et al. 2013). Interestingly, the magnitude of olfactory bulb interneuron reductions was similar (40-60%) in my study and that of Feng et al., suggesting that reduction of *Chd7* gene function below 50% may not lead to further impairments in olfactory bulb development. Additionally, I observed ventriculomegaly in *Chd7*-deficient adult mice, consistent with a recent study of 40 *CHD7* mutation positive human fetuses which demonstrated a variety of brain malformations including arrhinencephaly and ventriculomegaly (Legendre et al. 2012). Similar to my data, disruption of SVZ neural stem cell function results in ventriculomegaly in mouse models of Bardet-Biedl syndrome and *Sox2*-deficiency (Ferri et al. 2004; Carter et al. 2012). CHD7 has been shown to regulate neurogenesis in the adult dentate gyrus of the hippocampus (Feng et al. 2013) and is also implicated in autism spectrum disorder (O'Roak et al. 2012). My findings therefore add to a growing body of work supporting a specific role for CHD7 function in SVZ, SGZ and olfactory neural stem cells, and perhaps in other regions of the nervous system that are affected in CHARGE. Notably, CHARGE individuals can also present with hindbrain and cerebellar abnormalities (Jongmans et al. 2006; Sanlaville et al. 2006; Sanlaville et al. 2007; Legendre et al. 2012), and future studies should help clarify whether *CHD7* also regulates neural stem and progenitor cells in these regions. My work opens new avenues for investigation of CHD7 activity in stem

cell populations affected by CHARGE syndrome, and should help guide future work toward development of diagnostic and therapeutic treatments.

Acknowledgements

I would like to thank Wanda Layman for generating the original mice for these experiments, Sophia Frank for assistance with tissue preparation and immunofluorescence experiments, Mark Durham for assistance with neurosphere cultures, Elizabeth Hurd, Jennifer Skidmore and Donald Swiderski for assistance with the inner ear experiments and Ethan Sperry for assistance with the qPCR and ChIP experiments.

Chapter 2 Notes

A revised version of Chapter 2 has been published as Micucci, J.A, Layman, W.S, Hurd, E.A., Sperry, E.D., Frank, S.F., Durham, M.A., Swiderski, D.L., Skidmore, J.M., Scacheri, P.C., Raphael, Y., and Martin, D.M. (2013). CHD7 and retinoic acid signaling cooperate to regulate neural stem cell and inner ear development in mouse models of CHARGE syndrome. *Human Molecular Genetics*, 2013 Sep 17.

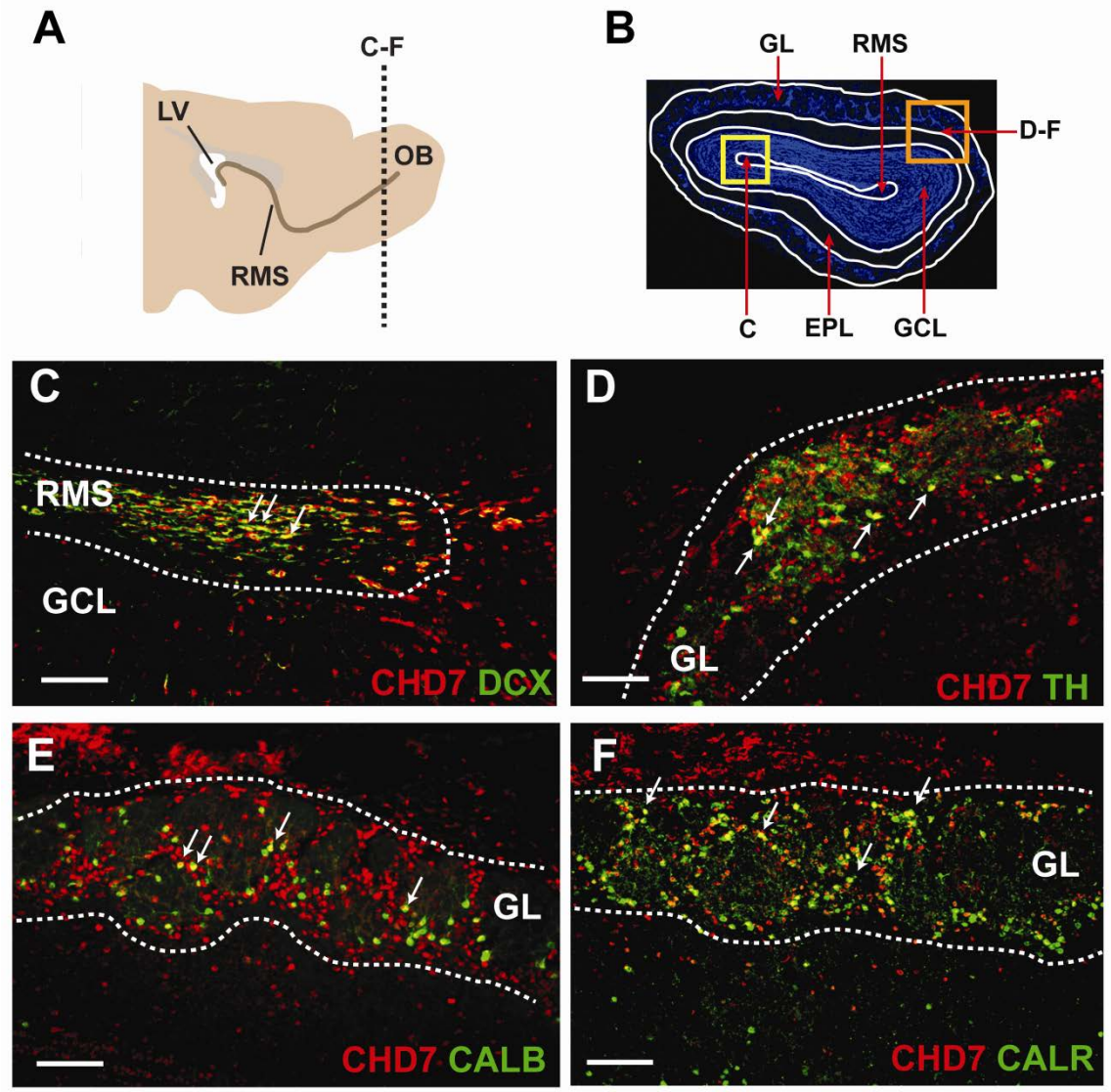

Figure 2.1: CHD7 co-localizes with immature and mature olfactory bulb neurons. (**A**) Schematic sagittal view of an adult mouse brain showing location of coronal sections through the olfactory bulb (OB) in (**C-F**) (dotted line, OB). (**B**) Schematic of a DAPI-stained coronal section through the olfactory bulb denoting location of panel **C** in the rostral migratory stream (RMS, yellow box) and panels (**D-F**) in the glomerular layer (GL, orange box). (**C-F**) Immunofluorescence on adult tissues shows CHD7 co-localization (denoted with white arrowheads) with Doublecortin (DCX) in immature neurons in the RMS (**C**), with Tyrosine hydroxylase (TH) in dopaminergic interneurons (**D**) and with Calbindin (CALB) and Calretinin (CALR) in GABAergic interneurons in the GL (**E,F**). Scale bars in (**C-F**): 75 μm.

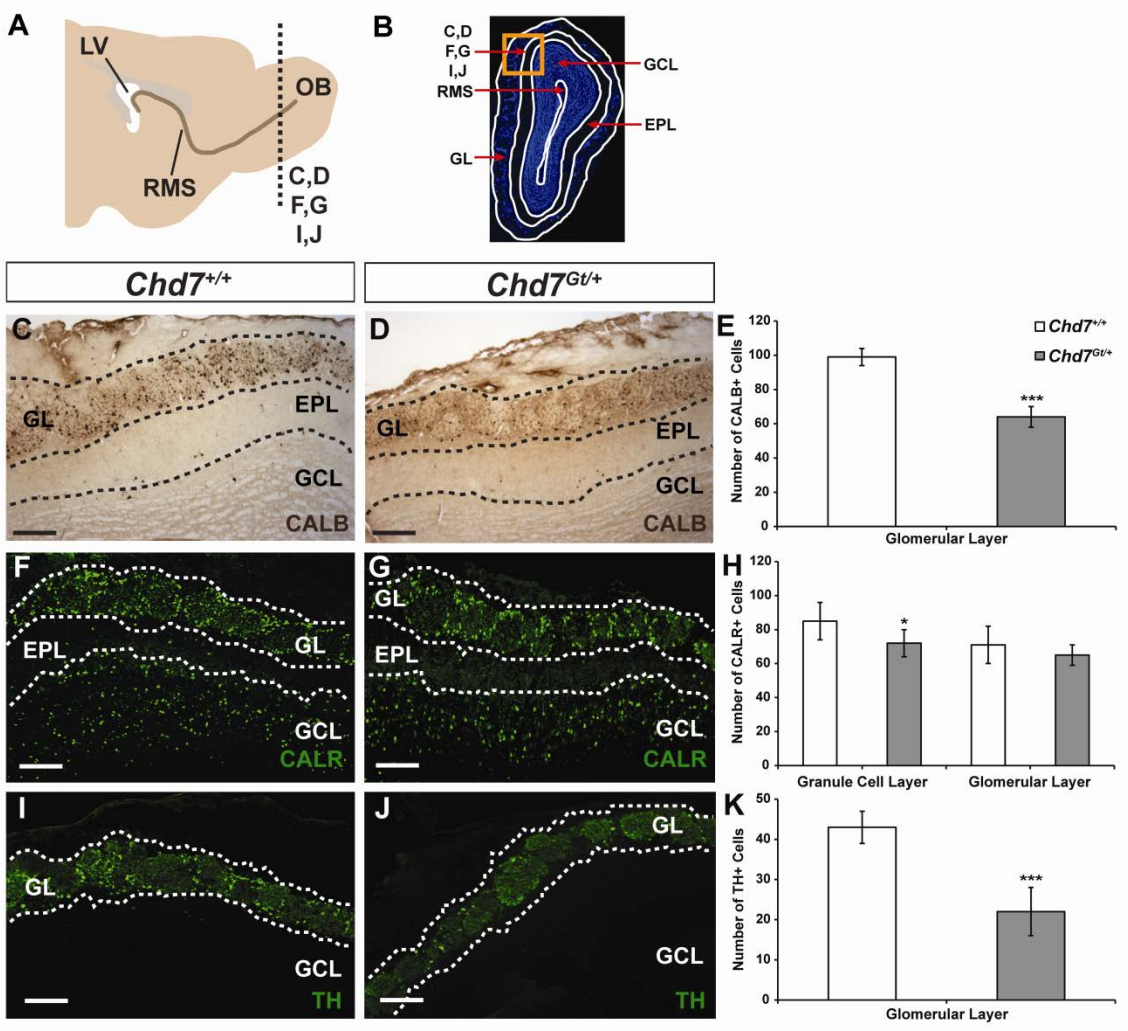

Figure 2.2: Adult heterozygous *Chd7* mice have fewer mature olfactory bulb interneurons. (**A**) Schematic sagittal view of an adult mouse brain showing location of coronal sections through the olfactory bulb (OB) in (**C,D,F,G,I,J**) (dotted line, OB). (**B**) Schematic of a DAPI-stained coronal section through the olfactory bulb denoting location of panels (**C,D,F,G,I,J**) in the glomerular and granule cell layers (GL, GCL, orange box). Immunolabeling with anti-Calbindin (CALB, **C,D**), anti-Calretinin (CALR, **F,G**) and anti-Tyrosine hydroxylase (TH, **I,J**) antibodies in wild type and *Chd7* heterozygous null (*Chd7*$^{Gt/+}$) mice shows 35% and 48% reductions in the number of CALB+ and TH+ interneurons in the GL, respectively, and 15% reduction in the number of CALR+ interneurons in the GCL of *Chd7*$^{Gt/+}$ mice compared to wild type (**E,H,K**). Scale bars in (**C,D**), (**F,G**), (**I,J**): 75 µm. Error bars in (**E,H,K**) indicate standard error of the mean (SEM) (n=3 per genotype). **p*<0.05, ****p*<0.001 by unpaired Student's t-test. Other abbreviations: EPL: external plexiform layer

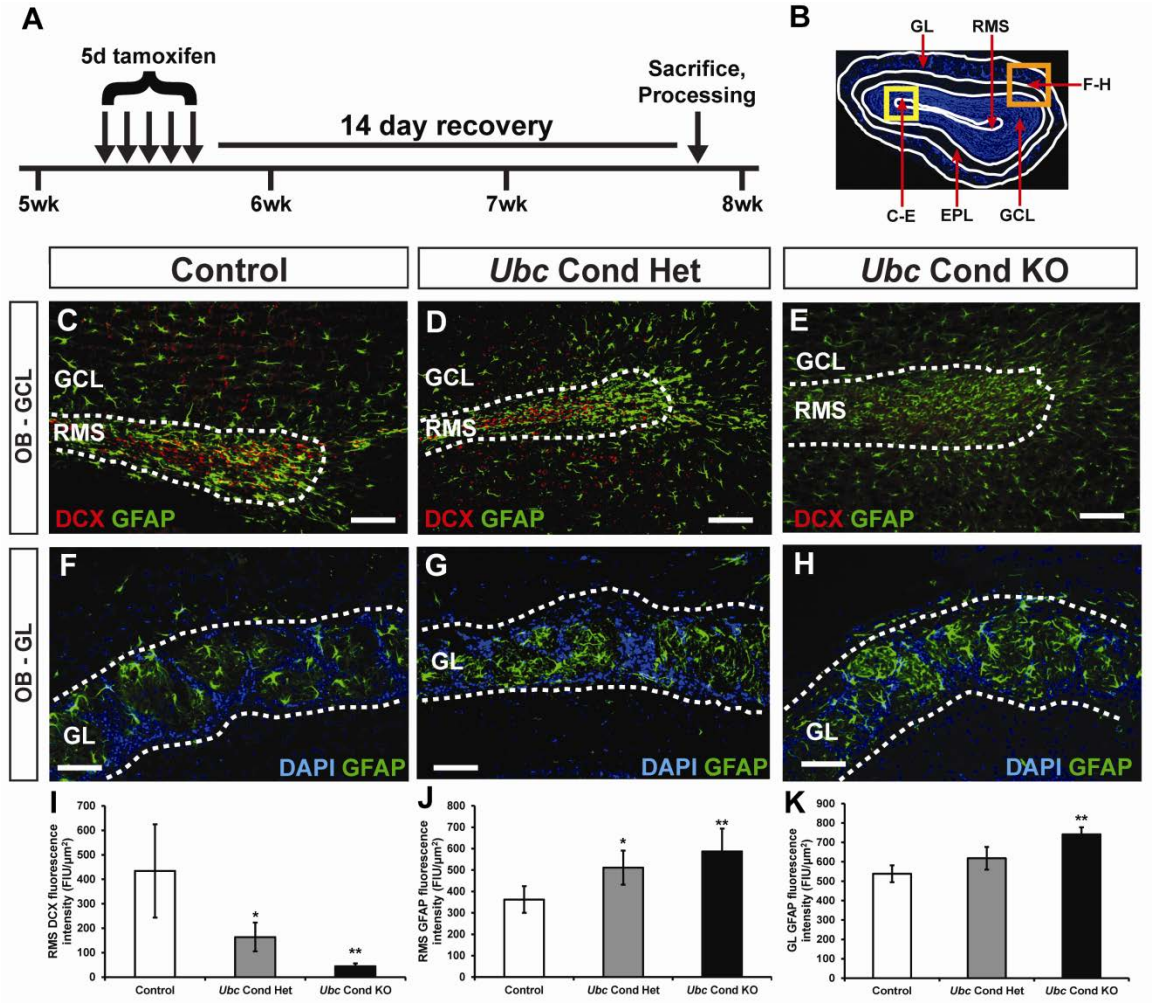

Figure 2.3: *Chd7*-deficiency results in fewer immature neurons with glial expansion in the adult olfactory bulb.
(**A**) Schematic showing the Tamoxifen dosing regimen for adult mice. At five weeks of age, mice were treated with a single dose of Tamoxifen (0.2 mg/gbw) by daily intraperitoneal injection for five days, allowed to recover for 14 days then processed for frozen sectioning. (**B**) Schematic of a DAPI-stained coronal section through the olfactory bulb denoting location of panels (**C-E**) in the rostral migratory stream (RMS, yellow box) and panels (**F-H**) in the glomerular layer (GL, orange box).
(**C-E**) Immunofluorescence on coronal sections through the OB showing reduced DCX+ neuroblasts in the RMS of *Ubc* Cond Het (**D**) and *Ubc* Cond KO (**E**) mice compared to control (**C,** quantified in **I**). Immunofluorescence on coronal sections through the OB showing increased glia in the RMS (**C-E**) and GL (**F-H**) of *Ubc* Cond Het (**D,G**) and *Ubc* Cond KO (**E,H**) mice compared to control (**C,F**, quantified in **J,K**). Scale bars in (**C-E**), (**F-H**): 75 μm. Error bars in (**I-K**) indicate SEM (n=3 per genotype). **p*<0.05, ***p*<0.01 by unpaired Student's t-test.

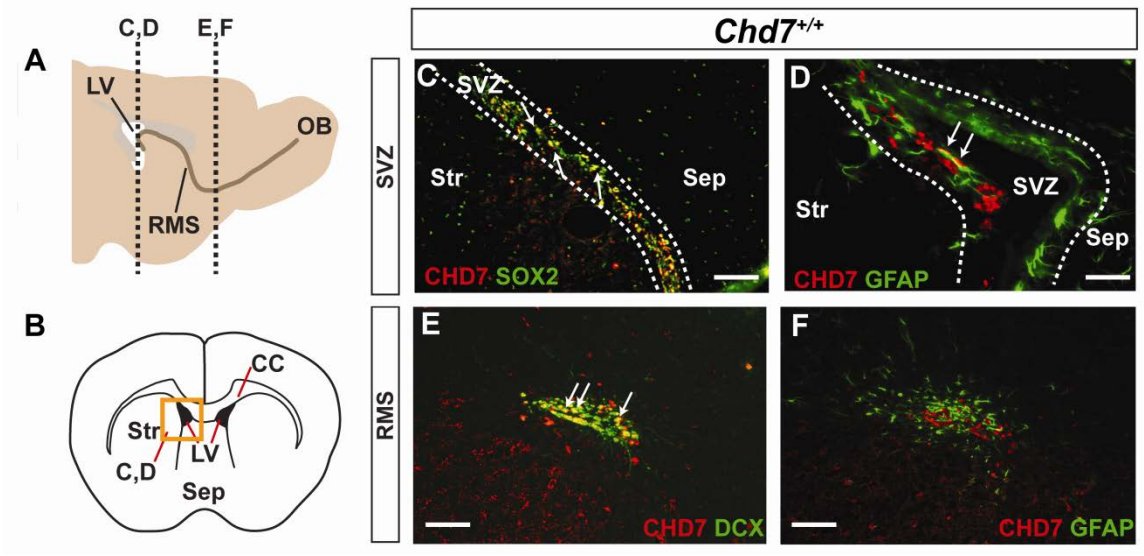

Figure 2.4: *Chd7* is expressed in neural stem cells and neuroblasts in the adult mouse SVZ and RMS.
(**A**) Schematic sagittal view of an adult mouse brain showing location of coronal sections through the subventricular zone (SVZ) of the lateral ventricle (LV) in (**C,D**) (dotted line, LV) and sections through the RMS in (**E,F**) (dotted line, RMS). (**B**) Diagram of a coronal section through adult mouse forebrain showing the area of SVZ (orange box) imaged in (**C,D**). Double immunofluorescence shows that CHD7 co-localizes with a subset of SOX2+ (white arrows, **C**) and GFAP+ (white arrows, **D)** neural stem and progenitor cells, but not with corpus callosum GFAP+ glial cells (**D**). In the RMS, CHD7 co-localizes with DCX in migrating neuroblasts and immature neurons (white arrows, **E**) and CHD7+ cells are surrounded by a sheath of GFAP+ glia (**F**). Scale bars in (**C,E,F**): 75 µm, (**D**): 25 µm. Other abbreviations: Str: striatum, Sep: septum, CC: corpus callosum.

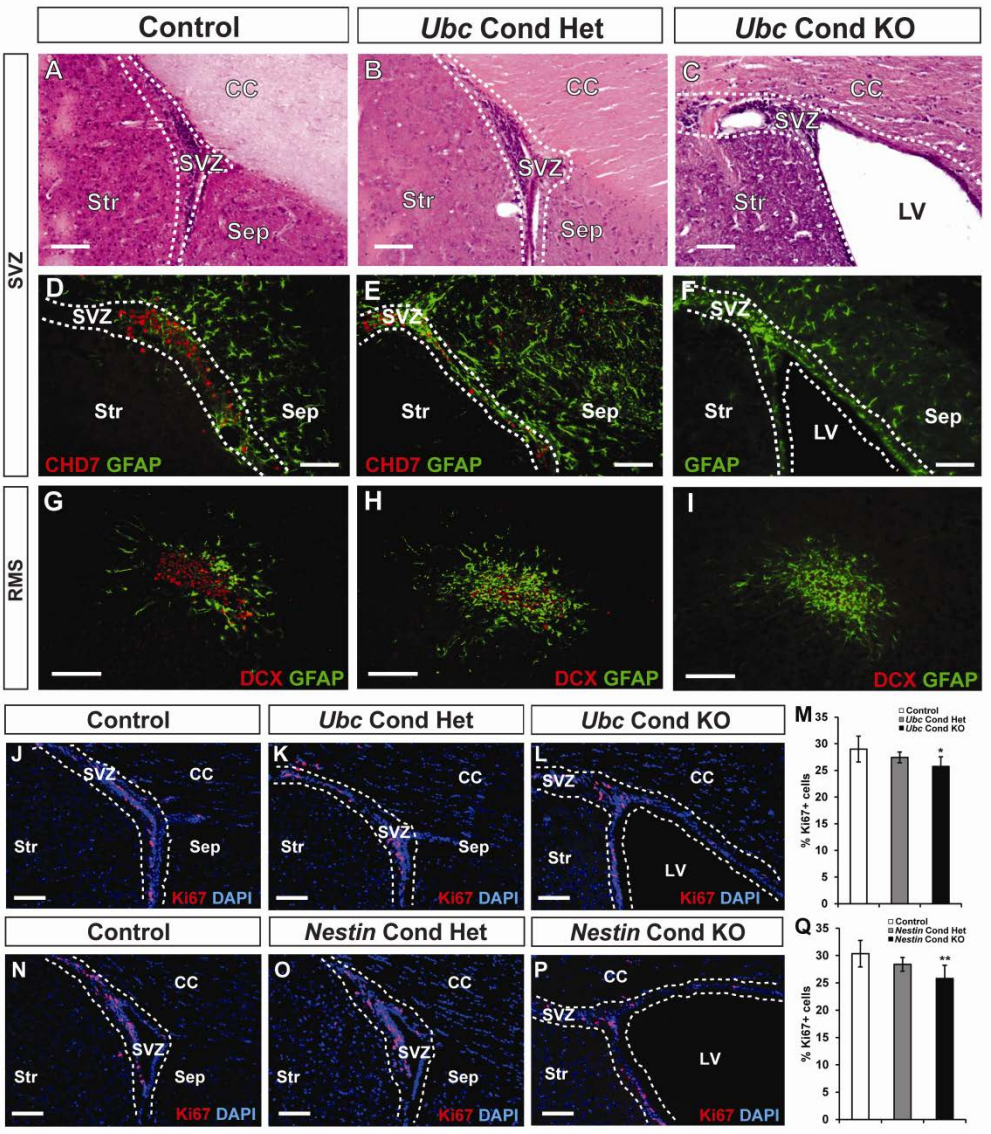

Figure 2.5: Loss of *Chd7* leads to ventriculomegaly and mild proliferative defects in the adult mouse SVZ.
(**A-I**) Hematoxylin and eosin staining and immunofluorescence analysis of adult SVZ in control, *Ubc* Cond Het and *Ubc* Cond KO mice. (**A-C**) Reduced *Chd7* dosage results in ventriculomegaly in *Ubc* Cond KO (**C**) mice compared to control and *Ubc* Cond Het (**A,B**). (**D-F**) CHD7 immunofluorescence is decreased in *Ubc* Cond Het (**E**) and *Ubc* Cond KO SVZ (**F**) compared to control (**D**), confirming gene deletion. (**G-I**) DCX-positive neuroblasts are reduced in the RMS in *Ubc* Cond Het (**H**) and *Ubc* Cond KO (**I**) mice compared to control (**G**). (**J-L**) and (**N-P**) Representative coronal sections through the SVZ of adult control (**J,N**), *Ubc* Cond Het (**K**), *Ubc* Cond KO (**L**), *Nestin* Cond Het (**O**) and *Nestin* Cond KO (**P**) mice processed for immunofluorescence with anti-Ki67 antibody and counterstained with DAPI.(**M,Q**) Quantification showing the percentage of Ki67+ cells relative to the total number of DAPI-stained cells in control, *Ubc* Cond Het and *Ubc* Cond KO and control, *Nestin* Cond Het and *Nestin* Cond KO. The percentage of Ki67+ cells in the SVZ of *Ubc* Cond KO and *Nestin* Cond KO adult mice is decreased by 11% and 15%, respectively, compared to controls. Scale bars in (**A-I**), (**J-L**), (**N-P**): 75 µm. Error bars in (**M,Q**) indicate SEM (n=3 per genotype). *p<0.05, **p<0.01 by unpaired Student's t-test.

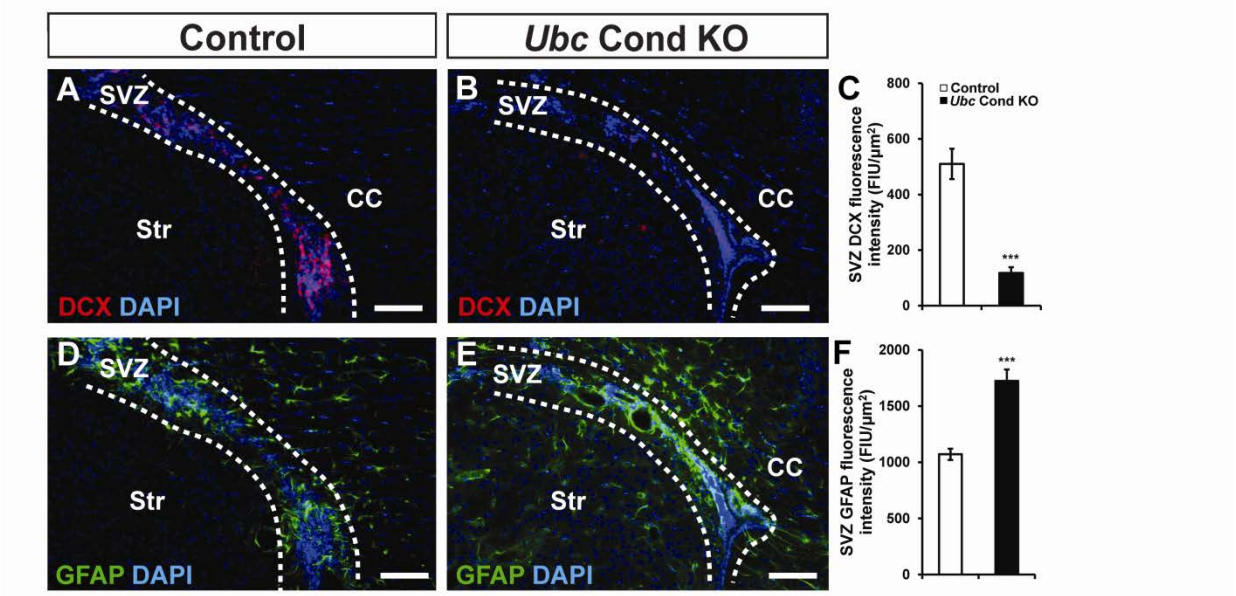

Figure 2.6: *Chd7*-deficient adult SVZ displays loss of neuroblasts and increased glia. (**A,B**) and (**D,E**) show immunofluorescence of coronal sections from adult control and *Ubc* Cond KO SVZ for neuroblasts (DCX, **A,B**) and neural stem cells/glia (GFAP, **D,E**). There is a 76% reduction in DCX immunofluorescence and a 61% increase in GFAP immunofluorescence between control and *Ubc* Cond KO brains (quantified in **C,F**) . Error bars in (**C,F**) indicate SEM (n=3 per genotype). ***p<0.001 by unpaired Student's t-test. Other abbreviations: FIU: fluorescence intensity unit. Scale bars in (**A,B,D,E**): 75 μm.

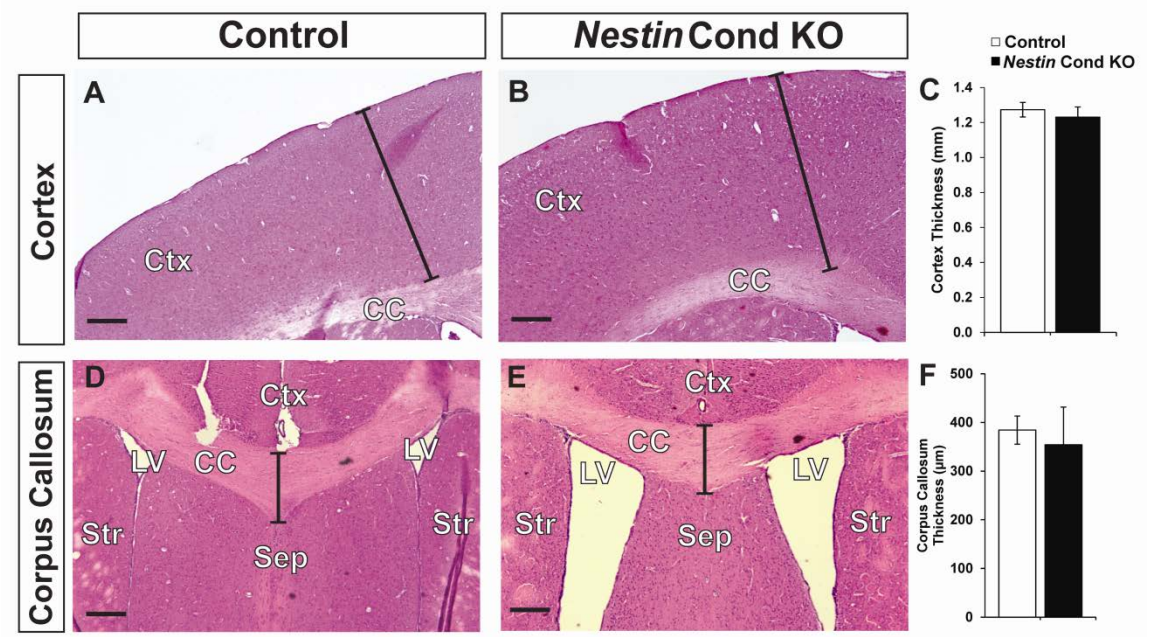

Figure 2.7: Cortex and corpus callosum size are unchanged in adult *Nestin-Cre* conditional *Chd7* knockout mice.
(**A,B**) and (**D,E**) show hematoxylin and eosin staining of coronal sections from adult control and *Nestin* Cond KO cortex (Ctx) and corpus callosum (CC), respectively. There are no differences in thickness of cortex and corpus callosum between control and *Nestin* Cond KO brains as quantified in (**C**) and (**F**), but enlarged lateral ventricles are present in *Nestin* Cond KO brains (**E**) as observed in *Ubc* Cond KO adult mice (**Fig. 2C**). Scale bars in (**A,B,D,E**): 250 µm.

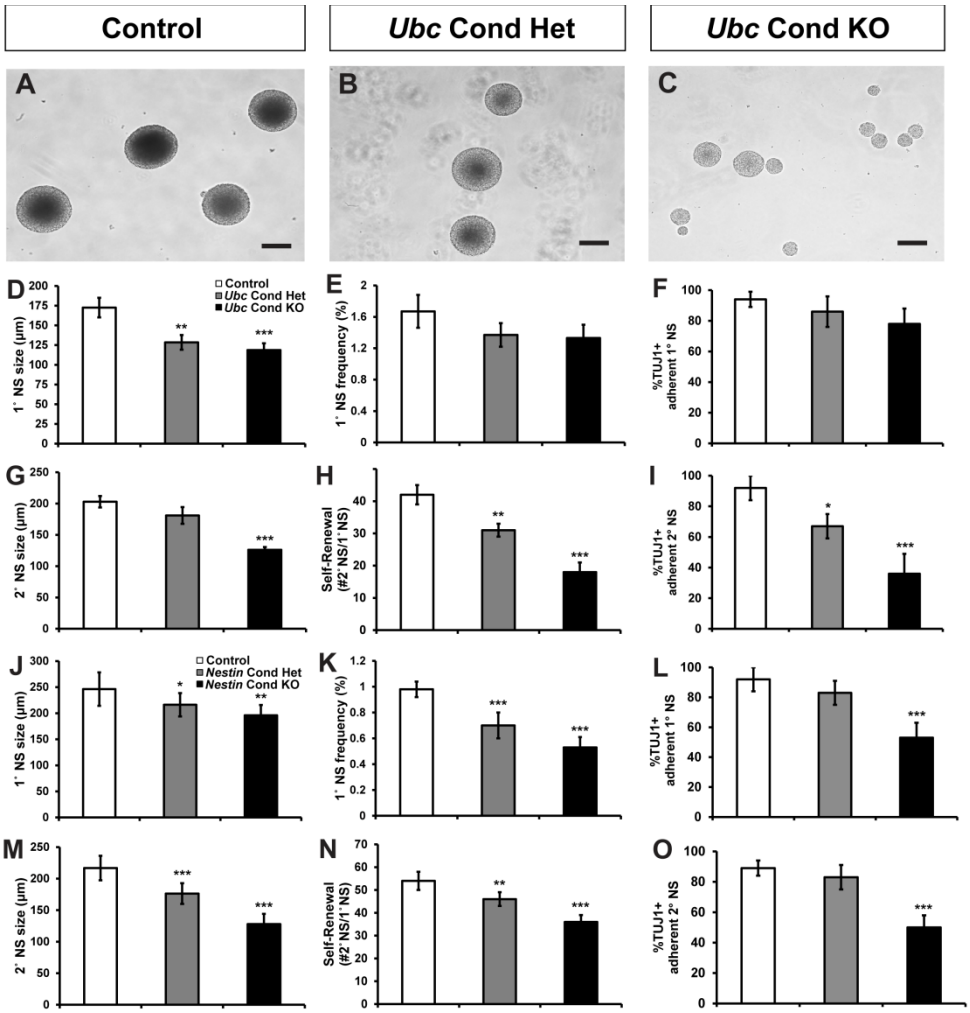

Figure 2.8: Neural stem cells derived from adult *Chd7* conditional knockout mice exhibit impaired proliferation, self-renewal, and neuronal potential.
(**A-C**) Representative images of neurospheres derived from SVZ tissue of adult control (**A**), *Ubc* Cond Het (**B**), and *Ubc* Cond KO (**C**) mice. (**D-F**), (**G-I**), (**J-L**), and (**M-O**) show quantification of primary and secondary neurosphere size (µm), primary neurosphere frequency, secondary neurosphere self-renewal (expressed as the number of secondary neurospheres formed from a single primary neurosphere) and percentage of neuronal lineage-positive (TUJ1+) differentiated adherent neurospheres from control, *Ubc* Cond Het, *Ubc* Cond KO, *Nestin* Cond Het, and *Nestin* Cond KO adult mice. Neurospheres derived from *Ubc* Cond Het and *Ubc* Cond KO adult mice exhibit *Chd7* dosage-dependent reductions in primary neurosphere size (**D**), as well as secondary neurosphere size (**G**) and self-renewal (**H**) compared to controls. Neurospheres generated from *Nestin* Cond Het and *Nestin* Cond KO adult mice show *Chd7* dosage-dependent reductions in primary neurosphere size (**J**) and frequency (**K**), and secondary neurosphere size (**M**) and self-renewal (**N**), compared to controls. (**E**) There is no change in *Ubc* Cond Het or *Ubc* Cond KO primary neurosphere frequency compared to controls. (**I,L,O**) Neuronal potential is reduced by 61% in *Ubc* Cond KO secondary neurospheres (**I**), 42% in *Nestin* Cond KO primary neurospheres (**L**) and 44% in *Nestin* Cond KO secondary neurospheres (**O**) compared to controls. There is no change in neuronal potential of *Ubc* Cond Het or *Ubc* Cond KO primary neurospheres compared to controls (**F**). Scale bars in (**A-C**): 100 µm. Error bars in (**D-O**) indicate SEM (n=3 per genotype). **p*<0.05, ***p*<0.01, ****p*<0.001 by unpaired Student's t-test. Other abbreviations: 1°NS: primary neurosphere, 2°NS: secondary neurosphere.

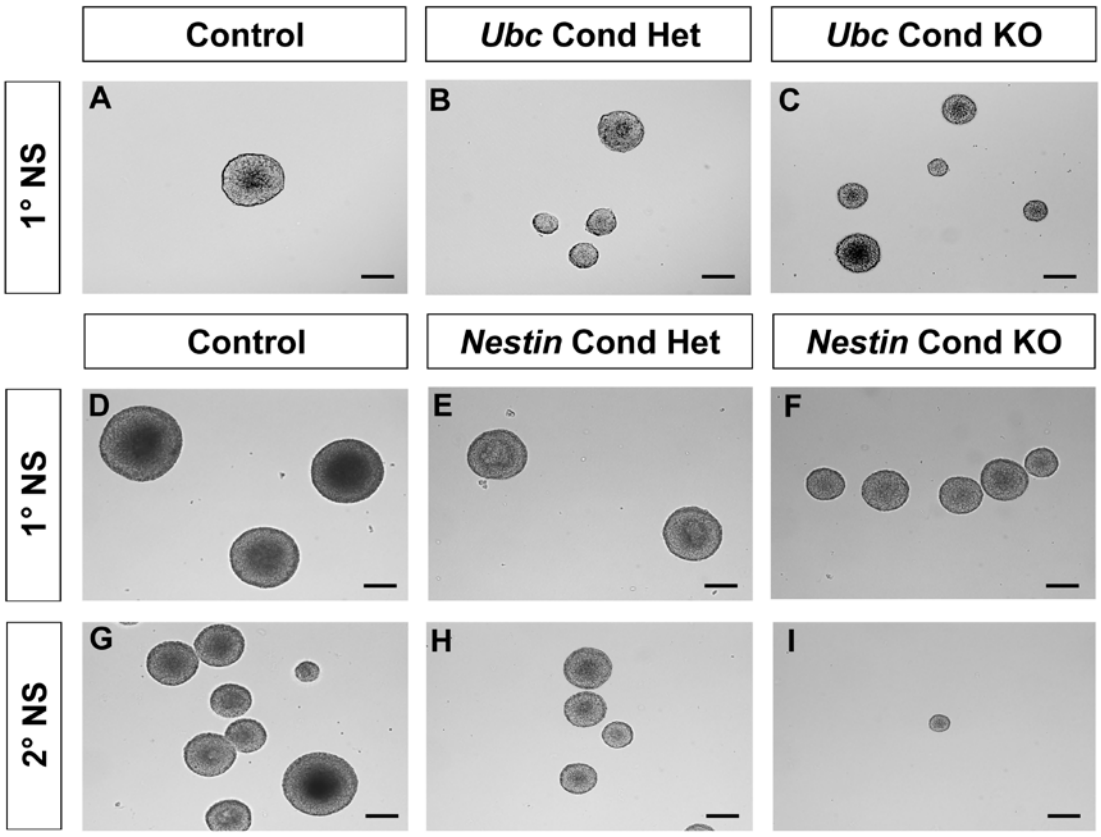

Figure 2.9: Reduction of *Chd7* dosage leads to decreased adult SVZ-derived neurosphere size. (**A-C**) Representative images of primary neurospheres derived from SVZ of adult control (**A**), *Ubc* Cond Het (**B**) and *Ubc* Cond KO mice (**C**). (**D-I**) Representative images of primary and secondary neurospheres derived from SVZ of adult control (**D,G**), *Nestin* Cond Het (**E,H**) and *Nestin* Cond KO mice (**F,I**). Scale bars in (**A-I**): 100 µm.

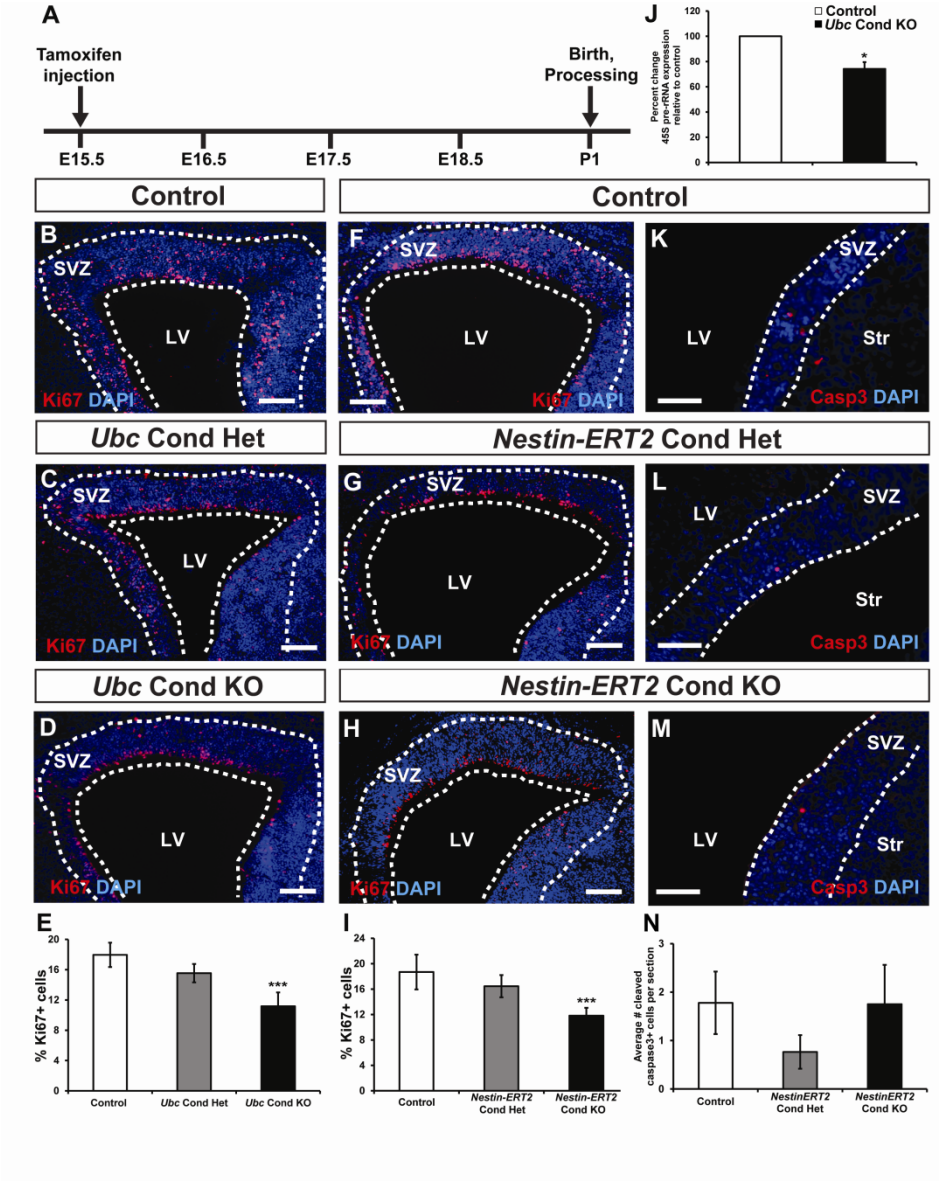

Figure 2.10: Postnatal day 1 *Chd7* conditional knockout mice display reduced SVZ proliferation. (**A**) Schematic showing the Tamoxifen dosing regimen where pregnant females received a single intraperitoneal injection of Tamoxifen (0.2 mg/gbw) at embryonic day 15.5 (E15.5). (**B-D**), (**F-H**), and (**K-M**) Representative coronal sections showing immunofluorescence for the proliferative marker Ki67 or apoptosis marker cleaved caspase 3 (Casp3) with DAPI counterstain in the SVZ of postnatal day 1 (P1) control (**B,F,J**), *Ubc* Cond Het (**C**), *Ubc* Cond KO (**D**), *Nestin-ERT2* Cond Het (**G,K**), and *Nestin-ERT2* Cond KO (**H,L**) mice. (**E,I**) Quantification showing the percentage of Ki67+ cells relative to the total number of DAPI-stained cells in control, *Ubc* Cond Het, and *Ubc* Cond KO (**E**), and *Nestin-ERT2* Cond Het and *Nestin-ERT2* Cond KO (**I**) P1 SVZ. The percentage of Ki67+ cells are reduced by 37% and 38% in the SVZ of *Ubc* Cond KO and *Nestin-ERT2* Cond KO P1 mice, respectively, compared to controls. (**J**) Quantitative PCR shows that 45S pre-rRNA is decreased by 26% in *Ubc* Cond KO SVZ compared to controls. (**K-N**) There is no change in the number of cleaved caspase 3+ (Casp3) cells per section in *Nestin-ERT2* Cond Het (**L**) and *Nestin-ERT2* Cond KO (**M**) P1 SVZ compared to control (**K**). Scale bars in (**B-D**), (**F-H**): 75 µm, (**K-M**): 50 µm. Error bars in (**E,I,J,N**) indicate SEM (n=3 per genotype). **p*<0.05, ****p*<0.001 by unpaired Student's t-test.

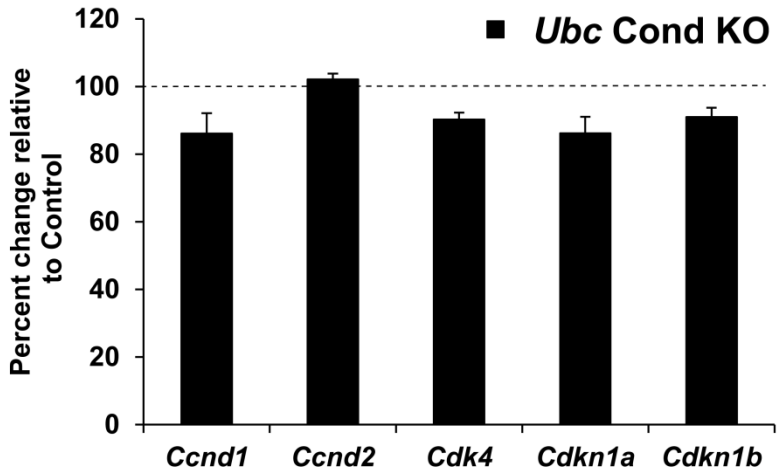

Figure 2.11: Cell cycle and proliferation markers are unchanged with loss of *Chd7* in the perinatal SVZ.
Quantitative RT-PCR on RNA isolated from SVZ of P1 control and *Ubc* Cond KO mice shows no changes in expression of proliferation or cell cycle regulatory genes CyclinD1 (*Ccnd1*), CyclinD2 (*Ccnd2*), Cdk4 (*Cdk4*), $p21^{Cip1}$ (*Cdkn1a*) and $p27^{Kip1}$ (*Cdkn1b*) . Black dashed line indicates control gene expression levels and error bars indicate SEM (n=3 per genotype).

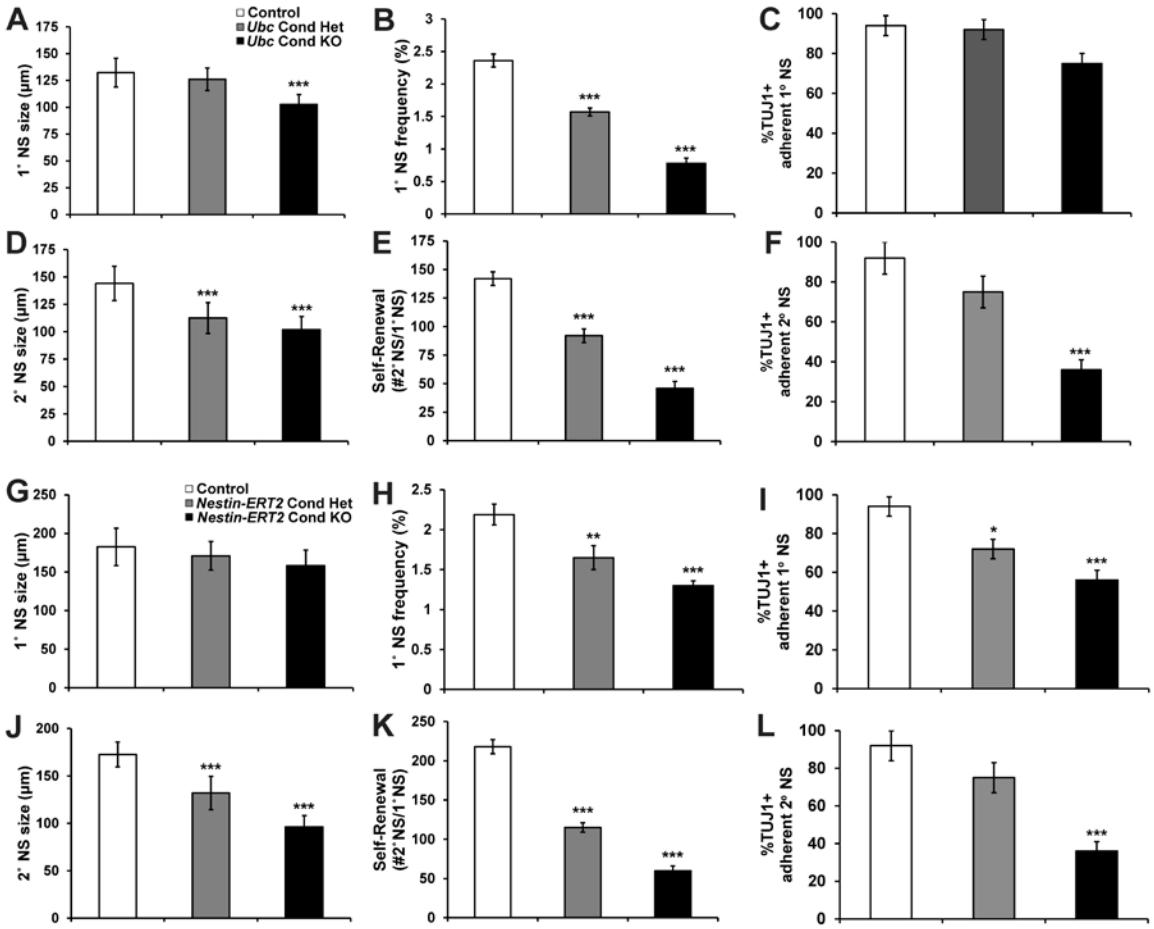

Figure 2.12: Neurospheres derived from postnatal day 1 *Chd7* conditional knockout mice exhibit impaired proliferation, self-renewal and neuronal potential.
(**A-L**) Quantification of the size (µm) of primary and secondary neurospheres, frequency of primary neurospheres, self-renewal and percentage of neuronal lineage-positive (TUJ1+) differentiated adherent neurospheres from control, *Ubc* Cond Het, *Ubc* Cond KO, *Nestin-ERT2* Cond Het and *Nestin-ERT2* Cond KO P1 mice. There are *Chd7* dosage-dependent reductions in primary neurosphere size (**A**) and frequency (**B**) and secondary neurosphere size (**D**) and self-renewal (**E**) from *Ubc* Cond Het and *Ubc* Cond KO P1 mice compared to controls. *Chd7* dosage-dependent reductions are also present in primary neurosphere frequency (**H**) and secondary neurosphere size (**J**) and self-renewal (**K**) in *Nestin-ERT2* Cond Het and *Nestin-ERT2* Cond KO P1 mice compared to controls. There are no changes in primary neurosphere size in *Ubc* Cond Het (**A**), *Nestin-ERT2* Cond Het (**G**) and *Nestin-ERT2* Cond KO (**G**) mice compared to controls. Among primary neurospheres, those from *Nestin-ERT2* Cond Het and *Nestin-ERT2* Cond KO P1 mice exhibit 22% and 40% reductions in neuronal potential, respectively, compared to controls (**F,L**). Neuronal potential is reduced by 79% for *Ubc* Cond KO secondary neurospheres (**F**) and 61% for *Nestin-ERT2* Cond KO secondary neurospheres (**L**) compared to controls. Neuronal potential of *Ubc* Cond Het primary and secondary neurospheres (**C,F**), *Ubc* Cond KO primary neurospheres (**C**) and *Nestin-ERT2* Cond Het secondary neurospheres (**L**) are unchanged compared to controls. Error bars in (**A-L**) indicate SEM (n=3 per genotype). *p<0.05, **p<0.01, ***p<0.001 by unpaired Student's t-test.

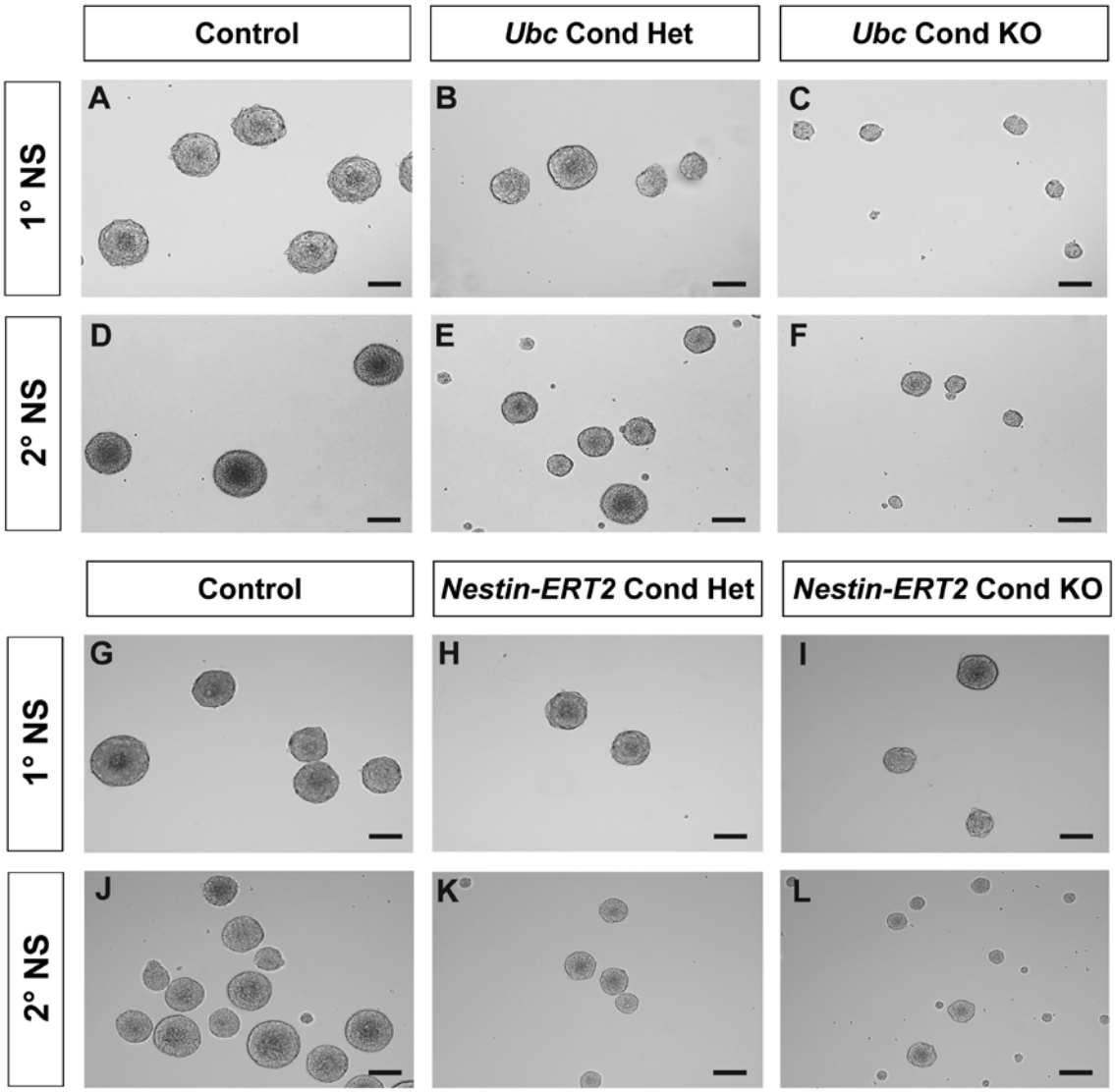

Figure 2.13 Loss of *Chd7* results in reduced size of perinatal SVZ-derived neurospheres. (**A-F**) Representative images of primary and secondary neurospheres derived from SVZ of adult control (**A,D**), *Ubc* Cond Het (**B,E**) and *Ubc* Cond KO mice (**C,F**). (**G-L**) Representative images of primary and secondary neurospheres derived from SVZ of adult control (**G,J**), *Nestin* Cond Het (**H,K**) and *Nestin* Cond KO mice (**I,L**). Scale bars in (**A-L**): 100 μm.

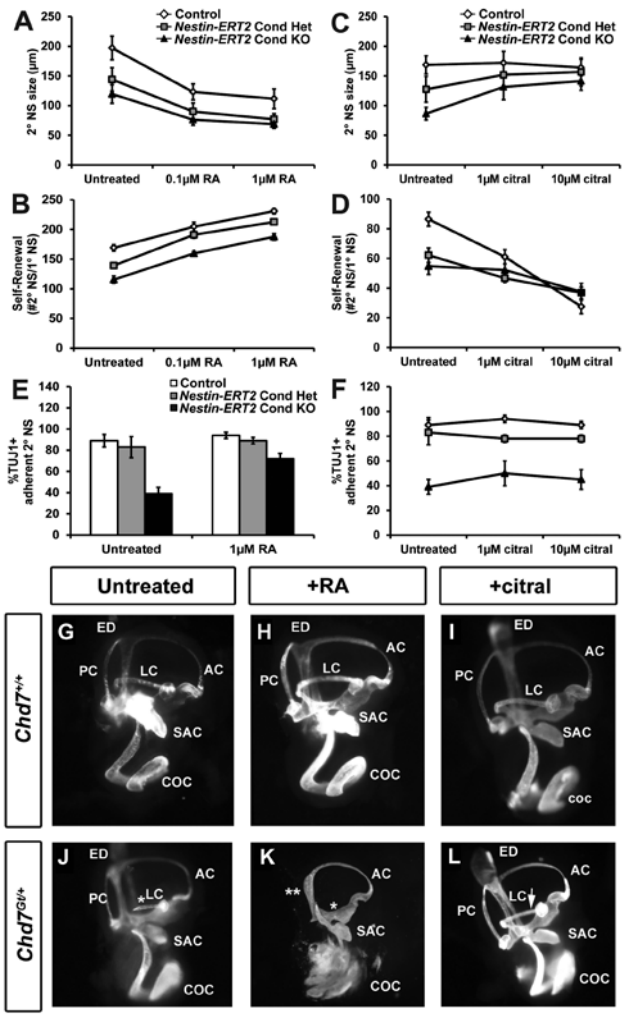

Figure 2.14: Modified retinoic acid signaling influences defects in *Chd7*-deficient neurospheres and semicircular canal development.
(**A-F**) Secondary neurospheres were derived from P1 control, *Nestin-ERT2* Cond Het and *Nestin-ERT2* Cond KO mice then treated with varying concentrations of all-trans retinoic acid (RA, **A,B,E**) or the retinoic acid signaling inhibitor citral (**C,D,F**), and assayed for changes in size, self-renewal, and neuronal potential. (**A,B**) Treatment with RA (0.1µM or 1µM) results in smaller neurospheres (**A**) and increased self-renewal (**B**) for all three genotypes. (**C,D**) Treatment with citral (1µM or 10µM) in non-adherent neurosphere cultures causes increased *Nestin-ERT2* Cond Het and *Nestin-ERT2* Cond KO neurosphere size (**C**), and reduced self-renewal (**D**) for all three genotypes. (**E**) Treatment of differentiating, adherent *Nestin-ERT2* Cond KO neurospheres with 1µM RA resulted in a 33% increase (from 39% to 72%) in the proportion of *Nestin-ERT2* Cond KO TUJ1+ colonies compared to control TUJ1+ colonies. (**F**) Neuronal potentials of *Nestin-ERT2* Cond KO differentiating neurospheres were unaffected by citral treatment. (**G-L**) Pregnant females were untreated or treated with either RA by oral gavage or citral by intraperitoneal injection at E7.5, then embryos were extracted at E14.5 and processed for inner ear paint-filling. (**G-I**) Wild type embryos are unaffected by treatment with either RA or citral. *Chd7*$^{Gt/+}$ embryos consistently display lateral semicircular canal truncation (LC, denoted by white asterisk) in untreated conditions (**J**) which worsen with RA treatment (**K**) while treatment with citral results in rescue of the LC truncation in 29% (8/28 ears) of mutant inner ears (denoted by white arrowhead, **L**). Error bars in (**A-F**) indicate SEM (n=3 per genotype). Other abbreviations: ED: endolymphatic duct, AC: anterior semicircular canal, SAC: saccule, COC: cochlea.

		Citral	Retinoic Acid
***Chd7*$^{+/+}$**	**normal**	18	6
	mutant	0	0
	total	18	6

***Chd7*$^{Gt/+}$**	**normal**	8	0
	mutant	20	8
	total	28	8

Figure 2.15 Inhibition of retinoic acid signaling by citral prevents semicircular canal defects in the developing *Chd7*-deficient inner ear.
Pregnant females were treated with citral by intraperitoneal injection or retinoic acid by oral gavage at E7.5, then embryos were extracted at E14.5 and processed for inner ear paintfilling. 29% (8/28 ears) of *Chd7*$^{Gt/+}$ embryos showed wild type inner ear morphology and rescue of semicircular canal hypoplasia (n=18 wild type ears, n=28 *Chd7*$^{Gt/+}$ ears). Retinoic acid treatment showed no effects on wild type inner ear morphology and did not rescue semicircular canal defects in *Chd7*$^{Gt/+}$ embryos (n= 6 wild type ears, n = 8 *Chd7*$^{Gt/+}$ ears).

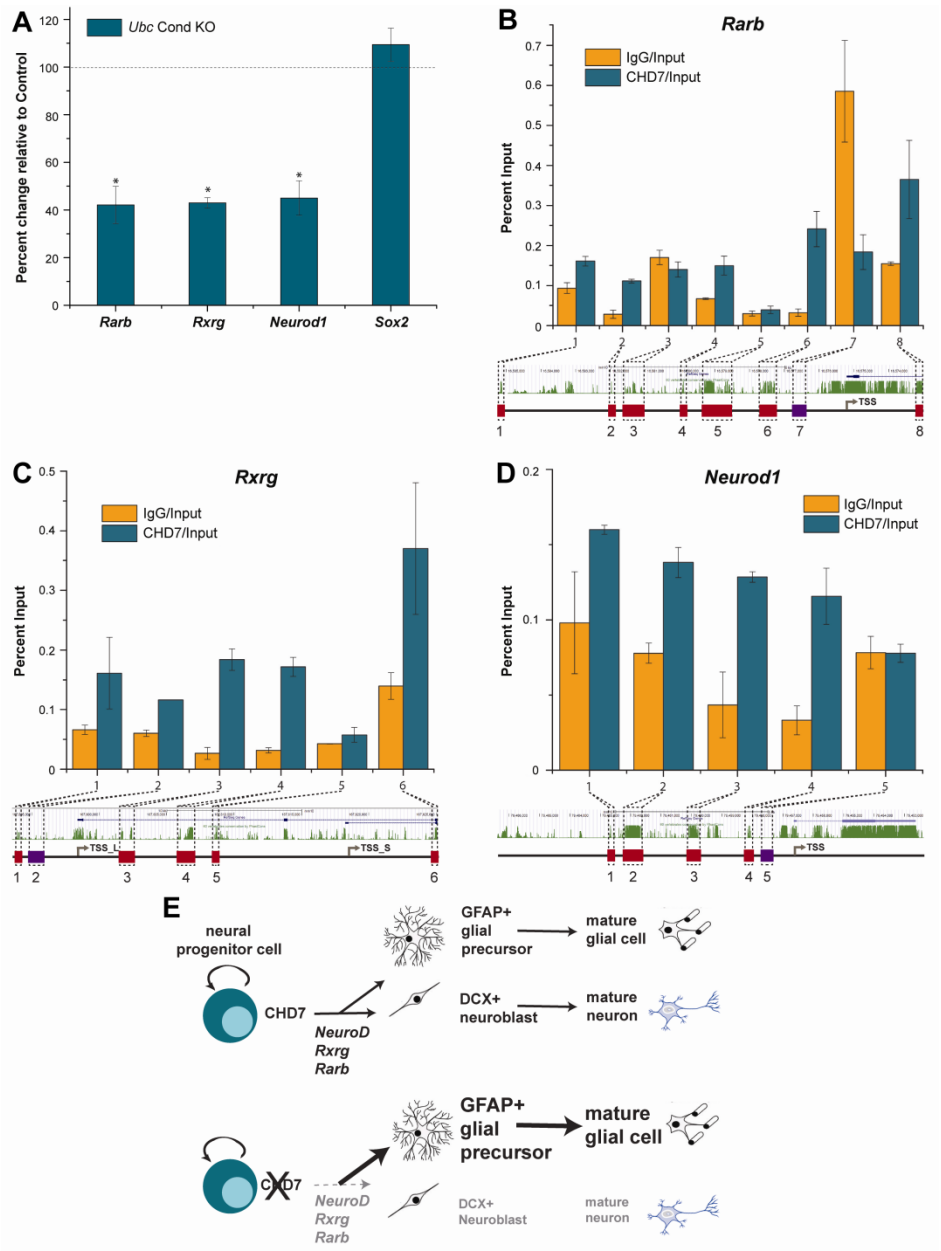

Figure 2.16 CHD7 binds to the promoters of retinoic acid receptor and pro-neuronal transcription factor genes and regulates their expression.
(**A**) qRT-PCR analysis of total RNA from P1 control and *Ubc* Cond KO microdissected SVZ shows expression levels of *Rarb*, *Rxrg*, *Neurod1,* and *Sox2*. Threshold cycles are normalized to *Gapdh*. In *Ubc* Cond KO P1 SVZ, expression levels of *Rarb, Rxrg,* and *Neurod1* are decreased by 55-58% compared to controls. *Sox2* expression is unchanged in *Ubc* Cond KO SVZ compared to controls. Black dashed line denotes control gene expression levels. (**B-D**) By ChIP-qPCR, CHD7 is enriched relative to IgG at conserved regions 1, 2, 4, 6, and 8 for *Rarb* (**B**), conserved regions 1, 3, 4, and 6 for *Rxrg* (**C**), and conserved regions 1-4 for *Neurod1* (**D**). Non-conserved regions are not enriched for CHD7 relative to IgG. (**E**) Proposed model showing CHD7 function in neural progenitors, including regulation of *Rarb*, *Rxrg,* and pro-neuronal gene transcription and promotion of differentiation into neuroblasts. *Chd7*-deficiency results in decreased *Rarb*, *Rxrg,* and pro-neuronal *Neurod1* gene transcription leading to fewer neuroblasts and a shift towards glial fates. Error bars in (**A-D**) indicate SEM. *$p < 0.05$.

References

Ables, J. L., N. A. Decarolis, M. A. Johnson, P. D. Rivera, Z. Gao, D. C. Cooper, F. Radtke, J. Hsieh and A. J. Eisch (2010). "Notch1 is required for maintenance of the reservoir of adult hippocampal stem cells." J Neurosci **30**(31): 10484-10492.

Alvarez-Buylla, A., J. M. Garcia-Verdugo and A. D. Tramontin (2001). "A unified hypothesis on the lineage of neural stem cells." Nat Rev Neurosci **2**(4): 287-293.

Anchan, R. M., D. P. Drake, C. F. Haines, E. A. Gerwe and A. S. LaMantia (1997). "Disruption of local retinoid-mediated gene expression accompanies abnormal development in the mammalian olfactory pathway." J Comp Neurol **379**(2): 171-184.

Anderson, S. A., D. D. Eisenstat, L. Shi and J. L. Rubenstein (1997). "Interneuron migration from basal forebrain to neocortex: dependence on Dlx genes." Science **278**(5337): 474-476.

Bergman, J. E., E. A. Bosman, C. M. van Ravenswaaij-Arts and K. P. Steel (2010). "Study of smell and reproductive organs in a mouse model for CHARGE syndrome." Eur J Hum Genet **18**(2): 171-177.

Bergman, J. E., N. Janssen, L. H. Hoefsloot, M. C. Jongmans, R. M. Hofstra and C. M. van Ravenswaaij-Arts (2011). "CHD7 mutations and CHARGE syndrome: the clinical implications of an expanding phenotype." J Med Genet **48**(5): 334-342.

Beukelaers, P., R. Vandenbosch, N. Caron, L. Nguyen, G. Moonen and B. Malgrange (2012). "Cycling or not cycling: cell cycle regulatory molecules and adult neurogenesis." Cell Mol Life Sci **69**(9): 1493-1503.

Bosman, E. A., A. C. Penn, J. C. Ambrose, R. Kettleborough, D. L. Stemple and K. P. Steel (2005). "Multiple mutations in mouse Chd7 provide models for CHARGE syndrome." Hum Mol Genet **14**(22): 3463-3476.

Bouazoune, K. and R. E. Kingston (2012). "Chromatin remodeling by the CHD7 protein is impaired by mutations that cause human developmental disorders." Proc Natl Acad Sci U S A **109**(47): 19238-19243.

Carter, C. S., T. W. Vogel, Q. Zhang, S. Seo, R. E. Swiderski, T. O. Moninger, M. D. Cassell, D. R. Thedens, K. M. Keppler-Noreuil, P. Nopoulos, D. Y. Nishimura, C. C. Searby, K. Bugge and V. C. Sheffield (2012). "Abnormal development of NG2+PDGFR-alpha+ neural progenitor cells leads to neonatal hydrocephalus in a ciliopathy mouse model." Nat Med **18**(12): 1797-1804.

Engelen, E., U. Akinci, J. C. Bryne, J. Hou, C. Gontan, M. Moen, D. Szumska, C. Kockx, W. van Ijcken, D. H. Dekkers, J. Demmers, E. J. Rijkers, S. Bhattacharya, S. Philipsen, L. H. Pevny, F. G. Grosveld, R. J. Rottier, B. Lenhard and R. A. Poot (2011). "Sox2 cooperates with Chd7 to regulate genes that are mutated in human syndromes." Nat Genet **43**(6): 607-611.

Feng, W., M. A. Khan, P. Bellvis, Z. Zhu, O. Bernhardt, C. Herold-Mende and H. K. Liu (2013). "The Chromatin Remodeler CHD7 Regulates Adult Neurogenesis via Activation of SoxC Transcription Factors." Cell Stem Cell **13**(1): 62-72.

Ferri, A. L., M. Cavallaro, D. Braida, A. Di Cristofano, A. Canta, A. Vezzani, S. Ottolenghi, P. P. Pandolfi, M. Sala, S. DeBiasi and S. K. Nicolis (2004). "Sox2 deficiency causes neurodegeneration and impaired neurogenesis in the adult mouse brain." Development **131**(15): 3805-3819.

Haskell, G. T. and A. S. LaMantia (2005). "Retinoic acid signaling identifies a distinct precursor population in the developing and adult forebrain." J Neurosci **25**(33): 7636-7647.

Hurd, E. A., M. E. Adams, W. S. Layman, D. L. Swiderski, L. A. Beyer, K. E. Halsey, J. M. Benson, T. W. Gong, D. F. Dolan, Y. Raphael and D. M. Martin (2011). "Mature middle and inner ears express Chd7 and exhibit distinctive pathologies in a mouse model of CHARGE syndrome." Hear Res **282**(1-2): 184-195.

Hurd, E. A., P. L. Capers, M. N. Blauwkamp, M. E. Adams, Y. Raphael, H. K. Poucher and D. M. Martin (2007). "Loss of Chd7 function in gene-trapped reporter mice is embryonic lethal and associated with severe defects in multiple developing tissues." Mamm Genome **18**(2): 94-104.

Hurd, E. A., J. A. Micucci, E. N. Reamer and D. M. Martin (2012). "Delayed fusion and altered gene expression contribute to semicircular canal defects in Chd7 deficient mice." Mech Dev **129**(9-12): 308-323.

Hurd, E. A., H. K. Poucher, K. Cheng, Y. Raphael and D. M. Martin (2010). "The ATP-dependent chromatin remodeling enzyme CHD7 regulates pro-neural gene expression and neurogenesis in the inner ear." Development **137**(18): 3139-3150.

Issekutz, K. A., J. M. Graham, Jr., C. Prasad, I. M. Smith and K. D. Blake (2005). "An epidemiological analysis of CHARGE syndrome: preliminary results from a Canadian study." Am J Med Genet A **133A**(3): 309-317.

Janssen, N., J. E. Bergman, M. A. Swertz, L. Tranebjaerg, M. Lodahl, J. Schoots, R. M. Hofstra, C. M. van Ravenswaaij-Arts and L. H. Hoefsloot (2012). "Mutation update on the CHD7 gene involved in CHARGE syndrome." Hum Mutat **33**(8): 1149-1160.

Jongmans, M. C., R. J. Admiraal, K. P. van der Donk, L. E. Vissers, A. F. Baas, L. Kapusta, J. M. van Hagen, D. Donnai, T. J. de Ravel, J. A. Veltman, A. Geurts van Kessel, B. B. De Vries, H. G. Brunner, L. H. Hoefsloot and C. M. van Ravenswaaij (2006). "CHARGE syndrome: the phenotypic spectrum of mutations in the CHD7 gene." J Med Genet **43**(4): 306-314.

Kikonyogo, A., D. P. Abriola, M. Dryjanski and R. Pietruszko (1999). "Mechanism of inhibition of aldehyde dehydrogenase by citral, a retinoid antagonist." Eur J Biochem **262**(3): 704-712.

LaMantia, A. S., M. C. Colbert and E. Linney (1993). "Retinoic acid induction and regional differentiation prefigure olfactory pathway formation in the mammalian forebrain." Neuron **10**(6): 1035-1048.

Layman, W. S., E. A. Hurd and D. M. Martin (2011). "Reproductive dysfunction and decreased GnRH neurogenesis in a mouse model of CHARGE syndrome." Hum Mol Genet **20**(16): 3138-3150.

Layman, W. S., D. P. McEwen, L. A. Beyer, S. R. Lalani, S. D. Fernbach, E. Oh, A. Swaroop, C. C. Hegg, Y. Raphael, J. R. Martens and D. M. Martin

(2009). "Defects in neural stem cell proliferation and olfaction in Chd7 deficient mice indicate a mechanism for hyposmia in human CHARGE syndrome." Hum Mol Genet **18**(11): 1909-1923.

Legendre, M., M. Gonzales, G. Goudefroye, F. Bilan, P. Parisot, M. J. Perez, M. Bonniere, B. Bessieres, J. Martinovic, A. L. Delezoide, F. Jossic, C. Fallet-Bianco, M. Bucourt, J. Tantau, P. Loget, L. Loeuillet, N. Laurent, B. Leroy, H. Salhi, N. Bigi, C. Rouleau, F. Guimiot, C. Quelin, A. Bazin, C. Alby, A. Ichkou, R. Gesny, A. Kitzis, Y. Ville, S. Lyonnet, F. Razavi, B. Gilbert-Dussardier, M. Vekemans and T. Attie-Bitach (2012). "Antenatal spectrum of CHARGE syndrome in 40 fetuses with CHD7 mutations." J Med Genet **49**(11): 698-707.

Lledo, P. M., F. T. Merkle and A. Alvarez-Buylla (2008). "Origin and function of olfactory bulb interneuron diversity." Trends Neurosci **31**(8): 392-400.

Luskin, M. B. (1993). "Restricted proliferation and migration of postnatally generated neurons derived from the forebrain subventricular zone." Neuron **11**(1): 173-189.

MacPherson, P. A., S. Jones, P. A. Pawson, K. C. Marshall and M. W. McBurney (1997). "P19 cells differentiate into glutamatergic and glutamate-responsive neurons in vitro." Neuroscience **80**(2): 487-499.

Marin, O. and J. L. Rubenstein (2001). "A long, remarkable journey: tangential migration in the telencephalon." Nat Rev Neurosci **2**(11): 780-790.

Mark, M., N. B. Ghyselinck and P. Chambon (2009). "Function of retinoic acid receptors during embryonic development." Nucl Recept Signal **7**: e002.

McBurney, M. W., K. R. Reuhl, A. I. Ally, S. Nasipuri, J. C. Bell and J. Craig (1988). "Differentiation and maturation of embryonal carcinoma-derived neurons in cell culture." J Neurosci **8**(3): 1063-1073.

O'Roak, B. J., L. Vives, S. Girirajan, E. Karakoc, N. Krumm, B. P. Coe, R. Levy, A. Ko, C. Lee, J. D. Smith, E. H. Turner, I. B. Stanaway, B. Vernot, M. Malig, C. Baker, B. Reilly, J. M. Akey, E. Borenstein, M. J. Rieder, D. A. Nickerson, R. Bernier, J. Shendure and E. E. Eichler (2012). "Sporadic autism exomes reveal a highly interconnected protein network of de novo mutations." Nature **485**(7397): 246-250.

Pagon, R. A., J. M. Graham, Jr., J. Zonana and S. L. Yong (1981). "Coloboma, congenital heart disease, and choanal atresia with multiple anomalies: CHARGE association." J Pediatr **99**(2): 223-227.

Pastrana, E., V. Silva-Vargas and F. Doetsch (2011). "Eyes wide open: a critical review of sphere-formation as an assay for stem cells." Cell Stem Cell **8**(5): 486-498.

Pinto, G., V. Abadie, R. Mesnage, J. Blustajn, S. Cabrol, J. Amiel, L. Hertz-Pannier, A. M. Bertrand, S. Lyonnet, R. Rappaport and I. Netchine (2005). "CHARGE syndrome includes hypogonadotropic hypogonadism and abnormal olfactory bulb development." J Clin Endocrinol Metab **90**(10): 5621-5626.

Reynolds, B. A. and S. Weiss (1992). "Generation of neurons and astrocytes from isolated cells of the adult mammalian central nervous system." Science **255**(5052): 1707-1710.

Rochette-Egly, C. and P. Germain (2009). "Dynamic and combinatorial control of gene expression by nuclear retinoic acid receptors (RARs)." Nucl Recept Signal **7**: e005.
Romand, R., W. Krezel, M. Beraneck, L. Cammas, V. Fraulob, N. Messaddeq, P. Kessler, E. Hashino and P. Dolle (2013). "Retinoic acid deficiency impairs the vestibular function." J Neurosci **33**(13): 5856-5866.
Roybon, L., T. Deierborg, P. Brundin and J. Y. Li (2009). "Involvement of Ngn2, Tbr and NeuroD proteins during postnatal olfactory bulb neurogenesis." Eur J Neurosci **29**(2): 232-243.
Ruzankina, Y., C. Pinzon-Guzman, A. Asare, T. Ong, L. Pontano, G. Cotsarelis, V. P. Zediak, M. Velez, A. Bhandoola and E. J. Brown (2007). "Deletion of the developmentally essential gene ATR in adult mice leads to age-related phenotypes and stem cell loss." Cell Stem Cell **1**(1): 113-126.
Sanlaville, D., H. C. Etchevers, M. Gonzales, J. Martinovic, M. Clement-Ziza, A. L. Delezoide, M. C. Aubry, A. Pelet, S. Chemouny, C. Cruaud, S. Audollent, C. Esculpavit, G. Goudefroye, C. Ozilou, C. Fredouille, N. Joye, N. Morichon-Delvallez, Y. Dumez, J. Weissenbach, A. Munnich, J. Amiel, F. Encha-Razavi, S. Lyonnet, M. Vekemans and T. Attie-Bitach (2006). "Phenotypic spectrum of CHARGE syndrome in fetuses with CHD7 truncating mutations correlates with expression during human development." J Med Genet **43**(3): 211-217.
Sanlaville, D. and A. Verloes (2007). "CHARGE syndrome: an update." Eur J Hum Genet **15**(4): 389-399.
Sclafani, A. M., J. M. Skidmore, H. Ramaprakash, A. Trumpp, P. J. Gage and D. M. Martin (2006). "Nestin-Cre mediated deletion of Pitx2 in the mouse." Genesis **44**(7): 336-344.
Siepel, A., G. Bejerano, J. S. Pedersen, A. S. Hinrichs, M. Hou, K. Rosenbloom, H. Clawson, J. Spieth, L. W. Hillier, S. Richards, G. M. Weinstock, R. K. Wilson, R. A. Gibbs, W. J. Kent, W. Miller and D. Haussler (2005). "Evolutionarily conserved elements in vertebrate, insect, worm, and yeast genomes." Genome Res **15**(8): 1034-1050.
Takada, I., M. Mihara, M. Suzawa, F. Ohtake, S. Kobayashi, M. Igarashi, M. Y. Youn, K. Takeyama, T. Nakamura, Y. Mezaki, S. Takezawa, Y. Yogiashi, H. Kitagawa, G. Yamada, S. Takada, Y. Minami, H. Shibuya, K. Matsumoto and S. Kato (2007). "A histone lysine methyltransferase activated by non-canonical Wnt signalling suppresses PPAR-gamma transactivation." Nat Cell Biol **9**(11): 1273-1285.
Thompson Haskell, G., T. M. Maynard, R. A. Shatzmiller and A. S. Lamantia (2002). "Retinoic acid signaling at sites of plasticity in the mature central nervous system." J Comp Neurol **452**(3): 228-241.
Tronche, F., C. Kellendonk, O. Kretz, P. Gass, K. Anlag, P. C. Orban, R. Bock, R. Klein and G. Schutz (1999). "Disruption of the glucocorticoid receptor gene in the nervous system results in reduced anxiety." Nat Genet **23**(1): 99-103.
Vissers, L. E., C. M. van Ravenswaaij, R. Admiraal, J. A. Hurst, B. B. de Vries, I. M. Janssen, W. A. van der Vliet, E. H. Huys, P. J. de Jong, B. C. Hamel,

E. F. Schoenmakers, H. G. Brunner, J. A. Veltman and A. G. van Kessel (2004). "Mutations in a new member of the chromodomain gene family cause CHARGE syndrome." Nat Genet **36**(9): 955-957.

Wang, T. W., H. Zhang and J. M. Parent (2005). "Retinoic acid regulates postnatal neurogenesis in the murine subventricular zone-olfactory bulb pathway." Development **132**(12): 2721-2732.

Wichterle, H., D. H. Turnbull, S. Nery, G. Fishell and A. Alvarez-Buylla (2001). "In utero fate mapping reveals distinct migratory pathways and fates of neurons born in the mammalian basal forebrain." Development **128**(19): 3759-3771.

Zentner, G. E., E. A. Hurd, M. P. Schnetz, L. Handoko, C. Wang, Z. Wang, C. Wei, P. J. Tesar, M. Hatzoglou, D. M. Martin and P. C. Scacheri (2010). "CHD7 functions in the nucleolus as a positive regulator of ribosomal RNA biogenesis." Hum Mol Genet **19**(18): 3491-3501.

Chapter 3

CHD7 regulates neuronal differentiation and maturation potentially through a complex with retinoic acid receptors.

Introduction

Neural stem cell populations are responsible for the production of neurons that impart the remarkable functions of the mammalian brain. While neural stem cell niches have been implicated in the development of the cortex, hippocampus, cerebellum and olfactory bulbs (OB), the exact cell type-specific gene expression patterns unique to these cells is currently poorly characterized. Elucidating the molecular mechanisms behind the subventricular zone (SVZ) neural stem cell self-renewal and neurogenic defects observed in *Chd7*-deficient mice is imperative to understanding forebrain and OB malformations observed in CHARGE syndrome (Pinto et al. 2005; Legendre et al. 2012).

The transcriptomes of neural stem and progenitor cells in the SVZ and neuroblasts populations in the rostral migratory stream (RMS) and OB have begun to be explored. Notably, human neural stem cells express genes involved in several of the signaling pathways observed to be active in mouse neural stem cells including: retinoic acid metabolism enzymes, Wnt signaling molecules and growth factors (Marei et al. 2012). SoxC transcription factors (*SOX4*, *SOX11* and *SOX12*) are also highly expressed in human SVZ neural stem cells, which have recently been shown to be directly regulated by CHD7 and overexpression of

SoxC transcription factors rescues *Chd7*-deficiency in the adult SVZ (Feng et al. 2013).

Laser capture microdissection of eGFP-expressing neuroblasts populations in the SVZ, RMS and OB followed by high throughput genetic analysis has demonstrated a remarkably elastic transcriptome for neuroblasts (Khodosevich et al. 2013). Neuroblasts captured in the SVZ and caudal RMS show high expression of cell cycle regulators such as *Ccnd2* (CyclinD2) and *Cdk6* (Khodosevich et al. 2013). As neuroblasts begin to move through the RMS and exit the cell cycle, genes responsible for neuronal migration and guidance become highly expressed including *Dcx* and *Robo2* (Khodosevich et al. 2013). In the rostral RMS and OB, neuroblasts begin to differentiate into immature and mature neurons, concomitant with up-regulation of pro-neuronal transcription factors (*Neurod1*) and neurotransmitter receptors for GABAergic (*Gabaara2*, *Gabaarb2*, *Gabaarb3* and *Gabaarg2*) and glutamatergic interneurons (*Glua1*, *Glua2* and *Glua4*) (Khodosevich et al. 2013). As shown in Chapter 2, loss of *Chd7* in the mouse results in a significant decrease in DCX+ neuroblasts (Figs. 2.5 and 2.6) without alteration of cell cycle genes (Fig. 2.11) (Micucci et al. 2013). These results indicate that CHD7 plays a major role in the cell fate of SVZ neuroblasts.

In order to thoroughly investigate changes in SVZ gene expression upon loss of *Chd7*, I performed whole genome microarray on microdissected SVZ tissue from postnatal day 1 (P1) control and ubiquitous conditional *Chd7* knockout mice to monitor for dysregulation of expression of key neural stem cell,

neural progenitor cell and neuroblasts genes. Gene ontology (GO) analysis revealed CHD7 to regulate genes important for neurogenesis, neuronal differentiation, neuron maturation and retinoic acid signaling. While high throughput methods for analyzing the transcriptome of SVZ cells generate large amounts of data from a very limited number of cells, biochemical analysis of cellular components responsible for neural stem and progenitor cell differentiation and cell fate is difficult due to the dearth of cells present in the perinatal and adult murine SVZ. In order to circumvent this issue, I also utilized P19 embryonal carcinoma cells, a well characterized cell line which differentiates into neurons upon treatment with retinoic acid (McBurney 1993; Magnuson et al. 1995; Soprano et al. 2007). Use of P19 cells enabled me to examine for evidence of direct regulation of and interaction between CHD7 and retinoic acid receptors. I also reduced *Chd7* expression by short hairpin RNA (shRNA) transfection to determine changes in P19 cell growth and pro-neural gene expression. My findings demonstrate that CHD7 is essential for proper neuronal differentiation, regulates pro-neural genes, and directly interacts with retinoic acid signaling.

Materials and Methods

Mouse strains, breeding and genotyping.

Chd7$^{flox/flox}$ mice were maintained as previously described (Hurd et al. 2007; Hurd et al. 2010). *Ubc-CreERT2* mice were maintained on a C57BL/6 background and mated with *Chd7*$^{flox/flox}$ mice to generate *Cre*;*Chd7*$^{flox/+}$ mice.

Cre;Chd7$^{flox/+}$ mice were crossed to *Chd7*$^{flox/flox}$ to produce control (*Chd7*$^{flox/+}$ and *Chd7*$^{flox/flox}$), *Chd7* conditional heterozygous (*Cre;Chd7*$^{flox/+}$), and conditional knockout (*Cre;Chd7*$^{flox/flox}$) mice. Genomic DNA was isolated from tail and brain tissue and PCR genotyped as previously described (Hurd et al. 2010). All procedures were approved by The University of Michigan University Committee on the Use and Care of Animals (UCUCA).

Tamoxifen administration.

Tamoxifen (Sigma-Aldritch, St. Louis, MO) was dissolved in sterile corn oil at a concentration of 10 mg/ml. A single dose of Tamoxifen (0.2 mg/gbw) was administered by intraperitoneal injection to pregnant females at embryonic day 15.5 and perinatal pups were processed for brain dissection.

Microarray and gene ontology analysis.

Subventricular zones from littermate control and *Ubc* Cond KO P1 mice (*n* = 4 per genotype) were microdissected and RNA was isolated using the RNAqueous-Micro RNA Isolation Kit (Ambion, Austin, TX, USA). Isolated RNA was treated with DNase I prior to microarray and cDNA synthesis. For microarray, cDNA was prepared and amplified using the Ovation Pico WTA System V2 (Nugen Technologies, San Carlos, CA) then hybridized to a whole genome Mous Gene ST 1.1 strip array (Affymetrix, Santa Clara, CA). Microarray data was quality controlled using a principal components analysis, analyzed in the affy, oligo, and limma packages of bioconductor implemented in the R statistical environment. Expression values were calculated using a robust multi-

array average. Gene ontology analysis was performed by entering the list of up- and down-regulated genes from the microarray into the Gene Ontology Term Finder (Lewis-Sigler Institute for Integrative Genomics, Princeton University, http://go.princeton.edu/cgi-bin/GOTermFinder).

Gene expression analysis.

For quantitative real-time PCR, cDNA was generated using the Superscript First-Strand cDNA Synthesis system with random hexamers (Life Technologies). Relative gene expression levels were assayed using TaqMan Gene Expression Master Mix and TaqMan probes (Applied Biosystems, Foster City, CA, USA) for *Gapdh*, *Rara*, *Rarb*, *Rarg*, *Rxra*, *Rxrb*, *Rxrg*, *Tbr1* and *Olig2* or SYBR Green Master Mix and SYBR Green probes (Applied Biosystems) for *Gapdh*, *Chd7*, *Otx2*, *Bmp4* and *Fgf10*. Each sample was run in triplicate using an Applied Biosystems StepOne-Plus Real-Time qPCR System. The gene expression level of *Gapdh* was used as an internal, positive control. The difference in threshold cycle (C_T) between the assayed gene and *Gapdh* for any given sample was defined as the change in threshold cycle (ΔC_T). The difference in ΔC_T between two samples was defined as $\Delta\Delta C_T$ which represents a relative difference in expression of the assayed gene. The fold change of the assayed gene relative to *Gapdh* was defined as $2^{-\Delta\Delta CT}$. Unpaired Student's t-test was performed on *Gapdh* normalized ΔC_T values for each sample to determine statistical significance.

P19 monolayer and neurosphere cultures.

For undifferentiated monolayers, P19 embryonal carcinoma cells were passaged in MEMα (Life Technologies) + 10% FBS (Life Technologies) + 1X penicillin/streptomycin (Life Technologies). For neurospheres, cells were passaged as monolayers, gently treated with 0.25% trypsin and plated on 0.7% agarose in bacterial culture plates in MEMα + 7.5% calf serum + 2.5% FBS + 1 μM retinoic acid + 1X penicillin/streptomycin. Neurospheres were confirmed to form two days after plating by bright field microscopy and medium was changed two and four days after initial plating. Six days after plating, neurospheres were collected by gentle centrifugation then prepared for experiments.

Nuclear extract preparation.

Undifferentiated and neurosphere P19 cells were treated with 0.25% trypsin (Life Technologies) for 5 min at 37°C, triturated into a single cell suspension then centrifuged. The cell pellets were rinsed twice with ice cold 1X PBS, resuspended in ice cold lysis buffer (15 mM HEPES, 10 mM KCl, 0.1 mM EDTA, 1 mM $MgCl_2$, 350 mM sucrose, pH 7.4) and homogenized by passing the cells through a 1 mL syringe with a 26 3/8G needle. The lysate was centrifuged, the supernatant (now called cytoplasmic extract 1) was removed and saved. The pellet was resuspended in ice cold lysis buffer, gently vortexed to homogenize, centrifuged and the supernatant retained (cytoplasmic extract 2). The process of resuspension and retention of the supernatant was repeated with nuclear lysis buffer (15 mM HEPES, 110 mM KCl, 250 mM NaCl, 0.1 mM EGTA, 5% glycerol,

pH 7.4) creating two nuclear extracts. Extracts were used directly for immunoprecipitation experiments or flash frozen in liquid nitrogen and stored at -80°C.

Co-immunoprecipitation and Western blotting.

Cytoplasmic and nuclear extracts from undifferentiated and neurosphere P19 cells were pre-cleared with 20 µl Protein A/G agarose beads (Santa Cruz Biotechnology, Dallas, TX) for 1 hr by rotation at 4°C, centrifuged and supernatant removed to a new microfuge tube. 1 µg retinoic acid receptor antibody (RAR, Santa Cruz Biotechnology) was added to cytoplasmic and nuclear extracts and rotated overnight at 4°C in a cold room. 20 µl Protein A/G agarose beads were added to protein-antibody complexes and rotated for 2 hrs at 4°C. The protein-antibody-bead complexes were washed in the following washing protocol: two low salt buffer washes (30 min per wash in 20mM Tris, 0.2 mM EDTA, 10% glycerol, 0.1% NP-40, 150 mM KCl pH 7.9), two high salt buffer washes (30 min per wash in 20mM Tris, 0.2 mM EDTA, 10% glycerol, 0.1% NP-40, 350 mM KCl pH 7.9) and two low salt buffer washes (30 min per wash). The washed complexes were resuspended in 1X LDS loading buffer (Life Technologies) and heated at 75°C for 5 min. 10 µl of input and each immunoprecipitation condition were run on a 10% tris-glycine gel with MOPS buffer at 200V for 75 min. The gel was placed in a NuPAGE transfer apparatus (Life Technologies) with two pieces of filter paper and a nitrocellulose membrane (Life Technologies) then transferred in 1X transfer buffer (Life Technologies) +

20% methanol overnight at 4°C. The membrane was blocked overnight in blocking buffer (50 mM Tris, 150 mM NaCl, 0.05% Tween-20, 10% nonfat milk powder), washed three times for 5 min in TBST (50 mM Tris, 150 mM NaCl, 0.05% Tween-20) and incubated overnight at 4°C with 1:1000 anti-CHD7 antibody (Cell Signaling) in blocking buffer. The membrane was washed three times for 5 min with TBST then incubated for 2 hrs at room temperature with 1:500 goat anti-rabbit IgG HRP-conjugated secondary (Pierce Biotechnology, Rockford, IL). The blot was then washed three times for 5 min with TBST and two times for 5 min with TBS, developed using SuperSignal West Pico Chemiluminescent system (Pierce Biotechnology) as per the manufacturer's instructions and imaged using the FluorChem M MultiFluor System (Protein Simple, Santa Clara, CA).

SIBR shRNA vectors and *Chd7* knockdown.

pUI4-SIBR-GFP and pCS2-puro vectors were obtained from Drs. David Turner and Anne Vojtek (Yu et al. 2005; Chung et al. 2006; Taylor et al. 2008). A concatemer of cDNA targeting exon 18 (5' AAAATCTACAGGCTGATTACAAGGAAC 3') and exon 34 (5' ACTTCAAAGTTTATCTTGCCTAA 3') of the mouse *Chd7* gene were cloned into pUI4-SIBR-GFP. Undifferentiated P19 cells were co-transfected with pCS2-puro puromycin resistance vector and pUI4-SIBR-GFP containing either the *Chd7* concatemer or a control sequence targeting luciferase using the TransIT-LT1 transfection reagent (Mirus, Madison, WI) as per the manufacturer's

instructions. Transfected cells were selected with 10 µg/ml puromycin for three days, changing the medium as necessary to avoid an excess of dead cells then recovered for two days. Selected cells were processed for RNA isolation and gene expression analysis as described above.

P19 growth curves.

Undifferentiated P19 cells were transfected with pUI4-SIBR-GFP containing either the *Chd7* concatemer or a control sequence targeting luciferase. Cells were harvested by treatment with 0.25% trypsin and counted on a hemacytometer.

Results

Microarray analysis of *Chd7*-deficient SVZ suggests role for CHD7 in neuronal differentiation.

I sought to investigate changes in gene expression in the perinatal SVZ upon loss of *Chd7*. I performed a whole mouse genome microarray using RNA isolated from the SVZ of control and *Ubc* Cond KO postnatal day 1 mice (n = 4 per genotype). The microarray identified 136 genes that were changed at least 1.5 fold (117 genes down-regulated and 19 genes up-regulated) compared to controls (Tables 3.1 and 3.2). The list of down-regulated genes was uploaded to the GO Term Finder to find broad classes of gene function for the genes changed upon loss of *Chd7*. The most enriched GO terms were involved in neuronal differentiation (*Rxrg*, *Rarb*, *Neurod1*, *Tbr1* and *Eomes*, also known as

Tbr2), neuron migration (*Reln*, *Cdh8*, *Epha7* and *Robo2*) and synaptic transmission/action potentials (*Gabra5*, *Grm3*, *Scn2a1*, *Grm5*, *Cacna1e* and *Gabrb1*) (Table 3.3). None of the up-regulated genes listed in Table 3.2 are currently implicated in SVZ neural stem cell niche development or function. I also performed GO analysis on the list of up-regulated genes, but due to the small number of genes, no statistically significant terms were recovered.

Interestingly, this microarray analysis showed that *Rarb*, *Rxrg* and *Neurod1* were down-regulated in *Chd7*-deficient SVZ, thereby confirming our qRT-PCR and chromatin immunoprecipitation data for the down-regulation and CHD7 binding of *Rarb*, *Rxrg* and *Neurod1* from Chapter 2 (Fig. 2.16) (Micucci et al. 2013). The down-regulation of neuronal migration genes *Reln*, *Cdh8*, *Epha7* and *Robo2* suggests that CHD7 may also play a role in guiding neuroblasts from the SVZ, through the RMS, and into the OB. This hypothesis is bolstered by the paucity of DCX+ neuroblasts in the RMS of *Chd7*-deficient mice (Figs. 2.5 and 2.6) (Micucci et al. 2013). Of particular note is *Robo2*, a well-established axon guidance transmembrane receptor that binds the soluble Slit proteins and is highly expressed in migrating neuroblasts (Wu et al. 1999; Nguyen-Ba-Charvet et al. 2004). Overall, these findings from the microarray analysis show that CHD7 may be necessary for regulating expression of genes that promote migration of SVZ-derived neuroblasts through the RMS.

Loss of *Chd7* in the SVZ also led to reduced expression of mature neuronal genes involved in synaptic transmission and neurotransmitter receptor genes including GABA receptors (*Gabra5* and *Gabrb1*), glutamate receptors

(*Grm3* and *Grm5*) and ion channels (*Scn2a1* and *Cacna1e*). These classes of genes have been shown to be up-regulated in the transcriptome of neuroblasts in the rostral RMS and OB (Khodosevich et al. 2013). Decreased expression of these neuronal maturation and integration genes underscores the reduction in mature OB interneurons observed in *Chd7*-deficient mice (Fig. 2.2) (Micucci et al. 2013). Reduction of *Chd7* in the SVZ also enriched for GO terms for learning, memory, behavior and cognition. While these GO terms are broad, they are reminiscent of cognitive and behavioral phenotypes associated with CHARGE syndrome (Hartshorne et al. 2005). Additionally, *CHD7* has recently been implicated as a gene involved in autism spectrum disorder, and may influence expression of genes involved in cognition and behavior (O'Roak et al. 2012; Jiang et al. 2013). I conclude that loss of *Chd7* in the perinatal SVZ leads to down-regulation of neuronal differentiation, migration and maturation genes, which may help explain the neurogenic defects, OB hypoplasia and anosmia observed in *Chd7*-deficient mice (Layman et al. 2009; Micucci et al. 2013).

CHD7 shows isoform specificity in regulation of retinoic acid signaling.

Our previous studies have shown that modulation of retinoic acid signaling can partially rescue inner ear and SVZ neural stem cell phenotypes associated with *Chd7*-deficiency (Figs. 2.14-2.16) (Micucci et al. 2013). In addition, I have shown that *Rarb* and *Rxrg* are down-regulated in the SVZ upon loss of *Chd7* by qRT-PCR and microarray (Fig. 2.16 and Table 3.1). In order to determine whether there is specificity for CHD7 regulation of retinoic acid and retinoid X

receptors, I performed qRT-PCR on all major isoforms of RAR (*Rara*, *Rarb* and *Rarg*) and RXR (*Rxra*, *Rxrb* and *Rxrg*). Loss of *Chd7* specifically reduced the expression of *Rarb* and *Rxrg* by 58% and 57%, respectively, but had no effect on the expression of *Rara*, *Rarg*, *Rxra* and *Rxrb* compared to control levels; thereby confirming the microarray results (Fig. 3.1A).

Consistent with a reduction in the number of RMS neuroblasts in *Chd7*-deficient mice (Figs. 2.3 and 2.5) and microarray analysis (Table 3.1), I found that expression of the neuroblast/immature neuron marker *Tbr1* was decreased by 82% in *Ubc* Cond KO SVZ compared to control. (Fig. 3.1A) (Micucci et al. 2013). I also investigated the expression level of *Olig2*, an important oligodendrocyte-lineage marker, due to the increase in GFAP+ glia present in *Chd7*-deficient mice (Figs 2.3 and 2.5) (Marshall et al. 2005; Micucci et al. 2013). Interestingly, *Olig2* expression was unchanged in *Ubc* Cond KO P1 SVZ compared to control levels (Fig. 3.1A). Unchanged *Olig2* expression is not surprising for the early perinatal period, considering that gliogenesis occurs predominantly in the postnatal period. While *Olig2* expression is unchanged in the SVZ of perinatal *Chd7*-deficient mice, an increase in postnatal *Olig2* expression may explain why there is an expansion of glia observed in adult *Chd7*-deficient mice (Micucci et al. 2013). These data show that CHD7 regulates expression of specific RAR and RXR genes and promotes pro-neural gene expression in neural progenitor cells and neuroblasts.

Prior studies showed by chromatin immunoprecipitation, qRT-PCR and microarray that CHD7 directly regulates the expression of *Rarb* and *Rxrg* (Fig.

2.16 and Table 3.1). However, whether CHD7 physically associates with retinoic acid receptors in cells is unknown. To address this, I performed co-immunoprecipitation experiments for CHD7 and RAR's using cytoplasmic and nuclear extracts from undifferentiated P19 cells and P19-derived neurospheres using a pan-RAR antibody that recognizes a common epitope for RARα, RARβ and RARγ, followed by western blotting using anti-CHD7 antibody. In undifferentiated P19 cells, CHD7 was present in the nuclear fraction and excluded from the cytoplasmic extract, which is consistent with its role as a chromatin remodeling enzyme (Fig. 3.1B). Interestingly, CHD7 binds RAR's in the nucleus of both undifferentiated P19 cells and P19-derived neurospheres, but appears to be more enriched in undifferentiated cells (Fig. 3.1B). These data demonstrate that CHD7 forms a complex with RAR's in the nuclei of stem cell-like and neuronal progenitor-like P19 cells. While this co-immunoprecipitation experiment shows that CHD7 binds to RAR's, the use of a pan-RAR antibody cannot distinguish whether CHD7 associates with specific RAR isoforms.

CHD7 regulates gene expression and cell growth in P19 cells.

In order to more rigorously test the *in vivo* biochemical activity of CHD7, I developed shRNA vectors to specifically target the *Chd7* transcript and ablate its translation into functional protein. I cloned sequences from Exons 18 and 34 from the mouse *Chd7* gene into pUI4-SIBR-GFP, a vector that co-expresses GFP and the *Chd7* shRNA from an intronic cassette based on the miR-155 microRNA precursor (Fig. 3.2A) (Yu et al. 2005; Chung et al. 2006; Taylor et al.

2008). Considering that *Chd7* is known to play a role in the proliferation of olfactory epithelium and SVZ neural stem cells, the developing otocyst and SVZ-derived neurospheres, I measured the effects of *Chd7* shRNA on growth of undifferentiated P19 embryonal carcinoma cells (Layman et al. 2009; Feng et al. 2013; Micucci et al. 2013). P19 cells were transfected with the *Chd7* shRNA construct or a control construct expressing a shRNA vector that targets luciferase, and cell number was assessed every 24 hrs for three days. For *Chd7* shRNA transfections, there were 10% and 21% fewer P19 cells 48 hrs and 72 hrs post-transfection, respectively, compared to control shRNA (Fig. 3.2B). There was no difference in cell number between *Chd7* shRNA and control shRNA treated cells at 24 hrs (Fig. 3.2B). These data are consistent with 28% fewer cells at 72 hrs post-transfection reported by Kita et al. in *Chd7* shRNA transfected HeLa cells (Kita et al. 2012).

Next, I confirmed knockdown of *Chd7* and three genes known to be down-regulated upon loss of *Chd7* in the developing mouse (*Otx2*, *Bmp4* and *Fgf10*) by qRT-PCR performed on total RNA from undifferentiated P19 cells that were co-transfected with a puromycin resistance vector and *Chd7* or control shRNA (Hurd et al. 2010). *Chd7* expression was reduced by 85% in *Chd7* shRNA transfections compared to controls (Fig. 3.2C), which is significantly higher than the 25% knockdown observed by Kita et al. in *Chd7* shRNA transfected HeLa cells (Kita et al. 2012). Consistent with *in situ* hybridization experiments on embryonic inner ears, *Chd7* shRNA transfection resulted in 72%, 77% and 51% reduction in expression of *Otx2*, *Bmp4* and *Fgf10*, respectively, compared to

control shRNA (Fig. 3.2C) (Hurd et al. 2010). Thus, our *Chd7* shRNA constructs are effective at significantly reducing *Chd7* mRNA levels and affect the expression of known CHD7 target genes. The availability of *Chd7* shRNA knockdown vectors allows for examination of *Chd7* function in a well-described cell line that circumvents some of the limitations of biochemical analysis in primary SVZ neurospheres or tissue.

Discussion

Here I showed that *Chd7* deficiency in the perinatal SVZ results in down-regulation of genes that facilitate retinoic acid signaling, neuronal differentiation, neuron migration and synaptic transmission. Co-immunoprecipitation using P19 embryonal carcinoma cell nuclear extract showed that CHD7 and at least one RAR directly bind and form a complex. shRNA knockdown of *Chd7* in P19 cells leads to decreased proliferation and reduced expression of known CHD7 target genes including *Otx2*, *Bmp4* and *Fgf10.* Together, these findings provide additional evidence that CHD7 regulates neuronal differentiation and maturation through the modulation of retinoic acid signaling.

Microarray analyses of neuroblast populations have demonstrated that these cells exhibit highly dynamic transcriptomes that change dependent upon their progression along the path from the SVZ to the OB (Khodosevich et al. 2013). Our microarray analysis of *Chd7*-deficient postnatal day 1 (P1) SVZ shows down-regulation of genes that are highly important for the identity (*Neurod1*, *Tbr1* and *Eomes*), migration (*Reln* and *Robo2*) and maturation

(*Gabra5*, *Grm3*, *Grm5* and *Gabrb1*) of neuroblasts. CHD7 is known to bind poised enhancer elements of ectodermal lineage (Zentner et al. 2011) and through this mechanism may facilitate the resolution of pro-neural enhancers to promote neuronal differentiation and maturation in neuronal progenitor cells and neuroblasts.

CHD7 influences the transcription of cell fate and identity genes by forming cell type-specific complexes in mesenchymal stem cells (adipose vs. bone), neural crest cells (epithelium vs. mesenchyme) and neural stem cells (neuron vs. oligodendrocyte/glia) (Takada et al. 2007; Bajpai et al. 2010; Engelen et al. 2011; Micucci et al. 2013). Here, I have shown that CHD7 is required for optimal transcription of *Rarb* and *Rxrg* by directly binding their promoters. I also showed that CHD7 forms a complex with at least one RAR, although the specific isoform is not defined. Further investigation is needed to determine whether (1) CHD7 binds only a single RAR or a specific RAR/RXR heterodimer, (2) the complex binds retinoic acid response elements (RARE) in promoters of known CHD7 target genes, and (3) the CHD7/RAR complex is specific for neural stem cells. Considering the similarities between *in utero* retinoic acid deficiency and CHARGE syndrome (Mark et al. 2009; Janssen et al. 2012; Legendre et al. 2012), exploration of the interaction of CHD7 and retinoic acid signaling components may prove vital for developing therapeutic and diagnostic techniques to address these common phenotypes.

Acknowledgements

I would like to thank Ethan Sperry for assistance with the gene ontology analysis and Mark Durham for assistance with western blotting, tissue culture and transfections.

Table 3.1. Genes down-regulated in SVZ of *Chd7*-deficient neonatal mice by whole mouse genome microarray.

Gene	Description	Fold Change
Tac1	tachykinin 1	-3.68
Reln	reelin	-2.53
Gabra5	gamma-aminobutyric acid (GABA) A receptor, subunit alpha 5	-2.46
Grm3	glutamate receptor, metabotropic 3	-2.35
Cdh8	cadherin 8	-2.16
Scn2a1	sodium channel, voltage-gated, type II, alpha 1	-2.16
Grm5	glutamate receptor, metabotropic 5	-2.06
Neurod1	neurogenic differentiation 1	-2.06
Rxrg	retinoid X receptor gamma	-2.06
Snca	synuclein, alpha	-1.99
Tbr1	T-box brain gene 1	-1.93
Rarb	retinoic acid receptor, beta	-1.91
Eomes	eomesodermin homolog (Xenopus laevis)	-1.87
Cntn1	contactin 1	-1.83
Nefl	neurofilament, light polypeptide	-1.80
Ppp1r1b	protein phosphatase 1, regulatory (inhibitor) subunit 1B	-1.79
Dscam	Down syndrome cell adhesion molecule	-1.73
Syt4	synaptotagmin IV	-1.72
Tnik	TRAF2 and NCK interacting kinase	-1.71
Camk2b	calcium/calmodulin-dependent protein kinase II, beta	-1.68
Lin7a	lin-7 homolog A (C. elegans)	-1.68
Plcb1	phospholipase C, beta 1	-1.68
Lingo1	leucine rich repeat and Ig domain containing 1	-1.65
Slc17a6	solute carrier family 17, member 6	-1.65
Grin2b	glutamate receptor, ionotropic, NMDA2B (epsilon 2)	-1.60
Zic1	zinc finger protein of the cerebellum 1	-1.60
Lrrc4c	leucine rich repeat containing 4C	-1.59
Rapgef4	Rap guanine nucleotide exchange factor (GEF) 4	-1.59
Cacna1e	calcium channel, voltage-dependent, R type, alpha 1E subunit	-1.57
Gabrb2	gamma-aminobutyric acid (GABA) A receptor, subunit beta 2	-1.57
Pclo	piccolo (presynaptic cytomatrix protein)	-1.57
Epha7	Eph receptor A7	-1.55
Scg2	secretogranin II	-1.55
Adcy1	adenylate cyclase 1	-1.52
Plk2	polo-like kinase 2	-1.52
Robo2	roundabout homolog 2 (Drosophila)	-1.51

Table 3.2. Genes up-regulated in SVZ of *Chd7*-deficient neonatal mice by whole mouse genome microarray.

Gene	Description	Fold Change
Hspa8	heat shock protein 8	2.13
Rsph4a	radial spoke head 4 homolog A (Chlamydomonas)	1.75
Serpina3n	serine (or cysteine) peptidase inhibitor, clade A, member 3N	1.75
Lhx6	LIM homeobox protein 6	1.71
Lrp2	low density lipoprotein receptor-related protein 2	1.61
Ccl3	chemokine (C-C motif) ligand 3	1.59
Ogn	osteoglycin	1.59
Emp1	epithelial membrane protein 1	1.57
Ndufs5	NADH dehydrogenase (ubiquinone) Fe-S protein 5	1.57
Car5b	carbonic anhydrase 5b, mitochondrial	1.55
Gemin8	gem (nuclear organelle) associated protein 8	1.55
Fbxo2	F-box protein 2	1.54
Olfml3	olfactomedin-like 3	1.54
Tspan15	tetraspanin 15	1.54
Duxbl	double homeobox B-like	1.53
Hmox1	heme oxygenase (decycling) 1	1.53
Afap1l2	actin filament associated protein 1-like 2	1.52
Sfrp5	secreted frizzled-related sequence protein 5	1.52
Iqub	IQ motif and ubiquitin domain containing	1.51

Table 3.3. Gene Ontology terms associated with genes down-regulated in SVZ of *Chd7*-deficient neonatal mice.

Gene Ontology term	Corrected P-value	Genes annotated to GO term
Transmission of nerve impulse	2.43e-8	*Gabrb2, Snca, Grm5, Pclo, Plk2, Reln, Camk2b, Cdh8, Lin7a, Scn2a1, Slc17a6, Rxrg, Syt4, Rapgef4, Grm3, Tac1, Grin2b, Cacna1e, Gabra5*
Synaptic transmission	4.46e-7	*Gabrb2, Snca, Grm5, Pclo, Plk2, Reln, Camk2b, Cdh8, Lin7a, Slc17a6, Syt4, Rapgef4, Grm3, Tac1, Grin2b, Gabra5*
Learning/Memory	8.25e-6	*Grm5, Adcy1, Plk2, Plcb1, Tac1, Reln, Grin2b, Cacna1e, Ppp1r1b, Gabra5*
Behavior	1.5e-5	*Snca, Scg2, Grm5, Adcy1, Plk2, Zic1, Plcb1, Dscam, Robo2, Cdh13, Tac1, Reln, Grin2b, Cacna1e, Ppp1r1b, Gabra5*
Cognition	1.55e-5	*Grm5, Adcy1, Plk2, Plcb1, Tac1, Reln, Grin2b, Cacna1e, Ppp1r1b, Gabra5*
Regulation of nervous system development	3.42e-5	*Lingo1, Grm5, Rapgef4, Lrrc4c, Dscam, Rxrg, Tbr1, Robo2, Reln, Neurod1, Nefl, Eomes, Camk2b, Tnik, Cntn1*
Regulation of neurogenesis	6.32e-5	*Lingo1, Grm5, Rapgef4, Lrrc4c, Dscam, Tbr1, Robo2, Reln, Neurod1, Nefl, Eomes, Camk2b, Cntn1, Tnik*
Nervous system development	1.4e-4	*Gabrb2, Neurod6, Lingo1, Grm5, Dscam, Reln, Nefl, Epha7, Eomes, Camk2b, Tnik, Cntn1, Scn2a1, Adcy1, Rapgef4, Lrrc4c, Zic1, Rxrg, Plcb1, Tbr1, Robo2, Neurod1, Rarb, Gabra5*
Regulation of transmission of nerve impulse	2.1e-4	*Snca, Grm5, Plk2, Rapgef4, Rxrg, Tac1, Reln, Grm3, Grin2b, Camk2b*
Regulation of cell projection organization	3.3e-4	*Rapgef4, Lrrc4c, Dscam, Tbr1, Robo2, Reln, Odz1, Nefl, Camk2b, Cntn1, Tnik*
Regulation of neuron differentiation	3.6e-4	*Rapgef4, Lrrc4c, Dscam, Tbr1, Robo2, Reln, Neurod1, Nefl, Eomes, Camk2b, Cntn1, Tnik*
Regulation of neurological system process	4.1e-4	*Snca, Grm5, Plk2, Rapgef4, Rxrg, Tac1, Reln, Grm3, Grin2b, Camk2b*
Regulation of neuron projection development	4.9e-4	*Rapgef4, Lrrc4c, Dscam, Tbr1, Robo2, Reln, Nefl, Camk2b, Cntn1, Tnik*
Regulation of synaptic transmission	7.4e-4	*Snca, Grm5, Plk2, Rapgef4, Tac1, Reln, Grm3, Grin2b, Camk2b*
Neurogenesis	8.5e-4	*Gabrb2, Lingo1, Grm5, Dscam, Reln, Nefl, Epha7, Eomes, Camk2b, Tnik, Cntn1, Adcy1, Lrrc4c, Rapgef4, Tbr1, Robo2, Rarb, Neurod1, Gabra5*

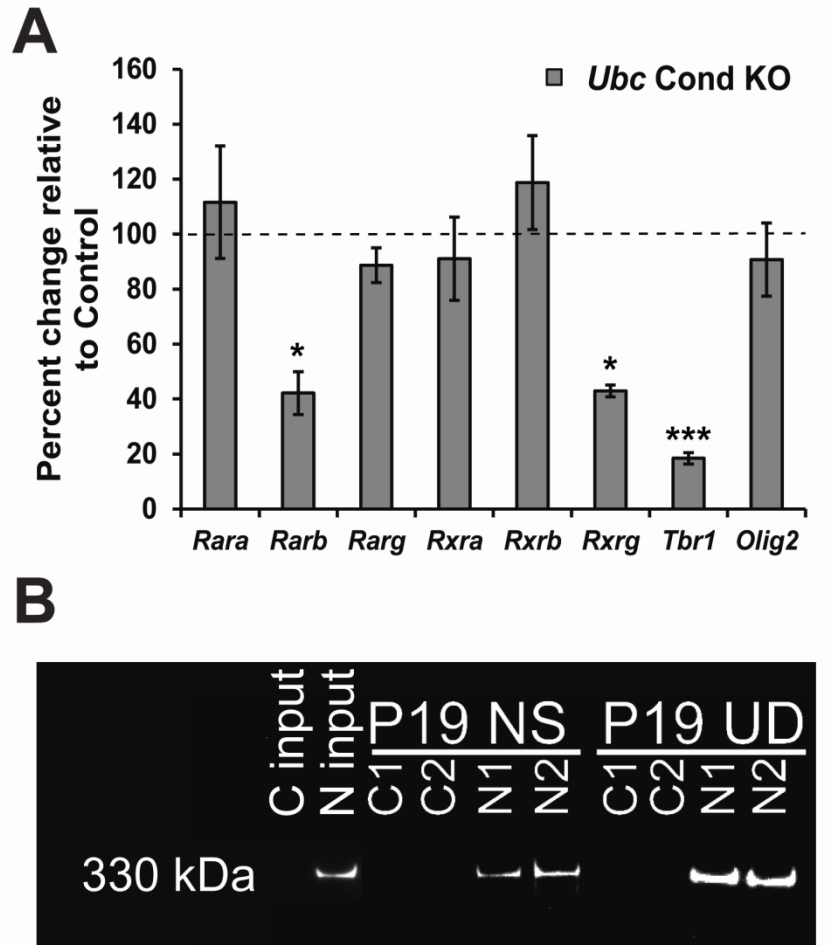

Figure 3.1. CHD7 regulates retinoic acid receptor expression and interacts with retinoic acid receptors *in vivo*.
(**A**) Quantitative RT-PCR on RNA isolated from SVZ of P1 control and *Ubc* Cond KO mice shows that loss of *Chd7* specifically reduces expression of *Rarb* and *Rxrg* by 58% and 57%, respectively, while expression of *Rara*, *Rarg*, *Rxra* and *Rxrb* are unaffected. Expression of *Tbr1*, a marker of neural progenitor cells, was decreased by 82%, while *Olig2*, an oligodendrocyte lineage marker, was unchanged at P1. (**B**) Co-immunoprecipitation was performed on undifferentiated (UD) and neurosphere (NS) P19 cells with anti-RAR antibody (recognizes RARα, RARβ and RARγ) followed by western blotting with anti-CHD7 antibody. CHD7 was present in the nuclear fraction (N input) and absent from cytoplasmic extracts (C input) of undifferentiated P19 cells. Anti-RAR immunoprecipitations performed with cytoplasmic extracts (C1, C2) of UD and NS P19 cells did not pull down CHD7, while CHD7 binds the nuclear RARs in both UD and NS P19 cells. Black dashed line in (**A**) indicates control gene expression levels and error bars indicate SEM (n=3 per genotype). *p<0.05, ***p<0.001 by unpaired Student's t-test.

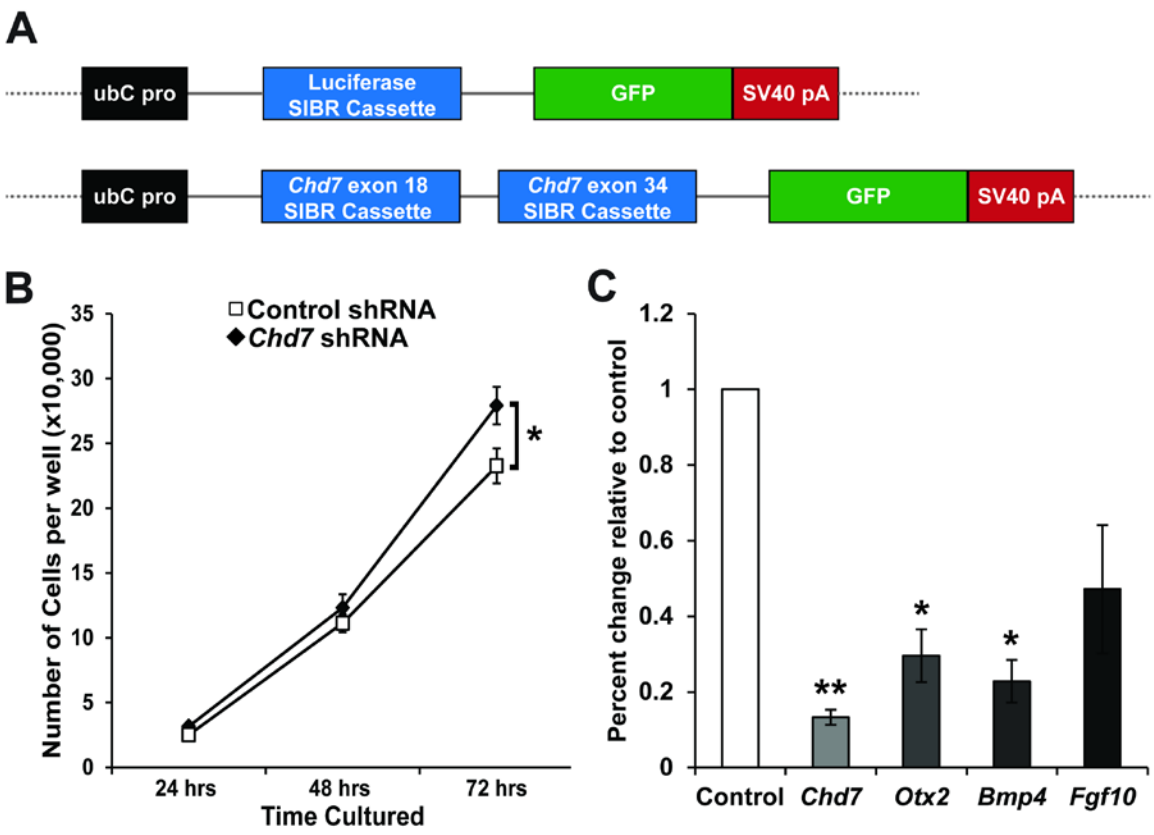

Figure 3.2. *Chd7* reduction leads to growth defects and decreased pro-neural gene expression. (**A**) Schematics showing the structure of the UI4-SIBR-GFP vectors containing either a single shRNA targeting Luciferase or a concatemer containing shRNAs targeting *Chd7* exons 18 and 34. (**B**) Growth curves for control (white squares) and *Chd7* shRNA (black diamonds) transfected undifferentiated P19 cells showed 17% fewer cells in *Chd7* knockdown cells compared to control. (**C**) Undifferentiated P19 cells were transfected with vectors encoding a control or *Chd7*-specific shRNA, selected with puromycin, total RNA was isolated, converted to cDNA and used for SYBR Green qPCR for pro-neural genes. *Chd7* expression was reduced by 85%, confirming knockdown of *Chd7*. Expression of *Otx2*, *Bmp4* and *Fgf10* was reduced by 72%, 77% and 51%, respectively, upon knockdown of *Chd7*. Other abbreviations: ubC pro: human ubC promoter, GFP: green fluorescent protein, SV40 pA: SV40 polyadenylation sequence. Error bars indicate SEM (n=3 per condition). *p<0.05, **p<0.01 by unpaired Student's t-test.

References

Bajpai, R., D. A. Chen, A. Rada-Iglesias, J. Zhang, Y. Xiong, J. Helms, C. P. Chang, Y. Zhao, T. Swigut and J. Wysocka (2010). "CHD7 cooperates with PBAF to control multipotent neural crest formation." Nature **463**(7283): 958-962.

Chung, K. H., C. C. Hart, S. Al-Bassam, A. Avery, J. Taylor, P. D. Patel, A. B. Vojtek and D. L. Turner (2006). "Polycistronic RNA polymerase II expression vectors for RNA interference based on BIC/miR-155." Nucleic Acids Res **34**(7): e53.

Engelen, E., U. Akinci, J. C. Bryne, J. Hou, C. Gontan, M. Moen, D. Szumska, C. Kockx, W. van Ijcken, D. H. Dekkers, J. Demmers, E. J. Rijkers, S. Bhattacharya, S. Philipsen, L. H. Pevny, F. G. Grosveld, R. J. Rottier, B. Lenhard and R. A. Poot (2011). "Sox2 cooperates with Chd7 to regulate genes that are mutated in human syndromes." Nat Genet **43**(6): 607-611.

Feng, W., M. A. Khan, P. Bellvis, Z. Zhu, O. Bernhardt, C. Herold-Mende and H. K. Liu (2013). "The Chromatin Remodeler CHD7 Regulates Adult Neurogenesis via Activation of SoxC Transcription Factors." Cell Stem Cell **13**(1): 62-72.

Hartshorne, T. S., T. L. Grialou and K. R. Parker (2005). "Autistic-like behavior in CHARGE syndrome." Am J Med Genet A **133A**(3): 257-261.

Hurd, E. A., P. L. Capers, M. N. Blauwkamp, M. E. Adams, Y. Raphael, H. K. Poucher and D. M. Martin (2007). "Loss of Chd7 function in gene-trapped reporter mice is embryonic lethal and associated with severe defects in multiple developing tissues." Mamm Genome **18**(2): 94-104.

Hurd, E. A., H. K. Poucher, K. Cheng, Y. Raphael and D. M. Martin (2010). "The ATP-dependent chromatin remodeling enzyme CHD7 regulates pro-neural gene expression and neurogenesis in the inner ear." Development **137**(18): 3139-3150.

Janssen, N., J. E. Bergman, M. A. Swertz, L. Tranebjaerg, M. Lodahl, J. Schoots, R. M. Hofstra, C. M. van Ravenswaaij-Arts and L. H. Hoefsloot (2012). "Mutation update on the CHD7 gene involved in CHARGE syndrome." Hum Mutat **33**(8): 1149-1160.

Jiang, Y. H., R. K. Yuen, X. Jin, M. Wang, N. Chen, X. Wu, J. Ju, J. Mei, Y. Shi, M. He, G. Wang, J. Liang, Z. Wang, D. Cao, M. T. Carter, C. Chrysler, I. E. Drmic, J. L. Howe, L. Lau, C. R. Marshall, D. Merico, T. Nalpathamkalam, B. Thiruvahindrapuram, A. Thompson, M. Uddin, S. Walker, J. Luo, E. Anagnostou, L. Zwaigenbaum, R. H. Ring, J. Wang, C. Lajonchere, A. Shih, P. Szatmari, H. Yang, G. Dawson, Y. Li and S. W. Scherer (2013). "Detection of Clinically Relevant Genetic Variants in Autism Spectrum Disorder by Whole-Genome Sequencing." Am J Hum Genet.

Khodosevich, K., J. Alfonso and H. Monyer (2013). "Dynamic changes in the transcriptional profile of subventricular zone-derived postnatally born neuroblasts." Mech Dev **130**(6-8): 424-432.

Kita, Y., M. Nishiyama and K. I. Nakayama (2012). "Identification of CHD7S as a novel splicing variant of CHD7 with functions similar and antagonistic to those of the full-length CHD7L." Genes Cells **17**(7): 536-547.

Layman, W. S., D. P. McEwen, L. A. Beyer, S. R. Lalani, S. D. Fernbach, E. Oh, A. Swaroop, C. C. Hegg, Y. Raphael, J. R. Martens and D. M. Martin (2009). "Defects in neural stem cell proliferation and olfaction in Chd7 deficient mice indicate a mechanism for hyposmia in human CHARGE syndrome." Hum Mol Genet **18**(11): 1909-1923.

Legendre, M., M. Gonzales, G. Goudefroye, F. Bilan, P. Parisot, M. J. Perez, M. Bonniere, B. Bessieres, J. Martinovic, A. L. Delezoide, F. Jossic, C. Fallet-Bianco, M. Bucourt, J. Tantau, P. Loget, L. Loeuillet, N. Laurent, B. Leroy, H. Salhi, N. Bigi, C. Rouleau, F. Guimiot, C. Quelin, A. Bazin, C. Alby, A. Ichkou, R. Gesny, A. Kitzis, Y. Ville, S. Lyonnet, F. Razavi, B. Gilbert-Dussardier, M. Vekemans and T. Attie-Bitach (2012). "Antenatal spectrum of CHARGE syndrome in 40 fetuses with CHD7 mutations." J Med Genet **49**(11): 698-707.

Lim, D. A., Y. C. Huang, T. Swigut, A. L. Mirick, J. M. Garcia-Verdugo, J. Wysocka, P. Ernst and A. Alvarez-Buylla (2009). "Chromatin remodelling factor Mll1 is essential for neurogenesis from postnatal neural stem cells." Nature **458**(7237): 529-533.

Lim, D. A., M. Suarez-Farinas, F. Naef, C. R. Hacker, B. Menn, H. Takebayashi, M. Magnasco, N. Patil and A. Alvarez-Buylla (2006). "In vivo transcriptional profile analysis reveals RNA splicing and chromatin remodeling as prominent processes for adult neurogenesis." Mol Cell Neurosci **31**(1): 131-148.

Magnuson, D. S., D. J. Morassutti, M. W. McBurney and K. C. Marshall (1995). "Neurons derived from P19 embryonal carcinoma cells develop responses to excitatory and inhibitory neurotransmitters." Brain Res Dev Brain Res **90**(1-2): 141-150.

Marei, H. E., A. E. Ahmed, F. Michetti, M. Pescatori, R. Pallini, P. Casalbore, C. Cenciarelli and M. Elhadidy (2012). "Gene expression profile of adult human olfactory bulb and embryonic neural stem cell suggests distinct signaling pathways and epigenetic control." PLoS One **7**(4): e33542.

Mark, M., N. B. Ghyselinck and P. Chambon (2009). "Function of retinoic acid receptors during embryonic development." Nucl Recept Signal **7**: e002.

Marshall, C. A., B. G. Novitch and J. E. Goldman (2005). "Olig2 directs astrocyte and oligodendrocyte formation in postnatal subventricular zone cells." J Neurosci **25**(32): 7289-7298.

McBurney, M. W. (1993). "P19 embryonal carcinoma cells." Int J Dev Biol **37**(1): 135-140.

Micucci, J. A., W. S. Layman, E. A. Hurd, E. D. Sperry, S. F. Frank, M. A. Durham, D. L. Swiderski, J. M. Skidmore, P. C. Scacheri, Y. Raphael and D. M. Martin (2013). "CHD7 and retinoic acid signaling cooperate to regulate neural stem cell and inner ear development in mouse models of CHARGE syndrome." Hum Mol Genet.

Molofsky, A. V., S. He, M. Bydon, S. J. Morrison and R. Pardal (2005). "Bmi-1 promotes neural stem cell self-renewal and neural development but not mouse growth and survival by repressing the p16Ink4a and p19Arf senescence pathways." Genes Dev **19**(12): 1432-1437.

Molofsky, A. V., R. Pardal, T. Iwashita, I. K. Park, M. F. Clarke and S. J. Morrison (2003). "Bmi-1 dependence distinguishes neural stem cell self-renewal from progenitor proliferation." Nature **425**(6961): 962-967.

Nguyen-Ba-Charvet, K. T., N. Picard-Riera, M. Tessier-Lavigne, A. Baron-Van Evercooren, C. Sotelo and A. Chedotal (2004). "Multiple roles for slits in the control of cell migration in the rostral migratory stream." J Neurosci **24**(6): 1497-1506.

O'Roak, B. J., L. Vives, S. Girirajan, E. Karakoc, N. Krumm, B. P. Coe, R. Levy, A. Ko, C. Lee, J. D. Smith, E. H. Turner, I. B. Stanaway, B. Vernot, M. Malig, C. Baker, B. Reilly, J. M. Akey, E. Borenstein, M. J. Rieder, D. A. Nickerson, R. Bernier, J. Shendure and E. E. Eichler (2012). "Sporadic autism exomes reveal a highly interconnected protein network of de novo mutations." Nature **485**(7397): 246-250.

Pinto, G., V. Abadie, R. Mesnage, J. Blustajn, S. Cabrol, J. Amiel, L. Hertz-Pannier, A. M. Bertrand, S. Lyonnet, R. Rappaport and I. Netchine (2005). "CHARGE syndrome includes hypogonadotropic hypogonadism and abnormal olfactory bulb development." J Clin Endocrinol Metab **90**(10): 5621-5626.

Soprano, D. R., B. W. Teets and K. J. Soprano (2007). "Role of retinoic acid in the differentiation of embryonal carcinoma and embryonic stem cells." Vitam Horm **75**: 69-95.

Takada, I., M. Mihara, M. Suzawa, F. Ohtake, S. Kobayashi, M. Igarashi, M. Y. Youn, K. Takeyama, T. Nakamura, Y. Mezaki, S. Takezawa, Y. Yogiashi, H. Kitagawa, G. Yamada, S. Takada, Y. Minami, H. Shibuya, K. Matsumoto and S. Kato (2007). "A histone lysine methyltransferase activated by non-canonical Wnt signalling suppresses PPAR-gamma transactivation." Nat Cell Biol **9**(11): 1273-1285.

Taylor, J., K. H. Chung, C. Figueroa, J. Zurawski, H. M. Dickson, E. J. Brace, A. W. Avery, D. L. Turner and A. B. Vojtek (2008). "The scaffold protein POSH regulates axon outgrowth." Mol Biol Cell **19**(12): 5181-5192.

Wu, W., K. Wong, J. Chen, Z. Jiang, S. Dupuis, J. Y. Wu and Y. Rao (1999). "Directional guidance of neuronal migration in the olfactory system by the protein Slit." Nature **400**(6742): 331-336.

Yu, J. Y., T. W. Wang, A. B. Vojtek, J. M. Parent and D. L. Turner (2005). "Use of short hairpin RNA expression vectors to study mammalian neural development." Methods Enzymol **392**: 186-199.

Zentner, G. E., P. J. Tesar and P. C. Scacheri (2011). "Epigenetic signatures distinguish multiple classes of enhancers with distinct cellular functions." Genome Res **21**(8): 1273-1283.

Chapter 4

Analysis of *Chd7* function during murine corticogenesis.

Introduction

The cerebral cortex of the mammalian brain is a complex, multilayered tissue that is responsible for processing sensory and motor inputs as well as mediating higher thought processes, language and memory. In order to provide the proper input of external signals into sensory perception and output to the body, the cortex is stratified into layers of neurons that facilitate these activities. The intricate, layered development of the cortex arises from the neural stem cell niche lining the lateral ventricles (LV) of the mammalian forebrain known as the ventricular/subventricular zone (VZ/SVZ) (Lois et al. 1993; Davis et al. 1994). Early in corticogenesis (embryonic day 11 in the mouse embryo), VZ/SVZ neural stem cells divide symmetrically with a vertical cleavage plane to expand the existing stem cell pool (Smart 1973; Chenn et al. 1995). As corticogenesis progresses, the neural stem cells switch to an asymmetric, horizontal cleavage pattern that produces a neural stem cell and a neural progenitor cell (Noctor et al. 2004; Shitamukai et al. 2011). Neural progenitor cells, also termed transit amplifying progenitors, rapidly divide symmetrically to produce more progenitor cells and asymmetrically to produce a large number of immature neurons (Noctor et al. 2008). During this time, the transit amplifying cell population is responsible for the exponential increase in neuron production (Kriegstein et al. 2006). It has

been hypothesized that the astronomical difference in the number of transit amplifying cells in the SVZ of the human cortex has led to the rapid evolution of higher thought processes present in humans as compared to other primates and mammals (Kriegstein et al. 2006).

At embryonic day 15 in the developing mouse, the SVZ neural stem cell niche stops creating neurons destined for migration into the cortex and shifts to making neurons that migrate to the olfactory bulb (OB) (Wichterle et al. 2001; Lledo et al. 2008). I have characterized the role of the chromatin remodeling enzyme CHD7 in the development and maintenance of the SVZ neural stem cell niche with regards to olfactory bulb development and maintenance (Micucci et al. 2013). Additionally, CHD7 is known to be required for proper development of the inner ear, nasal epithelium and eye, as evidenced by the high phenotypic penetrance of hearing, balance, olfaction and vision defects in individuals with CHARGE syndrome (Adams et al. 2007; Hurd et al. 2007; Layman et al. 2009; Hurd et al. 2010; Hurd et al. 2011). In contrast, there has been no exploration of CHD7 function in the development of the cortex, which processes inputs from all of the affected sensory organs and may impact the sensory capabilities of CHARGE individuals.

Chd7 is expressed in the embryonic mouse forebrain throughout the time period associated with active corticogenesis (embryonic day 11 to embryonic day 15) (Hurd et al. 2007). Here, I performed histological analyses of *Chd7* in the mouse forebrain during mid and late corticogenesis (embryonic days 13 and 15). CHD7 co-localizes with neural stem cells and neural progenitor cells in the SVZ.

Immunofluorescence analysis of *Chd7*-deficient brains during corticogenesis showed that there are no defects in proliferation or apoptosis. Neurosphere assays revealed that *Chd7*-deficiency resulted in a mild decrease in neurosphere size, but did not affect self-renewal or neuronal potential. Our findings show that *Chd7* is expressed during corticogenesis in neural stem and progenitor cells, but loss of *Chd7* does not appear to affect the process in an appreciable manner.

Materials and Methods

Mouse strains, breeding and genotyping.

Chd7$^{flox/flox}$ mice were maintained as previously described (Hurd et al. 2007; Hurd et al. 2010). Zsgreen Cre reporter mice (Madisen et al. 2010) were maintained on a C57BL/6/129 mixed background and bred with *Chd7*$^{flox/flox}$ to produce Zsgreen/Zsgreen; *Chd7*$^{flox/flox}$ mice. *Nestin-CreERT2* mice were maintained on a C57BL/6 background and mated with *Chd7*$^{flox/flox}$ or Zsgreen/Zsgreen; *Chd7*$^{flox/flox}$ mice to generate *Cre*;*Chd7*$^{flox/+}$ mice. *Cre;Chd7*$^{flox/+}$ mice were crossed to *Chd7*$^{flox/flox}$ to produce control (*Chd7*$^{flox/+}$ and *Chd7*$^{flox/flox}$), *Chd7* conditional heterozygous (*Cre;Chd7*$^{flox/+}$), and conditional knockout (*Cre;Chd7*$^{flox/flox}$) mice. Genomic DNA was isolated from tail and brain tissue and PCR genotyped as previously described (Hurd et al. 2010). All procedures were approved by The University of Michigan University Committee on the Use and Care of Animals (UCUCA).

Tamoxifen administration.

Tamoxifen (Sigma-Aldritch, St. Louis, MO) was dissolved in sterile corn oil at a concentration of 10 mg/ml. A single dose of Tamoxifen (0.2 mg/gbw) was administered by intraperitoneal injection to pregnant females at embryonic day 11.5 (E11.5) and embryos were processed for cryosectioning (at E13.5 and at E15.5) or neurosphere assays (at E14.5).

Histology and embedding.

E13.5 and E15.5 embryos were placed in 4% paraformaldehyde for 2 hrs, then cryoprotected in 30% sucrose, embedded in OCT (Tissue Tek, Torrance, CA), frozen and sectioned at 12 µm.

Immunofluorescence.

Cryosections from E13.5 and E15.5 embryos (*n* = 3 per genotype) were processed for immunofluorescence with antibodies against CHD7 (1:7500; Cell Signaling Technology, Beverly, MA), cleaved caspase 3 (1:800, Cell Signaling Technology), phospho-histone H3 (1:500, EMD Millipore), Nestin (1:500, Developmental Studies Hybridoma Bank, University of Iowa, Iowa City, IA), SOX2 (1:250; EMD Millipore), PAX6 (1:300, Covance, Princeton, NJ), TBR2 (1:2000, a gift from Robert Hevner), GFAP (1:500; Sigma), O4 (1:800; Developmental Studies Hybridoma Bank), Tuj1 (1:400; Covance). All secondary antibodies were used at 1:200 with Alexa Fluor 488, Alexa Fluor 555 or biotinylated secondary antibodies (Vector Laboratories) conjugated with

streptavidin-Horseradish Peroxidase and Alexa Fluor 488 Tyramide Signal Amplification or Alexa Fluor 555 Tyramide Signal Amplification (Life Technologies, Carlsbad, CA). Images were produced by single channel fluorescence microscopy on a Leica upright DMRB microscope (Leica Camera AG, Solms, Germany) and processed in Photoshop CS5.1 (Adobe, San Jose, CA).

SVZ proliferation and apoptosis studies.

E13.5 and E15.5 embryos (*n* = 3 per genotype) were processed for immunofluorescence with antibodies against phospho-histone H3 and cleaved caspase 3. Images were captured by single channel fluorescence microscopy on a Leica upright DMRB microscope and processed in Adobe Photoshop CS5.1. For quantification of pH3+ and caspase3+ cells, 12 images using the 10X (pH3) or 20X (caspase3) objective lens were taken of six SVZ sections per genotype and the number of pH3+ and caspase3+ cells were counted using the cell counter function of Image J (National Institutes of Health, Bethesda, MD).

Neurosphere cultures.

E14.5 embryos (*n* = 2 per genotype) were decapitated, skin was removed from the brain, the entire forebrain was dissected and dissociated in trypsin/EDTA (Life Technologies) and counted on a hemacytometer. For primary neurosphere formation assays, 1000 cells were plated on ultra-low binding 6 well plates (Corning, Corning, NY) under self-renewal conditions (media with EGF

and FGF), incubated at 37°C with 6.5% CO_2 for 8 days then measured and imaged using an Olympus IX81 motorized inverted microscope (Olympus, Tokyo, Japan). Secondary neurospheres were generated by dissociating single primary neurospheres and re-plating them under self-renewing conditions. For differentiation, single secondary neurospheres were plated under adherent conditions with FGF and without EGF (24 well tissue culture-treated plates (Corning) with poly-D-lysine and human fibronectin (Biomedical Technologies, Stoughton, MA)) then incubated at 37°C with 6.5% CO_2 for 12 days. Neurosphere diameter (*n*=150 per genotype) was measured using the arbitrary line tool in the Olympus cellSens Dimension software package. Neurosphere frequency was determined by counting the total number of neurospheres greater than 50 µm in diameter in each well of a 6 well plate and dividing by the total number of cells plated per well. Statistical significance was determined by unpaired Student's t-test.

Neurosphere differentiation, staining and scoring.

Secondary neurospheres were differentiated as described above then treated with 1:800 anti-O4 antibody for 1 hr and fixed with ice cold 95% ethanol/ 5% glacial acetic acid at -20ºC for 20 min. Fixed neurospheres were blocked for 1 h at room temperature with light rocking with blocking buffer (0.05% octylphenoxypolyethoxyethanol (NP-40, Sigma), 2 mg/ml bovine serum albumin (Sigma) in phosphate buffered saline). Alexa Fluor 647 conjugated goat anti-mouse IgM (1:500, Life Technologies) diluted in blocking buffer was added to

each well and incubated at room temperature for 1 h with light rocking. Each well was washed three times with blocking buffer then a cocktail of 1:500 anti-Tuj1 and 1:500 anti-GFAP primary antibodies was added to each well and incubated at room temperature for 1 h with light rocking. Each well was washed three times with blocking buffer then incubated in a cocktail of 1:500 Alexa Fluor 555 goat anti-mouse IgG_{2a} and 1:500 Alexa Fluor 488 goat anti-mouse IgG_1 at room temperature for 1 hr with light rocking. Each well was washed three times and nuclei were stained with 1:1000 DAPI for 15 min. Stained colonies were imaged with an Olympus IX81 motorized inverted microscope and scored for the presence or absence of cell type-specific immunofluorescence (*n* = 12 neurospheres per genotype). Statistical significance was determined by unpaired Student's t-test.

Retinoic acid and citral treatment of neurosphere cultures.

Neurosphere assays were performed as above on control, *Nestin-ERT2* Cond Het, and *Nestin-ERT2* Cond KO P1 mice. Secondary neurospheres (*n* = 2 per genotype) were plated in ultra-low binding 6 well plates in self-renewal medium or medium supplemented with 0.1 μM retinoic acid (Sigma), 1 μM retinoic acid, or 10 μM citral (Sigma) (*n* = 12 wells per genotype). For differentiation, untreated secondary neurospheres from each genotype were plated in 24 well plates in differentiation medium or medium supplemented with 1 μM retinoic acid, 1 μM citral, or 10 μM citral (*n* = 12 neurospheres per condition), and scored for differentiation as above.

Results

Chd7 is expressed in SVZ neural stem and progenitor cells during peak corticogenesis.

Chd7 is expressed throughout the mouse forebrain during embryogenesis (Hurd et al. 2007), but its cell type-specific co-localization during corticogenesis is currently unknown. To address this, I performed co-immunofluorescence for CHD7 and cell type-specific markers on coronal forebrain sections from wild type embryonic day 13.5 (E13.5) mouse embryos (Fig. 4.1B). CHD7 co-localizes with a subset of Nestin+ neural stem cells (Fig. 4.1C) and SOX2+ neural stem and progenitor cells (Fig. 4.1D) in the VZ/SVZ along the lateral wall of the LV. Additionally, CHD7 is present in PAX6+ and TBR2+ neural progenitor cells in the SVZ of wild type E13.5 embryos (Fig. 4.1E,F). These data are consistent with *Chd7* expression in neural stem and progenitor cells in the adult mouse SVZ (Fig. 2.4) and suggest that CHD7 may play a role in SVZ development and maintenance throughout life (Feng et al. 2013; Micucci et al. 2013).

In order to assess for potential defects in cortex development due to loss of *Chd7*, I utilized the *Nestin-CreERT2* allele and the Zsgreen reporter to conditionally knockout *Chd7* expression specifically in neural stem cells at the onset of corticogenesis at E11.5 and to mark cells in which recombination of the $Chd7^{flox}$ allele has occurred (Fig. 4.1A) (Ables et al. 2010; Madisen et al. 2010). *Chd7* is expressed throughout the E13.5 SVZ (Fig. 4.1G) and is absent in embryos with neural stem cell-specific *Chd7* conditional deletion (*NestinERT2* Cond KO, Fig. 4.1H). Activation of the Zsgreen reporter, combined with loss of

CHD7 immunofluorescence, confirms *Nestin-CreERT2* specific deletion of *Chd7* in the *NestinERT2* Cond KO embryonic SVZ (Fig. 4.1H).

Chd7-deficiency does not affect proliferation or apoptosis in the SVZ during mid-corticogenesis.

In studies outlined in Chapter 2, I examined the cortical thickness of adult *Nestin-Cre* conditional *Chd7* knockout mice, in which *Chd7* is deleted in *Nestin* lineage cells beginning at E8.5. Cortical thickness was used in this context as a measure of cumulative SVZ proliferation and neuronal migration during development and into adulthood. While I did not observe any changes in cortical thickness in *Nestin* Cond KO adult mice compared to controls (Fig. 2.7), the possibility remains that the crude measurement of cortical thickness may have masked a minor defect during a brief proliferative or migratory window during embryogenesis. In order to investigate this, I analyzed the E13.5 *Chd7*-deficient mouse SVZ for changes in cell proliferation that may arise due to *Chd7*-deficiency. Immunofluorescence detecting phosphorylated histone H3 (pH3), a marker of mitotic cells, revealed no changes in SVZ proliferation between control and *NestinERT2* Cond KO embryos (Fig. 4.2A-C). I also observed no changes in cellular apoptosis, marked by cleaved caspase3 (casp3), between control and *NestinERT2* Cond KO SVZ at E13.5 (Fig. 4.2D-F). While I did not observe proliferation or apoptosis defects between E11.5 and E13.5, these data leave open the possibility that CHD7 function may be more critical during later corticogenesis, between E13.5 and E15.5.

Loss of *Chd7* results in minor neurosphere size deficits while having no impact on self-renewal or neurogenesis.

In order to detect more subtle effects of *Chd7*-deficiency on stem and progenitor cell function, I performed neurosphere assays using control, *NestinERT2* Cond Het and *NestinERT2* Cond KO E14.5 embryonic forebrains (Fig. 4.3A) (Reynolds et al. 1992; Pastrana et al. 2011). Similar to perinatal and adult neurosphere analyses (Fig. 2.8 and 2.12), *NestinERT2* Cond Het and *NestinERT2* Cond KO showed a decrease in neurosphere size by 12% and 23%, respectively, compared to controls (Fig. 4.3B). Treatment with retinoic acid (RA) led to a reduction in neurosphere size regardless of genotype (Fig. 4.3B). The dosage dependent differences in neurosphere size observed among untreated controls, *NestinERT2* Cond Het and *NestinERT2* Cond KO neurospheres was preserved upon treatment with RA (Fig. 4.3B). Consistent with data obtained from citral-treated perinatal neurospheres (Fig. 2.14), inhibition of RA signaling resulted in a rescue of the size defect of *NestinERT2* Cond Het and *NestinERT2* Cond KO neurospheres which were only 2% and 4% smaller, respectively, compared citral-treated controls (Fig. 4.3B). These data show that there is a mild, but significant, proliferative defect in *Chd7*-deficient SVZ neural stem cells during corticogenesis that can be rescued by modulating RA signaling.

Chd7-deficient neurospheres derived from E14.5 forebrain did not display self-renewal or neurogenic defects (Figs. 4.3C,D). Additionally, modulation of retinoic acid signaling did not affect E14.5 SVZ neurosphere self-renewal and

differentiation (Figs. 4.3C,D). These data suggest that *Chd7* may be largely unnecessary for self-renewal and neuronal differentiation during corticogenesis. Conversely, using whole forebrain for neurosphere assays may mask any effects that may be observed if microdissected VZ/SVZ were used as the starting material.

Chd7 expression persists during late corticogenesis, but _Chd7_ deficiency exerts no effects on SVZ proliferation.

Corticogenesis proceeds in the mouse from E11 to E15. To test whether CHD7 regulates later aspects of cortex formation, I assayed CHD7 co-localization with neural stem and progenitor cell markers persisted at E15.5, immediately prior to the transition from cortical neurogenesis to olfactory bulb neurogenesis (Wichterle et al. 2001) (Fig. 4.4B). As observed at E13.5, CHD7 co-localizes with Nestin+ neural stem cells, SOX2+ neural stem and progenitor cells and TBR2+ neural progenitor cells at E15.5 (Fig. 4.4C-E).

Next, I generated E15.5 *NestinERT2* Cond KO embryos to address whether there is a proliferation defect present between E13.5 and E15.5 which would have been missed in E13.5 studies detailed above (Fig. 4.4A). I observed no differences in pH3 staining between control and *NestinERT2* Cond KO E15.5 SVZ corticogenesis period (Fig. 4.4F-H). Additionally, there were no detectable Caspase 3+ cells observed in control and *NestinERT2* Cond KO E15.5 SVZ. These data imply that there is no appreciable change in SVZ proliferation or apoptosis with loss of *Chd7* throughout the corticogenic period, but do not

investigate the possibility of CHD7 activity in neuroblast migration and maturation which may impact cortex function.

Discussion

Here I showed that *Chd7* is expressed in neural stem and progenitor cells during mid (E13.5) and late (E15.5) corticogenesis. Loss of *Chd7* through mid-corticogenesis (E11.5-E13.5) or late corticogenesis (E11.5-E15.5) did not result in changes in proliferation and apoptosis. Conversely, E14.5 *Chd7*-deficient neurospheres displayed a 23% reduction in size that is rescued with inhibition of retinoic acid signaling through citral treatment, but did not have self-renewal or neuronal differentiation deficits. Together, these findings demonstrate that *Chd7* is not required for the proper function of the SVZ neural stem cell niche during corticogenesis.

While there does not appear to be any aberration in neural stem and progenitor cell self-renewal or proliferation upon loss of *Chd7* during cortex formation, I did not characterize CHD7 function in the neuroblasts produced by neural progenitor cells or to the identity of cortical neuron layers. CHD7 could potentially play a role in the migration and maturation of neurons, as suggested by changes in expression of key neuronal migration genes in perinatal SVZ from *Chd7* mutant mice (Table 3.1). Analysis of the fate of *Chd7*-deficient neuroblasts born in the SVZ during corticogenesis may provide insights into the differentiation, migration and maturation of these neuron populations. Cortical neuron migration or maturation phenotypes in *Chd7*-deficient mice may indicate

a potential reason for further complication of sensory processing in CHARGE individuals.

CHD7 has been implicated in autism spectrum disorder (ASD), and the R in the CHARGE syndrome acronym originally represented mental retardation (Fernell et al. 1999; O'Roak et al. 2012). However, cognitive deficiencies observed in CHARGE individuals may be more related to extreme sensory impairment and difficulties in learning and communication than isolated intellectual disability (Hartshorne et al. 2005). Interestingly, *Chd7* is highly expressed in the neural stem cell niche of the dentate gyrus of the hippocampus, the region of the brain responsible for learning and memory (Feng et al. 2013). Preliminary studies of CHD7 function in the dentate gyrus indicate that CHD7 regulates production of neuroblasts, as well as neuronal differentiation and maturation (Feng et al. 2013). Further studies investigating the role of CHD7 in the function of the sensory cortex and hippocampus are clearly needed to inform diagnostics and therapeutic options for CHARGE individuals.

Acknowledgements

I would like to thank Sophia Frank for assistance with animal husbandry, tissue preparation and immunofluorescence experiments.

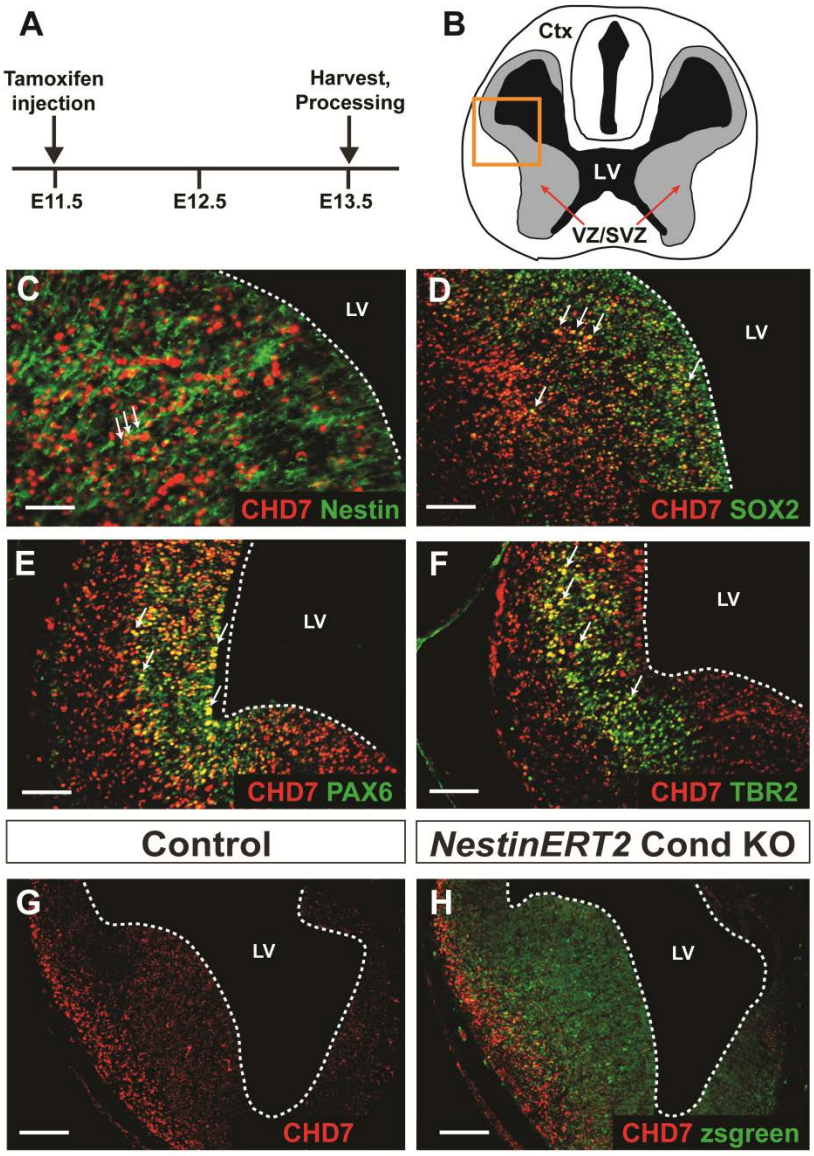

Figure 4.1. CHD7 co-localizes with neural stem and progenitor cells during early corticogenesis. (**A**) Schematic showing the Tamoxifen dosing regimen where pregnant females received a single intraperitoneal injection of Tamoxifen (0.2 mg/gbw) at embryonic day 11.5 (E11.5) and embryos were harvested for cryosectioning at E13.5. (**B**) Cartoon showing a coronal section of an E13.5 mouse forebrain showing the neural stem and progenitor cells in the ventricular/subventricular zones (VZ/SVZ, gray) lining the lateral ventricles (LV, black) with the orange box denoting the region shown in **C-H**. CHD7 co-localizes with the neural stem cell markers Nestin (**C**) and SOX2 (**D**) and the neural progenitor cell markers PAX6 (**E**) and TBR2 (**F**). The Zsgreen reporter was used to monitor deletion of *Chd7* in *Nestin*-lineage cells, also confirmed by CHD7 immunofluorescence in *NestinERT2* Cond KO E13.5 SVZ (**H**) compared to controls (**G**). White arrows denote co-localized yellow cells. Other abbreviations: Ctx: cortex. Scale bars in (**C**): 25 µm, (**D-F**): 75 µm and (**G**,**H**): 150 µm.

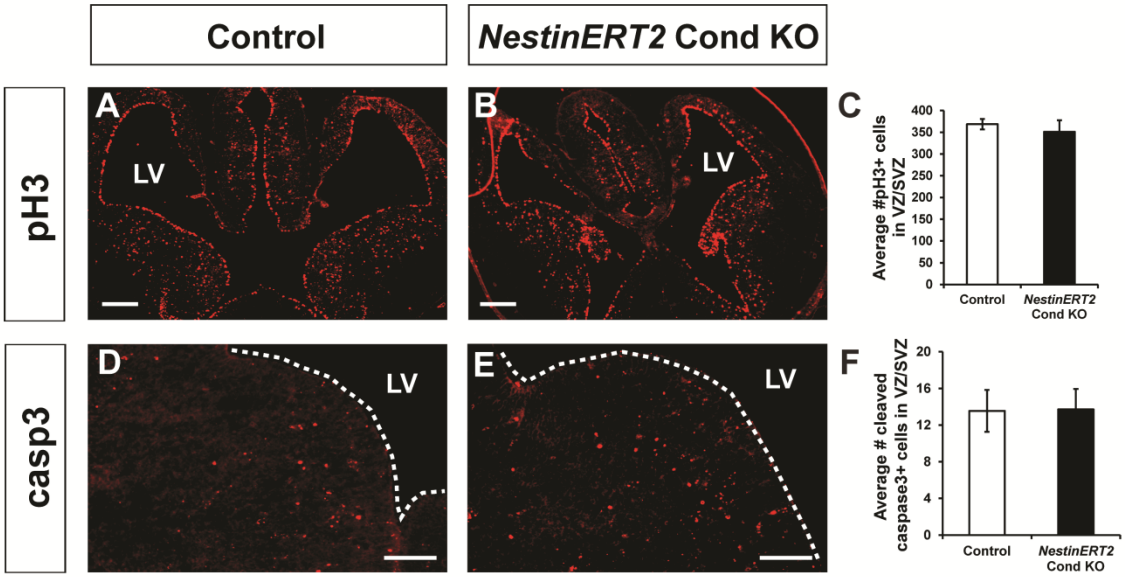

Figure 4.2. Proliferation and apoptosis are normal in *Chd7*-deficient SVZ during early corticogenesis.
Coronal cryosections of E13.5 SVZ from control and *NestinERT2* Cond KO embryos were processed for immunofluorescence for phospho-histone H3, marking mitotic cells (pH3, **A**,**B**) and cleaved caspase3, marking apoptotic cells (casp3, **C**,**D**). There was no difference in the number of pH3+ cells between control (**A**) and *NestinERT2* Cond KO (**B**) E13.5 SVZ (quantified in **C**). In addition, there was no difference in the number of casp3+ cells between control (**D**) and *NestinERT2* Cond KO (**E**) E13.5 SVZ (quantified in **F**). Other abbreviations: LV: lateral ventricles. Scale bars in (**A**,**B**): 250 µm and (**D**,**E**): 25 µm. Error bars in (**C, F**) indicate standard error of the mean (SEM, *n*=3 per genotype).

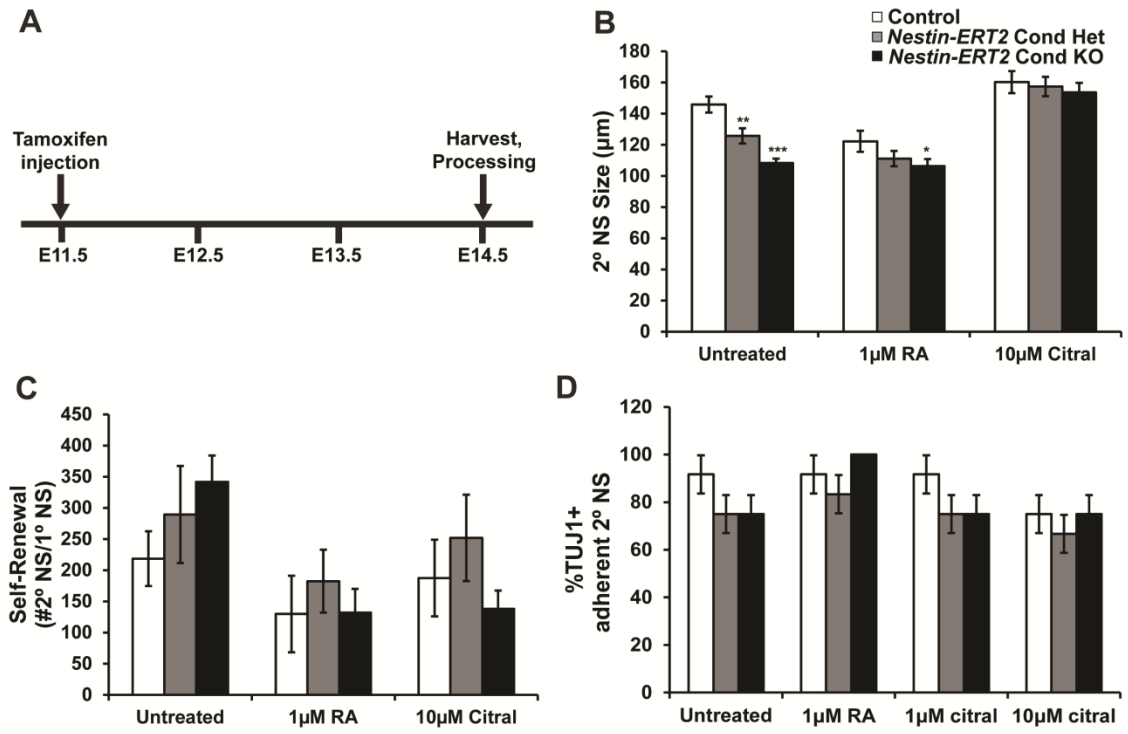

Figure 4.3. *Chd7*-deficient forebrain neurospheres display mild proliferative defects.
(A) Schematic showing the Tamoxifen dosing regimen where pregnant females received a single intraperitoneal injection of Tamoxifen (0.2 mg/gbw) at embryonic day 11.5 (E11.5) and embryos were harvested for neurosphere assays at E14.5. Secondary neurospheres were derived from P1 control, *Nestin-ERT2* Cond Het and *Nestin-ERT2* Cond KO mice then treated with varying concentrations of all-trans retinoic acid (RA) or the retinoic acid signaling inhibitor citral and assayed for changes in size (**B**), self-renewal (**C**), and neuronal potential (**D**). (**B**) Untreated neurospheres displayed a *Chd7* dosage dependent reduction in size, while treatment with 1µM RA resulted in slightly smaller control and *NestinERT2* Cond Het neurospheres and treatment with 1µM citral rescued *Nestin-ERT2* Cond Het and *Nestin-ERT2* Cond KO neurosphere size to control levels. (**C**) There were no discernible changes in self-renewal of E14.5 secondary neurospheres with *Chd7*-deficiency or alterations of retinoic acid signaling.
(**D**) Neuronal potentials of E14.5 *NestinERT2* Cond KO secondary neurospheres, regardless of treatment, were also unchanged compared to control. Error bars in (**B-D**) indicate SEM (*n*=2 per genotype).

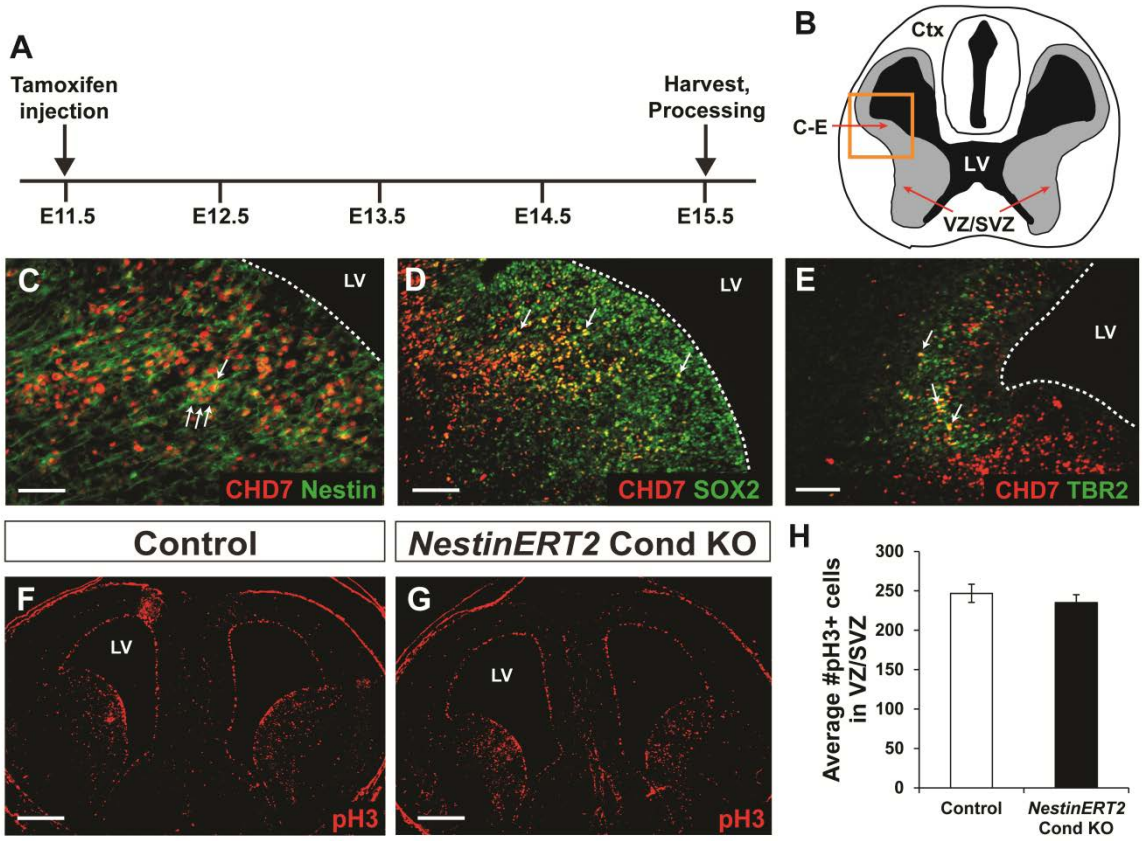

Figure 4.4. CHD7 is expressed in E15.5 SVZ neural stem and progenitor cells and does not regulate proliferation.
(**A**) Schematic showing the Tamoxifen dosing regimen where pregnant females received a single intraperitoneal injection of Tamoxifen (0.2 mg/gbw) at embryonic day 11.5 (E11.5) and embryos were harvested for cryosectioning at E15.5. (**B**) Cartoon showing a coronal section of an E15.5 mouse forebrain showing the neural stem and progenitor cells in the ventricular/subventricular zones (VZ/SVZ, gray) lining the lateral ventricles (LV, black) with the orange box denoting the region shown in **C-E**. CHD7 co-localizes with the neural stem cell markers Nestin (**C**) and SOX2 (**D**) and the neural progenitor cell marker TBR2 (**E**). There was no difference in the number of pH3+ cells between control (**F**) and *NestinERT2* Cond KO (**G**) E13.5 SVZ (quantified in **H**). White arrows denote co-localized yellow cells. Other abbreviations: Ctx: cortex. Scale bars in (**C-E**): 25 µm, (**F**,**G**): 250 µm. Error bars in (**H**) indicate (SEM) (*n*=3 per genotype).

References

Ables, J. L., N. A. Decarolis, M. A. Johnson, P. D. Rivera, Z. Gao, D. C. Cooper, F. Radtke, J. Hsieh and A. J. Eisch (2010). "Notch1 is required for maintenance of the reservoir of adult hippocampal stem cells." J Neurosci **30**(31): 10484-10492.

Adams, M. E., E. A. Hurd, L. A. Beyer, D. L. Swiderski, Y. Raphael and D. M. Martin (2007). "Defects in vestibular sensory epithelia and innervation in mice with loss of Chd7 function: implications for human CHARGE syndrome." J Comp Neurol **504**(5): 519-532.

Chenn, A. and S. K. McConnell (1995). "Cleavage orientation and the asymmetric inheritance of Notch1 immunoreactivity in mammalian neurogenesis." Cell **82**(4): 631-641.

Davis, A. A. and S. Temple (1994). "A self-renewing multipotential stem cell in embryonic rat cerebral cortex." Nature **372**(6503): 263-266.

Engelen, E., U. Akinci, J. C. Bryne, J. Hou, C. Gontan, M. Moen, D. Szumska, C. Kockx, W. van Ijcken, D. H. Dekkers, J. Demmers, E. J. Rijkers, S. Bhattacharya, S. Philipsen, L. H. Pevny, F. G. Grosveld, R. J. Rottier, B. Lenhard and R. A. Poot (2011). "Sox2 cooperates with Chd7 to regulate genes that are mutated in human syndromes." Nat Genet **43**(6): 607-611.

Feng, W., M. A. Khan, P. Bellvis, Z. Zhu, O. Bernhardt, C. Herold-Mende and H. K. Liu (2013). "The Chromatin Remodeler CHD7 Regulates Adult Neurogenesis via Activation of SoxC Transcription Factors." Cell Stem Cell **13**(1): 62-72.

Fernell, E., V. A. Olsson, C. Karlgren-Leitner, B. Norlin, B. Hagberg and C. Gillberg (1999). "Autistic disorders in children with CHARGE association." Dev Med Child Neurol **41**(4): 270-272.

Hartshorne, T. S., T. L. Grialou and K. R. Parker (2005). "Autistic-like behavior in CHARGE syndrome." Am J Med Genet A **133A**(3): 257-261.

Hurd, E. A., M. E. Adams, W. S. Layman, D. L. Swiderski, L. A. Beyer, K. E. Halsey, J. M. Benson, T. W. Gong, D. F. Dolan, Y. Raphael and D. M. Martin (2011). "Mature middle and inner ears express Chd7 and exhibit distinctive pathologies in a mouse model of CHARGE syndrome." Hear Res **282**(1-2): 184-195.

Hurd, E. A., P. L. Capers, M. N. Blauwkamp, M. E. Adams, Y. Raphael, H. K. Poucher and D. M. Martin (2007). "Loss of Chd7 function in gene-trapped reporter mice is embryonic lethal and associated with severe defects in multiple developing tissues." Mamm Genome **18**(2): 94-104.

Hurd, E. A., H. K. Poucher, K. Cheng, Y. Raphael and D. M. Martin (2010). "The ATP-dependent chromatin remodeling enzyme CHD7 regulates pro-neural gene expression and neurogenesis in the inner ear." Development **137**(18): 3139-3150.

Kriegstein, A., S. Noctor and V. Martinez-Cerdeno (2006). "Patterns of neural stem and progenitor cell division may underlie evolutionary cortical expansion." Nat Rev Neurosci **7**(11): 883-890.

Layman, W. S., D. P. McEwen, L. A. Beyer, S. R. Lalani, S. D. Fernbach, E. Oh, A. Swaroop, C. C. Hegg, Y. Raphael, J. R. Martens and D. M. Martin (2009). "Defects in neural stem cell proliferation and olfaction in Chd7 deficient mice indicate a mechanism for hyposmia in human CHARGE syndrome." Hum Mol Genet **18**(11): 1909-1923.

Lledo, P. M., F. T. Merkle and A. Alvarez-Buylla (2008). "Origin and function of olfactory bulb interneuron diversity." Trends Neurosci **31**(8): 392-400.

Lois, C. and A. Alvarez-Buylla (1993). "Proliferating subventricular zone cells in the adult mammalian forebrain can differentiate into neurons and glia." Proc Natl Acad Sci U S A **90**(5): 2074-2077.

Madisen, L., T. A. Zwingman, S. M. Sunkin, S. W. Oh, H. A. Zariwala, H. Gu, L. L. Ng, R. D. Palmiter, M. J. Hawrylycz, A. R. Jones, E. S. Lein and H. Zeng (2010). "A robust and high-throughput Cre reporting and characterization system for the whole mouse brain." Nat Neurosci **13**(1): 133-140.

Micucci, J. A., W. S. Layman, E. A. Hurd, E. D. Sperry, S. F. Frank, M. A. Durham, D. L. Swiderski, J. M. Skidmore, P. C. Scacheri, Y. Raphael and D. M. Martin (2013). "CHD7 and retinoic acid signaling cooperate to regulate neural stem cell and inner ear development in mouse models of CHARGE syndrome." Hum Mol Genet.

Noctor, S. C., V. Martinez-Cerdeno, L. Ivic and A. R. Kriegstein (2004). "Cortical neurons arise in symmetric and asymmetric division zones and migrate through specific phases." Nat Neurosci **7**(2): 136-144.

Noctor, S. C., V. Martinez-Cerdeno and A. R. Kriegstein (2008). "Distinct behaviors of neural stem and progenitor cells underlie cortical neurogenesis." J Comp Neurol **508**(1): 28-44.

O'Roak, B. J., L. Vives, S. Girirajan, E. Karakoc, N. Krumm, B. P. Coe, R. Levy, A. Ko, C. Lee, J. D. Smith, E. H. Turner, I. B. Stanaway, B. Vernot, M. Malig, C. Baker, B. Reilly, J. M. Akey, E. Borenstein, M. J. Rieder, D. A. Nickerson, R. Bernier, J. Shendure and E. E. Eichler (2012). "Sporadic autism exomes reveal a highly interconnected protein network of de novo mutations." Nature **485**(7397): 246-250.

Pastrana, E., V. Silva-Vargas and F. Doetsch (2011). "Eyes wide open: a critical review of sphere-formation as an assay for stem cells." Cell Stem Cell **8**(5): 486-498.

Reynolds, B. A. and S. Weiss (1992). "Generation of neurons and astrocytes from isolated cells of the adult mammalian central nervous system." Science **255**(5052): 1707-1710.

Shitamukai, A., D. Konno and F. Matsuzaki (2011). "Oblique radial glial divisions in the developing mouse neocortex induce self-renewing progenitors outside the germinal zone that resemble primate outer subventricular zone progenitors." J Neurosci **31**(10): 3683-3695.

Smart, I. H. (1973). "Proliferative characteristics of the ependymal layer during the early development of the mouse neocortex: a pilot study based on recording the number, location and plane of cleavage of mitotic figures." J Anat **116**(Pt 1): 67-91.

Wichterle, H., D. H. Turnbull, S. Nery, G. Fishell and A. Alvarez-Buylla (2001). "In utero fate mapping reveals distinct migratory pathways and fates of neurons born in the mammalian basal forebrain." Development **128**(19): 3759-3771.

Chapter 5

Conclusions and Future Directions

Summary

The focus of my thesis work has been to explore the role of CHD7 in the regulation of neural stem cells and their progeny from embryonic development into adulthood. Specifically, I have focused on the subventricular zone (SVZ) neural stem cell niche which creates neurons that populate the olfactory bulbs (OB) and cerebral cortex. While these two regions vary greatly in their functions in the mature brain, they are vital to the survival and function of most mammals. Human olfaction and processing of olfactory signals through the olfactory bulbs is vital to daily life (Lledo et al. 2006; Lledo et al. 2008). The cerebral cortex is the processing center for sensory, motor and cognitive information and its evolution has imbued higher mammals with sentience (Kriegstein et al. 2006). In CHARGE individuals with *CHD7* mutations, olfactory, motor and cognitive phenotypes may be caused by defects in neural stem cell function during embryogenesis and throughout life (Hartshorne et al. 2005; Issekutz et al. 2005; Legendre et al. 2012).

CHD7 in the perinatal and adult SVZ

Conclusions

In Chapter 2, I developed a mouse model of *Chd7*-deficiency in the adult and perinatal brain to investigate the role of *Chd7* in the maintenance and development of the SVZ. I found that adult *Chd7* heterozygous mice have reduced numbers of GABAergic and dopaminergic interneurons which are responsible for modulating olfactory signals to the olfactory cortex. This finding led me to observe *Chd7* expression from the neural stem cell niche in the SVZ, through the rostral migratory stream (RMS) and into the OB. Double immunofluorescence experiments with cell type specific markers showed that CHD7 co-localizes with a subset of neural stem cells, with the majority of neural progenitor cells and neuroblasts and with subsets of mature GABAergic and dopaminergic interneurons. In both adult and newborn SVZ, *in vivo* immunofluorescence and *in vitro* neurosphere assays demonstrated that *Chd7*-deficient neural stem and progenitor cells display proliferative and neurogenic defects. I also observed a drastic reduction in neuroblasts in the adult RMS of *Chd7*-deficient mice and a corresponding increase in glial cells indicating a potential cell fate switch. Interestingly, modulation of retinoic acid signaling was able to partially rescue the proliferative and neurogenic defects observed in perinatal neurospheres upon loss of *Chd7*. I confirmed direct regulation of retinoic acid signaling by chromatin immunoprecipitation which showed CHD7 binding to the promoter elements of retinoic acid receptor genes. Overall, I have demonstrated that *Chd7* is necessary for the proper function of the perinatal and

adult SVZ neural stem cell niche and its progeny. These studies are an important link to understanding the affected molecular mechanisms in *Chd7*-deficienct neural stem cell niches that may lead to some of the neurological phenotypes observed in CHARGE syndrome.

Future Directions

CHD7 is intimately tied to cell fate decisions in stem cells (Takada et al. 2007; Bajpai et al. 2010; Engelen et al. 2011; Feng et al. 2013) and our data suggest an important role for CHD7 regulation of the choice between neuronal cell fate and oligodendrocyte or glial cell fate in SVZ neural stem and progenitor cells (Micucci et al. 2013). Additionally, CHD7 binds to poised promoter and enhancer elements of ectodermal lineage genes (Zentner et al. 2011). Taken together, it can be hypothesized that CHD7 binds to poised genetic elements of pro-neuronal genes (such as *Ascl1*, *Tbr2*, *Tbr1* and *Neurod1*), recruits histone modifying enzymes such as H3K4 methyltransferases and activates transcription as neural stem and progenitor cells adopt a neuronal fate. This hypothesis could be tested by chromatin immunoprecipitation followed by massively parallel sequencing (ChIP-seq) in mouse or cell models of *Chd7*-deficiency. Chromatin preparations from wild type perinatal or adult mouse SVZ or P19 embryonal carcinoma neurospheres (McBurney et al. 1988; McBurney 1993; MacPherson et al. 1997) could be processed for immunoprecipitation with anti-CHD7 antibody, activating histone modifications (H3K4me1, H3K4me3, H3K27ac) or repressing histone modifications (H3K9me3, H3K27me3). Results of these experiments

would establish a baseline of CHD7 genomic binding in neural stem cells and its association with active, poised and repressed gene transcription, thereby creating a map of CHD7 binding in neural stem cells. Additionally, CHD7 ChIP-seq performed in neural stem cells would provide vital insight into the genomic binding properties of CHD7. For example, CHD7 may co-localize with SOX family consensus binding sequences or retinoic acid response elements (RARE). This binding information would be helpful in determining whether CHD7 is regulating pro-neural gene expression either through regulation of expression of retinoic acid signaling mediators or direct interaction with retinoic acid receptors at pro-neural target genes with RARE's.

An interesting extension of these ChIP-seq experiments would be to induce loss of *Chd7* expression, either through Cre recombination of the *Chd7*^{flox} allele *in vivo* (Hurd et al. 2010) or transfection with a *Chd7* shRNA vector *in vitro* (Yu et al. 2005) then monitor changes in chromatin modifications in known CHD7-bound genes. Upon loss of *Chd7*, formerly activated pro-neural genes may become poised or repressed, potentially leading to an inability to differentiate into neuronal cell types. Considering that I have observed a loss of neuronal differentiation and an increase in glia in the adult *Chd7*-deficient mouse (Micucci et al. 2013), it is necessary to know whether the promoter or enhancer status at gliogenic genes such as *Olig2* or *Gfap* changed from repressed to poised or active in neural stem cells upon loss of *Chd7*. Quantitative RT-PCR could be used to monitor for increases or decreases in gene expression between control and *Chd7*-deficient neural stem cells consistent with changes in promoter

or enhancer status. One would predict that since there is a significant increase in the amount of glial staining in the SVZ, RMS and OB of *Chd7*-deficient mice, there would be a deposition of activating histone marks at pro-glial genes and a corresponding increase in pro-glial gene expression. Overall, these experiments could provide mechanistic insight into the direct regulation of pro-neural genes in neural stem cells by CHD7 through modulation of histone modifications at promoter or enhancer elements.

While ChIP-seq experiments designed to observe the co-localization of CHD7 and various histone methylation marks at promoter and enhancer elements would provide important insight into the genomic location of CHD7 in neural stem cells, these experiments do not determine whether CHD7 is physically interacting with and resolving chromatin structures where these methylation marks are present. Bouazoune and Kingston have published the catalytic and chromatin remodeling activity of many recombinant CHD7 mutants (Bouazoune et al. 2012). Recombinant CHD7 containing CHARGE individual-observed missense mutations in the chromodomains show significant reductions in ATP hydrolysis and disruption of DNA-histone contacts (Bouazoune et al. 2012). To expand upon these studies by Bouazoune and Kingston and those proposed above, it is necessary to investigate the substrate specificity of the CHD7 chromodomains to determine the true physiologically relevant binding event between CHD7 and methylated histones at promoter and enhancer elements. In order to determine CHD7 chromodomain specificity, isothermal titration calorimetry (Ghai et al. 2012) would be performed with wild type or

chromodomain-mutant CHD7 (S834F, K907T and T917M) (Delahaye et al. 2007; Bartels et al. 2010) and covalently-modified, recombinant nucleosomes containing activating (H3K4me1, H3K4me3) or repressing (H3K9me3, H3K27me) histone marks. An appropriate control for these experiments would be unmodified recombinant histones or HeLA-purified nucleosomes to determine the level of non-specific binding. Considering the role of CHD7 in promoting gene expression and ChIP-seq data indicating that CHD7 specifically binds chromatin regions with H3K4me1, one would predict that CHD7 would most tightly bind to activating histone methylation marks and bind weakly or not at all to repressive histone methylation marks. These experiments would provide important clues as to the biochemically relevant substrate for CHD7 function and determine whether the co-localization of CHD7 with poised and active chromatin is a direct or indirect phenomenon.

CHD7 and retinoic acid signaling

Conclusions

In Chapter 3, I investigated changes in SVZ gene expression upon loss of *Chd7* as well as interactions between CHD7 and retinoic acid signaling. I performed whole genome microarray analysis on microdissected SVZ from control and *Chd7* knockout perinatal mice. The majority of genes with changes in expression were down-regulated. This abundance of down-regulated genes upon loss of *Chd7* is not entirely surprising considering that this trend is observed in several cell types and further strengthens the hypothesis that CHD7 acts a

potent activator of gene expression (Layman et al. 2011; Hurd et al. 2012). Gene ontology (GO) analysis revealed that down-regulated genes were involved in memory, cognition, neuronal differentiation, neuronal migration and neuronal maturation, which inform future studies of CHD7 function in brain regions that regulate these complex processes such as the cortex and dentate gyrus of the hippocampus. Consistent with studies presented in Chapter 2, *Rarb* and *Rxrg* were down-regulated which further strengthens the connection between CHD7 and retinoic acid signaling. In nuclear extract derived from P19 embryonal carcinoma cells, CHD7 physically interacts with retinoic acid receptors. To study *Chd7* function in a cell line that is more amenable to genetic and biochemical manipulation (Soprano et al. 2007), I used *Chd7* shRNA constructs based on the SIBR shRNA system to knockdown *Chd7* in P19 embryonal carcinoma cells (Yu et al. 2005). Knockdown of *Chd7* led to reduced expression of known CHD7 target genes and a decrease in P19 cell growth consistent with previously published growth studies (Kita et al. 2012). These studies have provided preliminary evidence that CHD7 may regulate neuronal migration and maturation. This further strengthens the genetic and biochemical link between CHD7 and retinoic acid signaling. Considering the striking similarity in phenotypes between CHARGE syndrome and retinoic acid deficiency (Sanlaville et al. 2006; Legendre et al. 2012; Rhinn et al. 2012), determination of the specific molecular mechanisms of CHD7 regulation of retinoic acid signaling may provide therapeutic interventions to potentially correct some CHARGE phenotypes through modulation of retinoic acid levels *in utero*.

Future Directions

I observed CHD7 binding directly to retinoic acid receptors by co-immunoprecipitation and found that *Rarb* and *Rxrg* expression are specifically down-regulated upon loss of *Chd7*. A confounding factor in the co-immunoprecipitation experiment is that I used a pan-retinoic acid receptor antibody that recognizes all three receptor isoforms. To identify the specific receptor isoforms that CHD7 binds, co-immunoprecipitation experiments should be repeated utilizing antibodies that specifically identify RARα, RARβ, RARγ, RXRα, RXRβ and RXRγ. After individually identifying which receptor isoforms CHD7 binds, one could determine whether CHD7 binds a specific RAR/RXR heterodimer. Similar to the ChIP-seq experiments proposed above, it is necessary to determine whether specific retinoic acid receptor isoforms co-localize at CHD7 bound genes in wild type mouse SVZ or P19 embryonal carcinoma neurospheres. These experiments would help determine which specific retinoic acid receptor isoforms help mediate CHD7 gene regulation and mediate CHD7 effects on pro-neuronal or RA-target gene expression. Additionally, it is necessary that all experiments involving RA signaling be performed both with and without retinoic acid treatment to determine if the association of CHD7 and RA signaling components is truly retinoic acid-dependent. Overall, CHD7 appears to be regulating gene expression of retinoic acid signaling modulators as well as potentially participating in RA-mediated gene regulation by binding RAR's. The CHD7 and RAR/RXR ChIP-seq experiments proposed in this chapter will help address whether CHD7 is co-

localizing with RAR/RXR complexes at pro-neural and RA-target genes at RARE's. The data presented in this dissertation lead me to hypothesize that CHD7 is likely functioning by binding to and activating the expression of RAR and RXR genes, not through direct association with RAR/RXR complexes at RA-target genes.

The studies outlined in this dissertation regarding retinoic acid signaling have largely been performed on microdissected SVZ tissue or P19 neurospheres, but have not assessed effects of *Chd7*-deficiency on retinoic acid signaling *in vivo*. Using *Nestin-CreERT2* and the *Chd7*^{flox} allele (Ables et al. 2010; Hurd et al. 2010; Madisen et al. 2010), one could induce knockout of *Chd7* in SVZ neural stem cells and investigate changes in localization of *Rarb* and *Rxrg* expression by *in situ* hybridization. This would test whether reduced expression observed by qRT-PCR and microarray also occurs *in vivo*. Alternatively, crossing the RARE-*lacZ* reporter (a reporter allele that activates β-galactosidase expression driven by a promoter with a retinoic acid response element) with wild type or *Chd7*-deficient mice would allow for monitoring of changes in activation of retinoic acid signaling in the SVZ (Rossant et al. 1991; Rajaii et al. 2008). Experiments utilizing the RARE-*LacZ* would only determine if *Chd7*-deficiency leads to general dysfunction in RA signaling and would not directly identify whether abnormal localization or intensity of *LacZ* signal is directly due to loss of CHD7 protein at RARE elements of RA-target genes or due to a global reduction in RAR and RXR protein.

Considering that modulation of retinoic acid signaling in *Chd7*-deficient neurospheres rescues defects in proliferation, self-renewal and neuronal differentiation, it would be interesting to determine whether intraventricular injection of retinoic acid or the retinoic acid synthesis inhibitor citral corrects the proliferative and neurogenic defects observed in *Chd7*-deficient mice and neurospheres. Overall, these studies would provide insight into the specific interactions between CHD7 and retinoic acid signaling to regulate pro-neuronal gene expression the SVZ neural stem cell niche.

CHD7 and corticogenesis

Conclusions

In Chapter 4, I investigated the role of CHD7 function in the development of the cerebral cortex, a brain region populated by neurons born in the SVZ. As in the adult SVZ, CHD7 co-localized with markers of neural stem and progenitor cells during corticogenesis. There were no changes in SVZ proliferation or apoptosis in the *Chd7*-deficient embryonic forebrain. In *Chd7*-deficient neurospheres derived from embryonic forebrain, there was a mild decrease in neurosphere size which was rescued by inhibition of retinoic acid signaling by citral. Interestingly, there were no changes in neurosphere self-renewal or neuronal differentiation. These data show that *Chd7* is expressed during corticogenesis, yet it does not appear to regulate neural stem and progenitor cell function between embryonic day 11 and embryonic day 15. Further study of CHD7 function is necessary to determine what role, if any, CHD7 plays during

cortex development due to the importance of cortex-mediated sensory processing.

Future Directions

While I have characterized the co-localization of CHD7 with a number of neural stem and progenitor cell markers, I did not explore its presence in neuroblasts and immature and mature cortical neurons. Double immunofluorescence at embryonic days 13 and 15 in the forebrain with CHD7 and neuroblast markers (DCX, Neurod1), immature neuron markers (TBR1) and mature neuron markers (CALB, CALR, TH) would reveal the complete spectrum of cell type-specific *Chd7* expression in the forebrain. These populations of cells are of particular interest due to their reduction in the *Chd7*-deficient SVZ neural stem cell niche and our microarray data showing that neuronal migration and maturation genes are down-regulated upon loss of *Chd7* (Feng et al. 2013; Micucci et al. 2013). Neuronal migration and maturation defects in *Chd7*-deficient forebrain could be observed by immunofluorescence and counting of neuroblasts as they migrate to their appropriate cortical layers and mature cortical GABAergic and dopaminergic neurons. Additionally, considering that the cortex consists of several distinct neuron layers, it would be interesting to see if this layering is disrupted in *Chd7* conditional knockout mice compared to controls. Abnormal layering would greatly affect the normal neural circuitry present in the cortex and could potentially lead to defects in information processing. Finally, microarray or RNA-seq analysis of the SVZ and cortex in

control and *Chd7*-deficient embryos would potentially reveal differentially expressed genes that are important for neuronal development. These studies would provide a basis for understanding the role of CHD7 in the development of the mammalian cortex and may give insight into some of the sensory and cognitive defects associated with CHARGE syndrome.

References

Ables, J. L., N. A. Decarolis, M. A. Johnson, P. D. Rivera, Z. Gao, D. C. Cooper, F. Radtke, J. Hsieh and A. J. Eisch (2010). "Notch1 is required for maintenance of the reservoir of adult hippocampal stem cells." J Neurosci **30**(31): 10484-10492.

Bajpai, R., D. A. Chen, A. Rada-Iglesias, J. Zhang, Y. Xiong, J. Helms, C. P. Chang, Y. Zhao, T. Swigut and J. Wysocka (2010). "CHD7 cooperates with PBAF to control multipotent neural crest formation." Nature **463**(7283): 958-962.

Bartels, C. F., C. Scacheri, L. White, P. C. Scacheri and S. Bale (2010). "Mutations in the CHD7 gene: the experience of a commercial laboratory." Genetic testing and molecular biomarkers **14**(6): 881-891.

Bouazoune, K. and R. E. Kingston (2012). "Chromatin remodeling by the CHD7 protein is impaired by mutations that cause human developmental disorders." Proc Natl Acad Sci U S A **109**(47): 19238-19243.

Delahaye, A., Y. Sznajer, S. Lyonnet, M. Elmaleh-Berges, I. Delpierre, S. Audollent, S. Wiener-Vacher, A. L. Mansbach, J. Amiel, C. Baumann, D. Bremond-Gignac, T. Attie-Bitach, A. Verloes and D. Sanlaville (2007). "Familial CHARGE syndrome because of CHD7 mutation: clinical intra- and interfamilial variability." Clinical genetics **72**(2): 112-121.

Engelen, E., U. Akinci, J. C. Bryne, J. Hou, C. Gontan, M. Moen, D. Szumska, C. Kockx, W. van Ijcken, D. H. Dekkers, J. Demmers, E. J. Rijkers, S. Bhattacharya, S. Philipsen, L. H. Pevny, F. G. Grosveld, R. J. Rottier, B. Lenhard and R. A. Poot (2011). "Sox2 cooperates with Chd7 to regulate genes that are mutated in human syndromes." Nat Genet **43**(6): 607-611.

Feng, W., M. A. Khan, P. Bellvis, Z. Zhu, O. Bernhardt, C. Herold-Mende and H. K. Liu (2013). "The Chromatin Remodeler CHD7 Regulates Adult Neurogenesis via Activation of SoxC Transcription Factors." Cell Stem Cell **13**(1): 62-72.

Ghai, R., R. J. Falconer and B. M. Collins (2012). "Applications of isothermal titration calorimetry in pure and applied research--survey of the literature from 2010." Journal of molecular recognition : JMR **25**(1): 32-52.

Hartshorne, T. S., T. L. Grialou and K. R. Parker (2005). "Autistic-like behavior in CHARGE syndrome." Am J Med Genet A **133A**(3): 257-261.

Hurd, E. A., J. A. Micucci, E. N. Reamer and D. M. Martin (2012). "Delayed fusion and altered gene expression contribute to semicircular canal defects in Chd7 deficient mice." Mech Dev **129**(9-12): 308-323.

Hurd, E. A., H. K. Poucher, K. Cheng, Y. Raphael and D. M. Martin (2010). "The ATP-dependent chromatin remodeling enzyme CHD7 regulates pro-neural gene expression and neurogenesis in the inner ear." Development **137**(18): 3139-3150.

Issekutz, K. A., J. M. Graham, Jr., C. Prasad, I. M. Smith and K. D. Blake (2005). "An epidemiological analysis of CHARGE syndrome: preliminary results from a Canadian study." Am J Med Genet A **133A**(3): 309-317.

Kita, Y., M. Nishiyama and K. I. Nakayama (2012). "Identification of CHD7S as a novel splicing variant of CHD7 with functions similar and antagonistic to those of the full-length CHD7L." Genes Cells **17**(7): 536-547.

Kriegstein, A., S. Noctor and V. Martinez-Cerdeno (2006). "Patterns of neural stem and progenitor cell division may underlie evolutionary cortical expansion." Nat Rev Neurosci **7**(11): 883-890.

Layman, W. S., E. A. Hurd and D. M. Martin (2011). "Reproductive dysfunction and decreased GnRH neurogenesis in a mouse model of CHARGE syndrome." Hum Mol Genet **20**(16): 3138-3150.

Legendre, M., M. Gonzales, G. Goudefroye, F. Bilan, P. Parisot, M. J. Perez, M. Bonniere, B. Bessieres, J. Martinovic, A. L. Delezoide, F. Jossic, C. Fallet-Bianco, M. Bucourt, J. Tantau, P. Loget, L. Loeuillet, N. Laurent, B. Leroy, H. Salhi, N. Bigi, C. Rouleau, F. Guimiot, C. Quelin, A. Bazin, C. Alby, A. Ichkou, R. Gesny, A. Kitzis, Y. Ville, S. Lyonnet, F. Razavi, B. Gilbert-Dussardier, M. Vekemans and T. Attie-Bitach (2012). "Antenatal spectrum of CHARGE syndrome in 40 fetuses with CHD7 mutations." J Med Genet **49**(11): 698-707.

Lledo, P. M., M. Alonso and M. S. Grubb (2006). "Adult neurogenesis and functional plasticity in neuronal circuits." Nat Rev Neurosci **7**(3): 179-193.

Lledo, P. M., F. T. Merkle and A. Alvarez-Buylla (2008). "Origin and function of olfactory bulb interneuron diversity." Trends Neurosci **31**(8): 392-400.

MacPherson, P. A., S. Jones, P. A. Pawson, K. C. Marshall and M. W. McBurney (1997). "P19 cells differentiate into glutamatergic and glutamate-responsive neurons in vitro." Neuroscience **80**(2): 487-499.

Madisen, L., T. A. Zwingman, S. M. Sunkin, S. W. Oh, H. A. Zariwala, H. Gu, L. L. Ng, R. D. Palmiter, M. J. Hawrylycz, A. R. Jones, E. S. Lein and H. Zeng (2010). "A robust and high-throughput Cre reporting and characterization system for the whole mouse brain." Nat Neurosci **13**(1): 133-140.

McBurney, M. W. (1993). "P19 embryonal carcinoma cells." Int J Dev Biol **37**(1): 135-140.

McBurney, M. W., K. R. Reuhl, A. I. Ally, S. Nasipuri, J. C. Bell and J. Craig (1988). "Differentiation and maturation of embryonal carcinoma-derived neurons in cell culture." J Neurosci **8**(3): 1063-1073.

Micucci, J. A., W. S. Layman, E. A. Hurd, E. D. Sperry, S. F. Frank, M. A. Durham, D. L. Swiderski, J. M. Skidmore, P. C. Scacheri, Y. Raphael and D. M. Martin (2013). "CHD7 and retinoic acid signaling cooperate to regulate neural stem cell and inner ear development in mouse models of CHARGE syndrome." Hum Mol Genet.

Rajaii, F., Z. T. Bitzer, Q. Xu and S. Sockanathan (2008). "Expression of the dominant negative retinoid receptor, RAR403, alters telencephalic progenitor proliferation, survival, and cell fate specification." Dev Biol **316**(2): 371-382.

Rhinn, M. and P. Dolle (2012). "Retinoic acid signalling during development." Development **139**(5): 843-858.

Rossant, J., R. Zirngibl, D. Cado, M. Shago and V. Giguere (1991). "Expression of a retinoic acid response element-hsplacZ transgene defines specific domains of transcriptional activity during mouse embryogenesis." Genes Dev **5**(8): 1333-1344.

Sanlaville, D., H. C. Etchevers, M. Gonzales, J. Martinovic, M. Clement-Ziza, A. L. Delezoide, M. C. Aubry, A. Pelet, S. Chemouny, C. Cruaud, S. Audollent, C. Esculpavit, G. Goudefroye, C. Ozilou, C. Fredouille, N. Joye, N. Morichon-Delvallez, Y. Dumez, J. Weissenbach, A. Munnich, J. Amiel, F. Encha-Razavi, S. Lyonnet, M. Vekemans and T. Attie-Bitach (2006). "Phenotypic spectrum of CHARGE syndrome in fetuses with CHD7 truncating mutations correlates with expression during human development." J Med Genet **43**(3): 211-217.

Soprano, D. R., B. W. Teets and K. J. Soprano (2007). "Role of retinoic acid in the differentiation of embryonal carcinoma and embryonic stem cells." Vitam Horm **75**: 69-95.

Takada, I., M. Mihara, M. Suzawa, F. Ohtake, S. Kobayashi, M. Igarashi, M. Y. Youn, K. Takeyama, T. Nakamura, Y. Mezaki, S. Takezawa, Y. Yogiashi, H. Kitagawa, G. Yamada, S. Takada, Y. Minami, H. Shibuya, K. Matsumoto and S. Kato (2007). "A histone lysine methyltransferase activated by non-canonical Wnt signalling suppresses PPAR-gamma transactivation." Nat Cell Biol **9**(11): 1273-1285.

Yu, J. Y., T. W. Wang, A. B. Vojtek, J. M. Parent and D. L. Turner (2005). "Use of short hairpin RNA expression vectors to study mammalian neural development." Methods Enzymol **392**: 186-199.

Zentner, G. E., P. J. Tesar and P. C. Scacheri (2011). "Epigenetic signatures distinguish multiple classes of enhancers with distinct cellular functions." Genome Res **21**(8): 1273-1283.